

# Metallurgical Characteristics of High Strength Structural Materials

[EIGHTH QUARTERLY REPORT]

P. P. PUZAK, K. B. LLOYD, R. J. GOODE, R. W. HUBER,  
D. G. HOWE, R. W. JUDY, JR., T. W. CROOKER, R. E. MOREY,  
E. A. LANGE, AND C. N. FREED

*Metallurgy Division*

August 1965

APPROVED FOR PUBLIC  
RELEASE - DISTRIBUTION  
UNLIMITED



U.S. NAVAL RESEARCH LABORATORY  
Washington, D.C.

## PREVIOUS REPORTS IN THIS SERIES

First Quarterly Report - "Metallurgical Characteristics of High Strength Structural Materials," P.P. Puzak, K.B. Lloyd, E.A. Lange, R.J. Goode, R.W. Huber, E.P. Dahlberg, and C.D. Beachem, NRL Memo. Rept. 1438, June 30, 1963

Second Quarterly Report - "Metallurgical Characteristics of High Strength Structural Materials," P.P. Puzak, K.B. Lloyd, E.A. Lange, R.J. Goode, and R.W. Huber, NRL Memo. Rept. 1461, Sept. 1963

Third Quarterly Report - "Metallurgical Characteristics of High Strength Structural Materials," P.P. Puzak, K.B. Lloyd, R.J. Goode, R.W. Huber, D.G. Howe, T.W. Crooker, E.A. Lange, and W.S. Pellini, NRL Report 6086, Jan. 1964

Fourth Quarterly Report - "Metallurgical Characteristics of High Strength Structural Materials," R.J. Goode, R.W. Huber, D.G. Howe, R.W. Judy, Jr., T.W. Crooker, R.E. Morey, E.A. Lange, P.P. Puzak, and K.B. Lloyd, NRL Report 6137, June 1964

Fifth Quarterly Report - "Metallurgical Characteristics of High Strength Structural Materials," T.W. Crooker, R.E. Morey, E.A. Lange, R.W. Judy, Jr., C.N. Freed, R.J. Goode, P.P. Puzak, K.B. Lloyd, R.W. Huber, D.G. Howe, and W.S. Pellini, NRL Report 6196, Sept. 1964

Sixth Quarterly Report - "Metallurgical Characteristics of High Strength Structural Materials," W.S. Pellini, R.J. Goode, R.W. Huber, D.G. Howe, R.W. Judy, Jr., P.P. Puzak, K.B. Lloyd, E.A. Lange, E.A. DeFelice, T.W. Crooker, R.E. Morey, E.J. Chapin, and L.J. McGeady, NRL Report 6258, Dec. 1964

Seventh Quarterly Report - "Metallurgical Characteristics of High Strength Structural Materials," R.J. Goode, D.G. Howe, R.W. Huber, P.P. Puzak, K.B. Lloyd, T.W. Crooker, R.E. Morey, E.A. Lange, R.W. Judy, Jr., and C.N. Freed, NRL Report 6327, May 1965.

## CONTENTS

Abstract	iii
Problem Status	iii
Authorization	iii
INTRODUCTION	1
HIGH STRENGTH STEELS	4
Fracture Toughness Index Diagram	4
DWTT of 9-4-.XXC Alloy High Strength Steels	11
DWTT of 12% Nickel Maraging Steels	19
Fracture Toughness Evaluation and Control of High Strength Weld Metals	22
TITANIUM ALLOYS	39
Fracture Toughness Index Diagram for Titanium	39
Alloy Development Studies	41
Welding Studies	42
Heat Treatment Studies on Some Titanium Alloys	47
ALUMINUM ALLOYS	58
Explosion Tear Test Results	58
Fracture Toughness Index Diagram	61
A COMPARATIVE EVALUATION OF LOW CYCLE FATIGUE CRACK PROPAGATION IN 5Ni-Cr-Mo-V STEELS	67
Materials and Experimental Procedure	68
Test Results	72
Comparative Fatigue Performance	82
Conclusions	82

CONTENTS - Continued

PLANE-STRAIN FRACTURE TOUGHNESS OF THE HIGH STRENGTH TITANIUM ALLOYS Ti-6Al-4V AND Ti-6Al-6V-2.5Sn	84
Test Results on 1-in.-Thick Ti-6Al-4V Plate	84
Test Results on 1-in.-Thick Ti-6Al-6V-2.5Sn	87
Effect of Thickness on $K_{Ic}$	89
REFERENCES	91

Copies available from  
Clearinghouse for Federal Scientific and  
Technical Information (CFSTI)  
Sills Building, 5285 Port Royal Road  
Springfield, Virginia 22151  
\$3.00

## ABSTRACT

A progress report covering research studies in high strength structural materials conducted in the period May 1965 to July 1965 is presented. The report includes fracture toughness studies on the 12% Ni maraging and 9Ni-4Co-.XXC steels, a variety of titanium alloy MIG, EB, and plasmarc weldments, and some aluminum alloys. The current fracture toughness index diagrams are presented for steels, titanium alloys, and aluminum alloys. Results are presented of (1) a study of the plane-strain fracture toughness of the alloys Ti-6Al-4V and Ti-6Al-6V-2.5Sn over respective yield strength ranges of 130-140 ksi and 147-186 ksi; (2) heat-treatment studies on several titanium alloys; and (3) a low cycle fatigue crack propagation study of 5Ni-Cr-Mo-V steel in dry and wet environments in which considerable microcrack formation and growth was encountered.

## PROBLEM STATUS

This is a progress report; work is continuing.

## AUTHORIZATION

NRL Problem FO1-17; Project SP-01426:  
NRL Problem MO1-05; Projects RR-007-01-46-5405,  
SR-007-01-02-0704, and SP-01426:  
NRL Problem MO1-18; Projects RR-007-01-46-5420,  
SF-020-01-05-0731, SP-01426, MIPR-ENG-NAV-66-2:  
NRL Problem MO3-01; Projects RR-007-01-46-5414,  
SF-020-01-01-0850, and SP- 01426

Manuscript submitted October 12, 1965.

METALLURGICAL CHARACTERISTICS  
OF HIGH STRENGTH STRUCTURAL MATERIALS

[Eighth Quarterly Report]

INTRODUCTION

This is the eighth status report covering the U.S. Naval Research Laboratory Metallurgy Division's long-range program of determining the performance characteristics of high strength metals. The program is primarily concerned with determining the fracture toughness characteristics of these materials using standard and recently developed laboratory test methods and is directed towards establishing the significance of the laboratory tests for predicting the service performance of the materials in large complex structures. Although the program is aimed at Navy requirements, the information that is developed is pertinent to all structural uses of these high strength materials. Titanium and aluminum alloys, quenched and tempered (Q&T) steels, and maraging steels are the principal high strength metals currently under investigation.

The fracture toughness index diagram for steel has been modified to indicate the expected yield strength regions of high and low fracture toughness for optimized or nearly optimized material. The yield strength range of low fracture toughness indicates the region where the linear elastic fracture mechanics approach to fracture toughness determination will be required. The fracture toughness index diagrams for titanium and aluminum alloys are also presented. All the diagrams reflect the most recent test results; a comparison of the weak and strong direction optimum materials trend line for aluminum indicates considerable anisotropy for all but the highest strength commercially-produced alloys.

The results of recent fracture toughness investigations using the drop-weight tear test for 12% Ni maraging and 9Ni-4Co-.XXC steels are reported. The fracture toughness evaluation and control of high strength steel weld metals are also discussed. The available test results for the various groups of steels are compared to the optimum materials trend lines obtained for plate material.

Preliminary heat-treatment studies on the fracture toughness of two NRL-produced alloys (Ti-6Al-2Mo-2V-2Sn and Ti-6Al-3Mo-1V-2Sn) are reported. Both alloys were aimed at the 130-ksi yield strength level. Drop-weight tear test studies on a Ti-2.5Al-16V all-beta alloy indicate a very low fracture toughness capability for this material.

Preliminary welding studies on Ti-6Al-2Mo MIG weldments show that considerable improvement in the fracture toughness can be obtained in the weld by a solution anneal and aging treatment after welding. For electron beam welds in the same alloy, it was found that heat treating the plate to a high fracture toughness prior to welding more than doubled the toughness of the as-deposited EB weld.

Plasmarc welds in Ti-7Al-2.5Mo and Ti-6Al-4V were evaluated in the drop-weight tear test. A study of the effect of heat treatment on 1/2-in.-thick Ti-6Al-4V, Ti-5Al-2.5Sn, Ti-7Al-2Cb-1Ta, and Ti-6Al-2Mo using EB welds has been completed. The results of both of these investigations are reported along with the very favorable drop-weight tear test results on Ti-7Al-2Cb-1Ta short circuit MIG and spray arc MIG weldments furnished by the U.S. Naval Applied Science Laboratory. The drop-weight tear test results on three high strength titanium experimental alloys, prepared by the New York University, are also presented.

Heat-treatment studies on Ti-6Al-2Mo and Ti-7Al-2.5Mo are described. There is some indication from the results obtained in this study that the fracture toughness properties of Ti-6Al-2Mo might be more sensitive to the rate of cooling from solution annealing temperatures than the Ti-7Al-2.5Mo alloy. The Charpy V notch properties for a number of alloys are reported for specific conditions of heat treatment or in the as-received condition.

Explosion tear test results are reported for the aluminum alloys 6061-T651, 5086-H112, and 5083-0. All of the alloys in the designated tempered conditions were seen to require high levels of plastic strain for fracture propagation. The 6061-T651 provided an index of 12% plastic strain required for fracture propagation in aluminum alloys of 750 ft-lb drop-weight tear test energy.

Low cycle fatigue crack propagation studies on 5Ni-Cr-Mo-V steels in air and a 3.5% salt water environment were conducted. These studies have shown that the intrinsic fatigue crack propagation resistance of the 5Ni-Cr-Mo-V steel at about 130-140 ksi yield strength is the same as that for HY-80 steel. The results also indicate that fatigue cracks propagate four to five times faster in the 5Ni-Cr-Mo-V steel than in the HY-80 steel at the same percentage of yield strength and that fatigue performance is not seriously affected by wet environments. Considerable microcrack formation and growth was experienced in advance of the main fatigue crack tip for both the wet and dry test conditions. Sequence photographs of this phenomenon are presented in this report.

The plane-strain fracture toughness of the alloys Ti-6Al-4V (T-27) and Ti-6Al-6V-2.5Sn (T-21) have been determined at the yield strength ranges of 132-140 ksi and 147-186 ksi respectively. Some additional data concerning the effect of thickness on  $K_{Ic}$  of heat-treated Ti-6Al-6V-2.5Sn are also presented.

## HIGH STRENGTH STEELS

(P.P. Puzak and K.B. Lloyd)

Since the original development of crack-starter test methods (1), the Metallurgy Division studies for steels have especially been aimed at determining the factors which affect the performance of steels in structural applications. The test methods used and information developed are basic to all structural use of steels and particular emphasis has been given to determining information required to provide fracture-safe design of complex, welded steel structures. The NRL-developed drop-weight test (DWT) for determining nil-ductility transition (NDT) temperatures (2) and the fracture analysis diagram concept (3, 4) provide the only available and proven engineering procedure for fracture-safe design with intermediate and low strength steels, commonly referenced as the structural grades. This test method has not been applicable for thin (less than 5/8-in.-thick) structural steels, or the nonferrous metals and ultrahigh strength steels which can develop low-energy-tear fractures via fracture modes not encountered with the structural grade steels (5).

The present broad scope fracture toughness evaluation studies for steels have been continuing to provide more definitive information relative to the fracture-safe design utilization of the high strength steels. New tests for determining the fracture toughness characteristics of high strength steels under a variety of test conditions were developed at the U.S. Naval Research Laboratory (6, 7). A two-step performance, using the drop-weight tear test (DWTT) and the structural prototype explosion tear test (ETT), was shown to establish criteria for selection, specification, and quality control of the ultrahigh strength steels required for new advanced designs (8). Modifications of the basic DWTT specimen design for steels have also been evolved and used successfully since 1962 to develop similar criteria for titanium and aluminum alloys, and more recently for the thin structural steels.

### FRACTURE TOUGHNESS INDEX DIAGRAM

The DWTT procedures are practical and suitable to any laboratory and the analysis has been simplified for understanding in the general engineering field. The DWTT and ETT methods

allow for determining the resistance to fracture propagation in a metal at elastic and plastic stress levels. Interpretation of the data has led to the evolution of new fracture toughness index diagrams (FTID) of similar simplicity to that of the fracture analysis diagram but with the potential of application "across the board" to all types and thicknesses of metals. The FTID chart relating specifically to all 1-in.-thick steel plates evaluated to date is presented in Fig. 1. The FTID summarizes the DWTT energy vs yield strength (YS) values obtained in extensive DWTT studies coupled with ETT correlations for tests of the steels at 30°F. Correlations with ETT data served to index the strain levels for fracture propagation to specific DWTT energy levels, irrespective of YS. Basic guidelines are given to indicate relative resistance to fracture propagation for steels characterized by DWTT energy levels above, between, or below, the strain levels illustrated by the horizontal cross-hatched lines. The shaded region from 1000 to 1250 ft-lb is used to denote the range of DWTT energy level separating materials capable of propagating fractures at elastic stress levels from the materials that require plastic strain overloads for propagation of fracture. This change-over point--from above yield to below yield stress levels for fracture propagation--is the primary evaluation criteria for suitability of steels in most large, complex, welded structures at this present stage of development of the FTID chart.

The curves given in the FTID, Fig. 1, separate the data into characteristic groups relating to the processing variables (melting practice and/or cross-rolling) of the steels. For each characteristic group of steels, a wide range of fracture toughness may be developed by different alloy steels of the same YS level. The various curves indicate that fracture toughness decreases with increasing strength level for all characteristic groups of steels. The limiting ceiling curves for each group have been designated as the "optimum materials trend lines" (OMTL) for the group. The OMTL may be recognized as the reference "yardstick" for evaluation of new steels with respect to the practicable upper limits of fracture toughness for any given strength level as a function of conventional or special processing variables.

The FTID data are particularly significant with respect to general conclusions that may be derived for steels

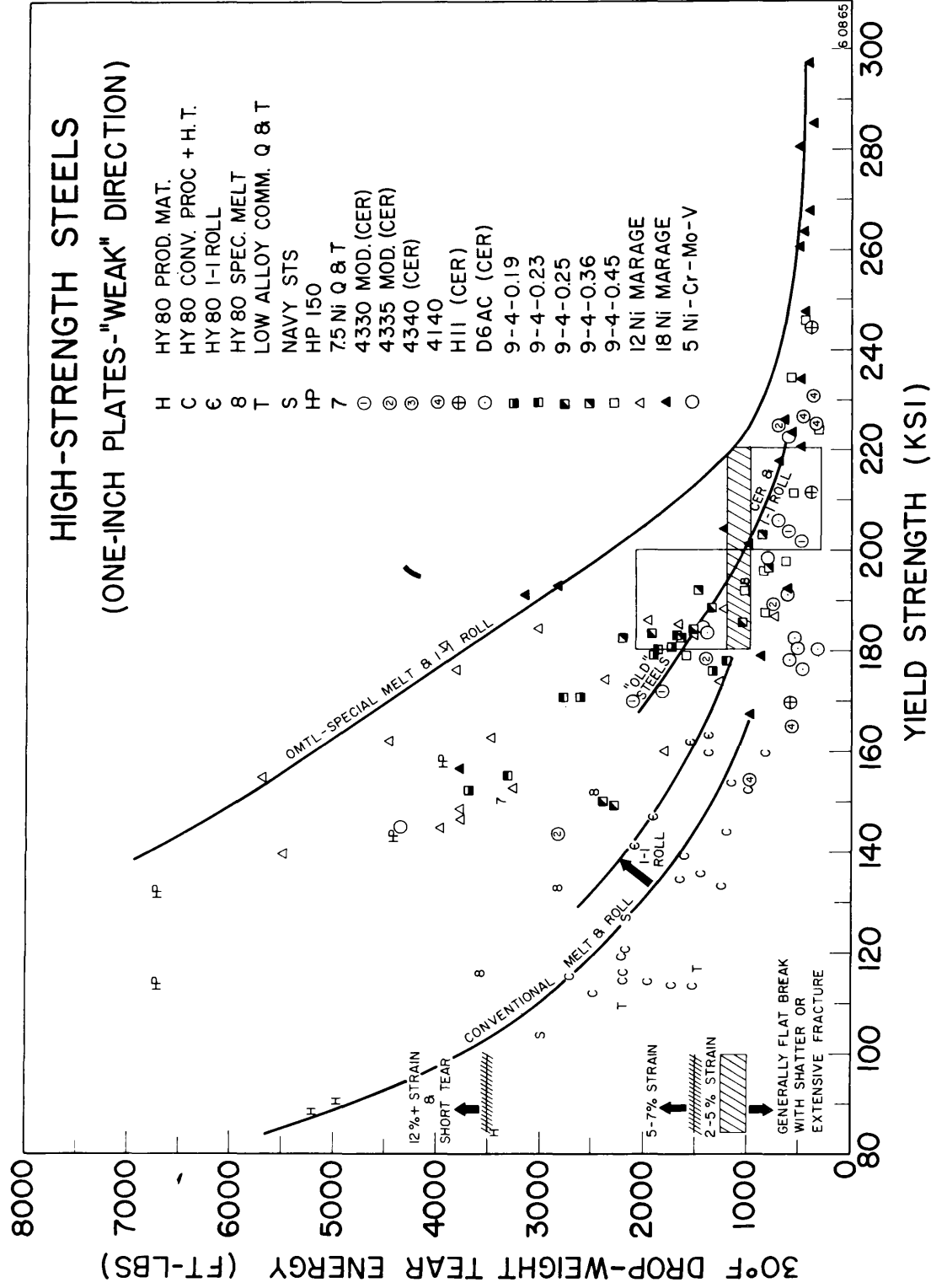


Fig. 1 - Spectrum of DWTT data for high-strength steels as a function of yield strength and processing practices. By referencing the specific OMTL to the ETT performance index points (percent strain for fracture propagation), the chart evolves to a fracture-toughness index diagram (FTID) for all steels represented.

of 180-ksi and higher yield strengths. Note that the shaded region denoting the DWTT-ETT correlation index level of change from elastic to plastic loading requirements for fracture propagation is also located in the 180/220-ksi YS range and that "boxes" have been drawn to encompass the population of steel data points above and below 200-ksi YS. There are major implications immediately apparent from consideration of these data:

(1) Above 200-ksi YS, the preponderance of data for steels reside in regions of the FTID where propagation of fracture at elastic stress levels should be expected and are so confirmed by ETT results. It is thus considered that valid fracture mechanics toughness measurements should be obtainable for these steels.

(2) In the 180/220-ksi YS range, many of the "old" steel types (4330, 4340, etc.) are also characterized by similar low resistance to fracture propagation so as to predict valid fracture mechanics determinations.

(3) The upper "box" located in the 200/220-ksi YS range encompasses many of the "new" steel alloys (maraging steels, 9Ni-4Co steels, etc.) which are characterized by high DWTT toughness and as such, these steels should (and ETT prove) resist propagation of fracture unless subjected to at least 2% to 5% levels of plastic strain.

The standard method for evaluating fracture toughness available generally to industry has been the Charpy V ( $C_v$ ) test. Correlations between the DWTT and  $C_v$  tests have provided a means for calibrating the significance of the  $C_v$  test for steels. Figure 2 depicts the general relationships between DWTT and  $C_v$  data for all of the 1-in.-thick steels studied to date. It should be emphasized that the surprisingly good correlation of DWTT energy values with  $C_v$  values applies to steels involving 100% shear fractures in the  $C_v$  test--i.e., the correlation relates to tests at temperatures of maximum  $C_v$  upper shelf energy. Investigations of the effects of temperature on DWTT and  $C_v$  test energies in the transition temperature range were shown to indicate that the  $C_v$  test can be highly misleading for cases involving mixed fracture of the  $C_v$  specimens (9). Apparently "high"  $C_v$  energy numbers for test specimens featuring the presence of even small amounts of cleavage (values in the transition range) do not signify high fracture toughness as would be the case for shelf-level temperature (100% shear)  $C_v$  values.

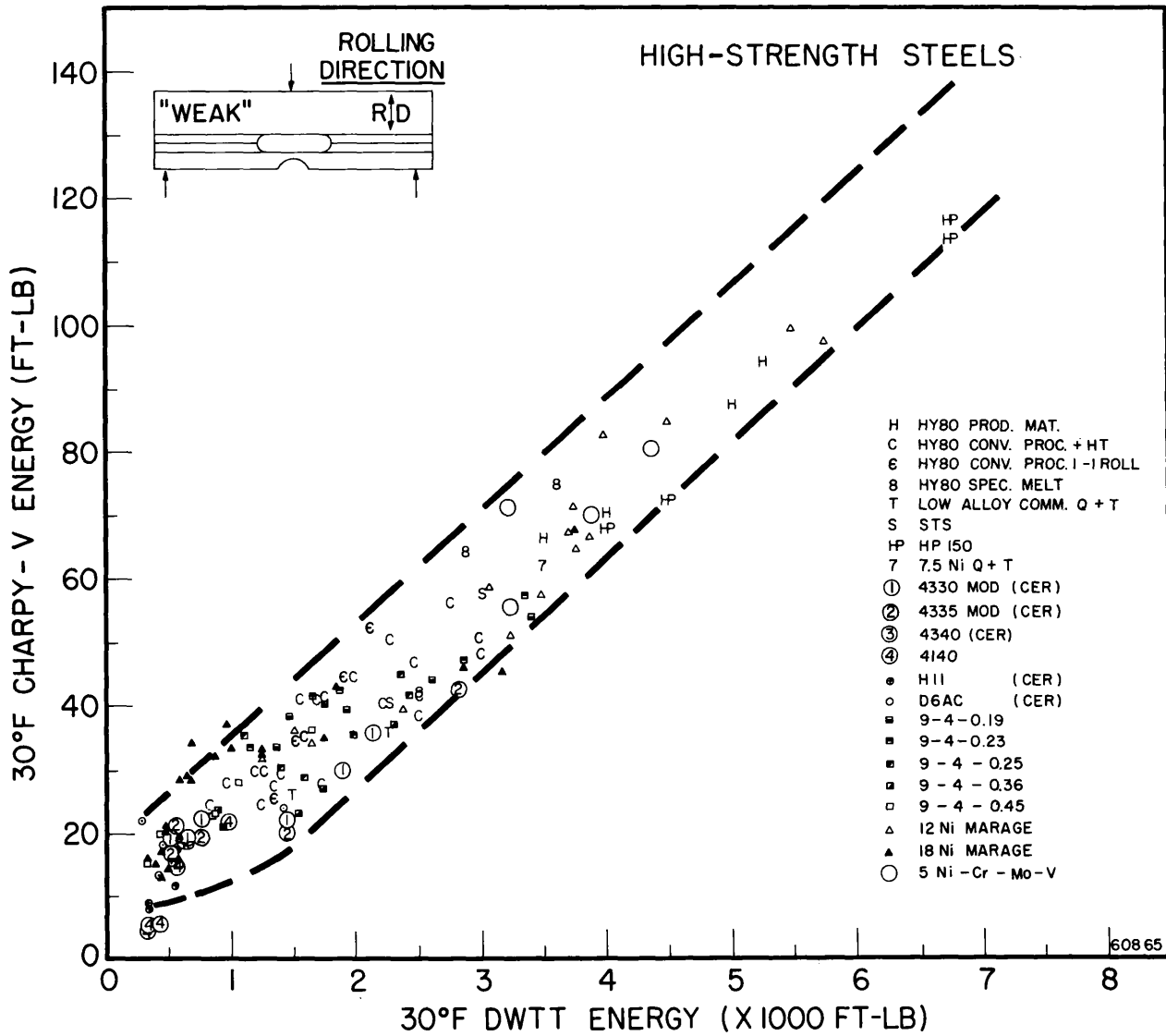


Fig. 2 - Correlation of  $C_v$  shelf energy with DWTT shelf energy. Shelf energies, for both tests, relate to test temperatures for which the fractures are of the fully ductile mode.

The DWTT and ETT index procedures have been used to evolve a FTID chart for  $C_v$  and YS data for all 1-in.-thick steels tested to date, Fig. 3. The curves in this figure separate these data into characteristic groups relating to the processing variables of the steels closely similar to those illustrated in Fig. 1. It is significant to note from the "two box" definition described for the data given in Fig. 1, that the  $C_v$  test also characterizes a high population density of steels in the 200/220-ksi YS range as materials capable of sustaining propagation of fractures at elastic stress levels. Also, that many steels of 180/200-ksi YS range may be expected to exhibit resistance to fracture propagation at plastic deformation overload levels. These data provide for useful application of  $C_v$  tests (within the described limitations) for high strength steels for fracture-safe design analysis in terms of simple FTID reference.

Figures 1 to 3 summarize all data developed to date for 1-in.-thick steel plates, including new data (to be reported) developed for 1-in.-thick steels during this reporting period. In addition much of the work during this past reporting period has been expended to validate the DWTT energy values obtained for the different steels with recheck values of DWTT energy for various steels using the electron-beam-embrittled weld technique for the crack-starter portion of the DWTT specimen as previously described (9). The initiation of a sharp crack which is directed into the test steel section for evaluation of fracture propagation resistance with minimum absorption of energy in fracture initiation is of critical importance to the DWTT. Exploratory tests are being conducted to determine whether prepared DWTT specimens using the electron-beam-embrittled weld can be subjected to heat-treatment studies without affecting the "brittleness" of the weld, i.e., the DWTT results.

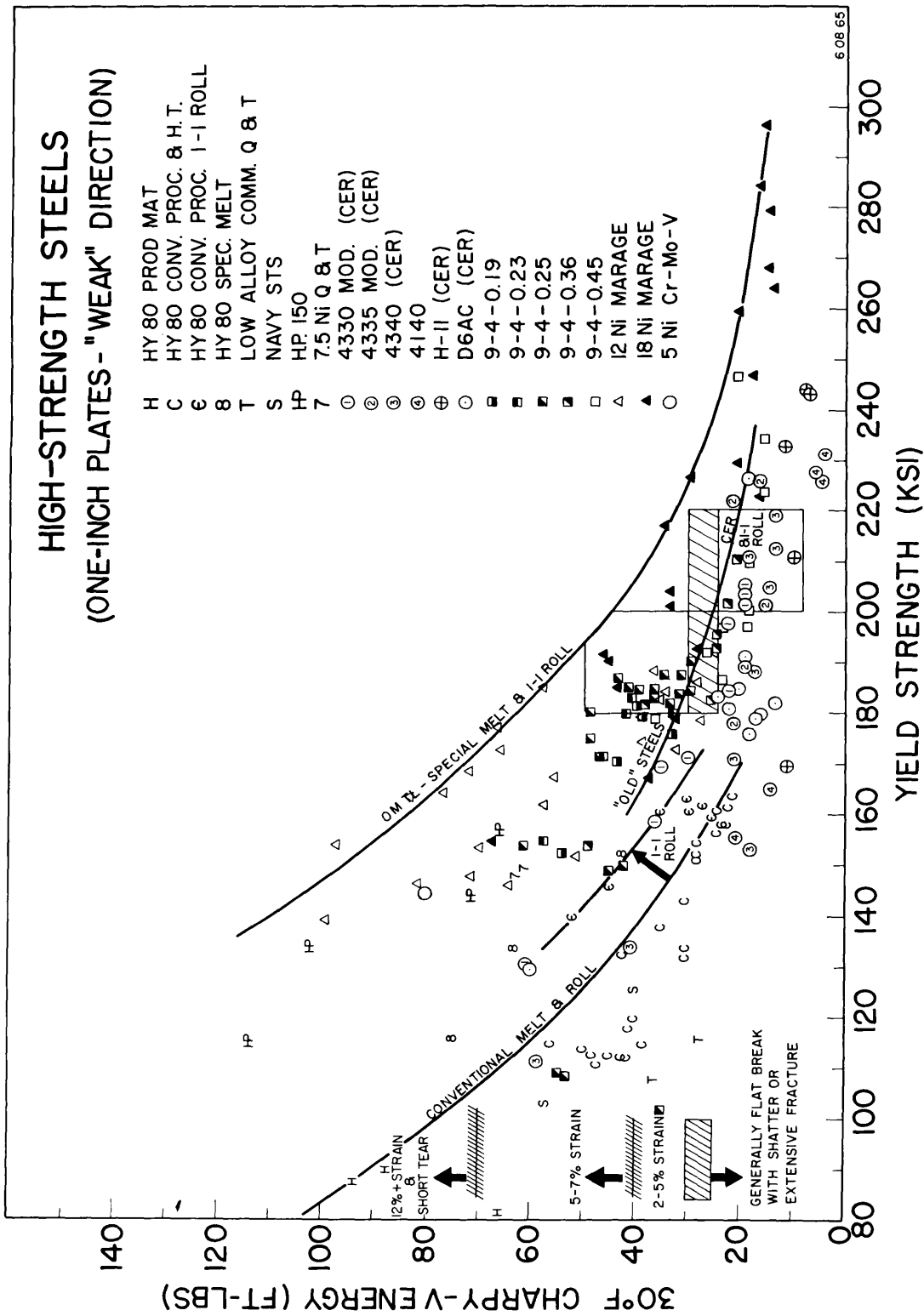


Fig. 3 - Spectrum of Cy test data for high-strength steels as a function of yield strength and of processing practices. Note the various optimum materials trend line (OMTL) curves. By indexing to DWT and ET data, the fracture-toughness index diagram (FTID) emerges. (Compare with Fig. 1.)

New steels obtained for study during this reporting period have included materials of the 9-4-.XXC and maraging steels capable of developing YS levels ranging from 150 to 200-ksi. DWTT results for these steels will be reported by using the basic features of the FTID charts (Figs. 1 and 3) to illustrate comparison of results for these new steels with previously tested and reported data.

#### DWTT OF 9-4-.XXC ALLOY HIGH STRENGTH STEELS

For high strength alloy steels conventionally strengthened by quench and temper (Q&T) heat treatments, the recently developed Ni-Co family of alloy compositions designated 9-4-.XXC appear very promising for high strength applications. The proprietary designation of 9-4 may be partly misleading in that the steels of this alloy family are all reported to contain 7.0 to 8.5% Ni, 3.5 to 4.5% Co, and 0.06 to 0.12% V. The two basic compositions of this alloy family, available commercially since 1962, contain approximately 0.45% C and 0.24% C, and these were designed to develop approximately 250-ksi and 180-ksi yield strengths respectively, for appropriate Q&T heat treatments. In all cases, commercial production of these steels have involved a special melt practice comprised of vacuum-carbon-deoxidation (VCD) of an electric furnace air-melt heat followed with a vacuum-consumable-electrode-remelt (CER). Present facilities for the CER process have limited the size of production heats of 9-4-.XXC steels from approximately 5 to 15 tons.

In addition to the nominal 180 and 250-ksi yield strengths of the two commercial alloys, the basic 9-4 composition can be adjusted or the heat treatment varied to develop YS levels ranging from approximately 150-ksi to 250-ksi as required for specific applications. Composition modifications involving carbon contents ranging from 0.10 to 0.45%, Co contents ranging from 2.0 to 4.0%, and higher ranges of Cr, Mo, or V than presently specified in the basic compositions (intended to promote secondary hardening characteristics upon tempering in the range of 1000°F) have been under intensive research investigation by the steel producer. The composition adjustments are generally made to maintain the Co addition in solid solution, to promote martensite "self-tempering" characteristics by raising the martensite transformation temperature of the alloy to above 450°F, and to decrease the amount of austenite that might be retained at room temperature after quenching.

Fracture toughness data for two steels, containing 0.25 and 0.36% C, of the basic 9-4 alloy composition were presented in previous investigations (10, 11). Additional 1-in.-thick plate sections of 9-4 alloy steels were received for this study: two of these steels (Nos. H-81 and H-82) represent lower carbon content and higher Cr-Mo content modifications of the basic 9-4-.25 alloy steel; one plate (No. G-99) represents the basic 9-4-.45 alloy steel; three of the plates (Nos. H-2, J-14, and J-15) represent the basic 9-4-.25 alloy. Excepting plate No. H-2 which measured 13/16-in., the above plates had been rolled to 1-in.-thickness. Essentially 1 to 1 cross-rolling was employed in producing each of the above plates excepting plate No. J-14 which was deliberately procured in the straightaway-rolled condition. The chemical compositions of these steels are given in Table 1.

Only two of these 9-4-.XXC alloy steels had been received in the mill Q&T heat-treatment condition, as noted in Table 1. The plates received in the annealed heat-treatment condition were cut into DWTT specimens and then Q&T heat treated by NRL. A spectrum of strength levels was developed in these alloys by tempering individual DWTT specimens at different temperatures. In addition to conventional Q&T heat treatments, isothermal transformation heat treatments at 475°F were conducted to develop a bainitic microstructure in the 9-4-.45 alloy steel. After DWTT of all plates had been conducted, the fractured specimens were sectioned to provide the necessary blanks for machining of tensile and C<sub>3</sub> specimens. The test data developed for this study for the various 9-4-.XXC steels are given in Tables 2, 3, 4, and 5.

A graphical summary of the changes in strength developed by these 9-4-.XXC steels as a function of the tempering temperatures employed is given in Fig. 4. With increasing tempering temperatures from 400° to 900°F, both the 9-4-.25 and 9-4-.45 steels display a continual decrease in ultimate tensile strength (UTS); the YS of the 9-4-.45 steel also decreases continually, however, the YS of the 9-4-.25 steel does not vary significantly with tempering temperatures of 400° to 900°F. Slightly higher UTS and YS properties are developed in the various 9-4-.XXC steels with the 1000°F tempering temperature treatment than those developed by the respective alloys

Table 1  
Chemical Composition of 9-4-.XXC Steels  
(Weight - percent)

NRL No.	As-Received Heat Treatment	C	Mn	Si	P	S	Ni	Cr	Mo	Co	V
H-2	Mill annealed	0.26	0.23	0.02	0.008	0.006	8.10	0.57	0.47	3.90	0.16
J-14	Mill Q&T	0.25	0.29	0.01	0.004	0.008	8.62	0.40	0.48	3.76	0.11
J-15	Mill Q&T	0.25	0.28	0.01	0.006	0.008	8.31	0.40	0.48	3.78	0.11
H-81	Mill annealed	0.21	0.37	0.02	0.004	0.007	7.13	1.13	1.12	3.98	0.10
H-82	Mill annealed	0.19	0.35	0.01	0.004	0.007	6.81	1.17	1.20	4.17	0.09
G-99	Mill annealed	0.43	0.28	0.01	0.003	0.006	7.63	0.40	0.31	3.90	0.13

Table 2  
 Test Data for 9-4-.25C Steel—Codes H-2, J-14, J-15  
 (Normalized 1600°F 1 hr, air-cooled; austenitized 1500°F 1 hr,  
 oil-quenched; tempered 2 + 2 hr, air-cooled)

Code	Tempering Temperature (°F)	Direction of Test *	0.505-In. -Diam. Tension Test Data				Charpy V at 30°F (ft-lb)	Drop-Weight Tear at 30°F (ft-lb)
			0.2% YS (ksi)	UTS (ksi)	El. in 2 in. (%)	R.A. (%)		
H-2	400	Weak	186.7	237.6	14.5	54.5	35	870
H-2	400	Strong	189.1	238.2	14.8	56.7	36	-
H-2	500	Weak	189.2	224.3	12.5	54.0	30	750
H-2	500	Strong	192.5	225.7	13.3	56.9	31	-
H-2	600	Weak	187.0	212.7	13.0	55.5	32	931
H-2	600	Strong	186.6	212.6	13.5	60.5	32	-
H-2	700	Weak	182.6	203.1	13.0	56.5	32	1113
H-2	700	Strong	185.7	204.2	13.0	56.9	33	-
H-2	800	Weak	181.0	196.5	15.5	56.3	34	1784
H-2	800	Strong	182.5	196.7	15.5	57.9	34	-
H-2	900	Weak	181.0	194.4	16.0	58.5	39	1784
H-2	900	Strong	181.3	195.0	16.3	60.0	40	-
H-2	950	Weak	183.8	196.6	16.3	57.8	40	1723
H-2	950	Strong	-	-	-	-	41	-
H-2	1000	Weak	185.9	194.8	16.5	61.1	44	1784
H-2	1000	Strong	-	-	-	-	42	-
H-2	1050	Weak	179.8	188.7	16.8	61.5	49	-
H-2	1050	Strong	178.4	186.9	18.0	65.4	49	-
H-2	1100	Weak	173.8	185.4	17.5	61.2	49	-
H-2	1100	Strong	175.9	185.6	18.0	64.1	53	-
H-2	1150	Weak	153.1	173.9	19.5	60.0	62	-
H-2	1150	Strong	155.4	174.5	20.0	64.4	59	-
H-2	1200	Weak	108.6	179.0	20.0	52.6	55	-
H-2	1200	Strong	109.5	177.6	21.0	56.0	58	-
H-2	1250	Weak	99.4	201.1	18.8	43.9	35	1228
H-2	1250	Strong	101.4	190.8	20.0	50.0	32	-
J-14	Mill heat tr.	Weak	180.3	196.4	15.0	48.0	30	1173
J-14	Str. rolled	Strong	180.0	196.2	16.8	61.0	38	1844
J-15	Mill heat tr.	Weak	183.2	195.0	17.0	61.0	40	1966
J-15	1X1 X-rolled	Strong	-	-	-	-	38	-

\*NOTE: Test direction is defined in terms of fracture path in specimen, i.e.,  
 "Weak" = specimen fracture parallel to principal (or final) rolling direction;  
 "Strong" = specimen fracture transverse to principal (or final) rolling direction.

**Table 3**  
**Test Data for 9-4-.23 Steel—Code H-81**  
(Austenitized 1 hr 1550° F; oil quenched; tempered 2 + 2 hr)

Tempering Temperature (°F)	Direction of Test*	0.505-in.-Diam. Tension Test Data				Charpy V at 30° F (ft-lb)	Drop-Weight Tear at 30° F (ft-lb)
		0.2% YS (ksi)	T.S. (ksi)	El. in 2 in. (%)	R.A. (%)		
900	Weak	177.9	214.8	15.0	52.2	33	1173
900	Strong	177.8	215.9	16.3	57.6	34	1113
950	Weak	-	-	-	-	38	-
950	Strong	181.5	212.2	16.0	60.0	40	1296
1000	Weak	182.9	212.3	16.3	58.7	41	1662
1000	Strong	183.6	212.3	16.0	60.0	42	1812
1050	Weak	179.9	208.2	15.8	57.3	42	1844
1050	Strong	181.6	209.2	16.0	59.3	44	2066
1100	Weak	171.4	196.1	16.5	59.6	47	2780
1100	Strong	166.8	192.4	17.0	60.5	52	3122
1150	Weak	154.8	183.4	17.8	59.4	58	3333
1150	Strong	148.0	179.5	19.3	63.0	63	3910

\*NOTE: Test direction is defined in terms of fracture path in specimen, i.e.,  
"Weak" = specimen fracture parallel to principal (or final) rolling direction;  
"Strong" = specimen fracture transverse to principal (or final) rolling direction.

**Table 4**  
**Test Data for 9-4-.19 Steel—Code H-82**  
(Austenitized 1 hr. 1550° F; oil quenched; tempered 2+2 hr.)

Tempering Temperature (°F)	Direction of Test*	0.505-in.-Diam. Tension Test Data				Charpy V at 30° F (ft-lb)	Drop-weight tear at 30° F (ft-lb)
		0.2% YS (ksi)	T.S. (ksi)	El. in 2" (%)	R.A. (%)		
900	Weak	176.1	210.3	15.1	51.8	33	1356
900	Strong	175.2	209.6	15.5	54.8	33	1326
950	Weak	-	-	-	-	38	1478
950	Strong	174.7	210.4	17.5	61.8	40	1601
1000	Weak	181.4	207.8	16.5	59.9	40	1723
1000	Strong	183.4	206.7	15.8	59.2	39	1723
1050	Weak	178.6	201.3	16.5	57.3	39	1933
1050	Strong	181.0	205.3	16.0	58.2	40	1994
1100	Weak	170.8	191.3	18.3	60.9	44	2618
1100	Strong	174.6	190.2	17.5	60.7	45	-
1150	Weak	152.7	174.8	19.0	61.3	54	3383
1150	Strong	153.9	176.4	19.5	64.6	57	-

\*NOTE: Test direction is defined in terms of fracture path in specimen; i.e.,  
"Weak" = specimen fracture parallel to principal (or final) rolling direction;  
"Strong" = specimen fracture transverse to principal (or final) rolling direction.

Table 5  
Test Data for Specially Processed CEVM Proprietary Ni-Co Steel – Code G-99

Tempering Temperature (°F)	Direction of Test *	0.505-in.-Diam. Tension Test Data				Charpy V at 30° F (ft-lb)	Drop-Weight Tear at 30° F (ft-lb)
		0.2% YS (ksi)	T.S. (ksi)	El. in 2 in. (%)	R.A. (%)		
400	Weak	246.4	298.2	10.5	42.0	20	485
400†	Strong	203.0	290.8	12.0	40.5	20	-
500	Weak	234.2	274.7	10.3	42.9	15	573
600	Weak	224.0	252.1	10.5	43.1	15	309
700	Weak	210.9	230.8	10.8	45.0	18	573
800	Weak	200.2	215.9	12.5	45.4	18	-
900	Weak	197.5	210.0	13.5	48.5	18	612
1000†	Weak	186.9	206.7	15.0	48.2	23	811
1000†	Strong	187.7	206.4	14.5	45.9	23	-
1000‡	Weak	196.9	207.3	14.5	49.5	23	811
1000‡	Strong	196.0	206.1	14.0	46.5	23	931
1100	Weak	179.0	188.4	16.0	54.3	36	1601
475¶	Weak	192.0	234.0	14.0	55.3	27	1052
475¶	Strong	188.6	233.2	12.8	54.4	28	-

\*Test direction is defined in terms of fracture path in specimen; i.e., "Weak" = specimen fracture parallel to principal (or final) rolling direction; "Strong" = specimen fracture transverse to principal (or final) rolling direction.

NOTE: All steel normalized 1 hour at 1600°F, air-cooled, austenitized 1 hour at 1450°F, oil-quenched, refrigerated 2 hours at -110°F, tempered 2 hours, air-cooled, refrigerated 2 hours at -110°F, tempered 2 hours, and air-cooled, except:

†Austenitized 1 hour at 1450°F, oil-quenched, tempered 1000°F 2+2 hours, air-cooled;

‡Austenitized 1 hour 1450°F, oil-quenched, refrigerated 2 hours at -120°F, tempered at 1000°F for 2 hours, refrigerated 2 hours at -108°F, tempered 1000°F 2 hours, air-cooled;

¶Normalized 1 hour at 1600°F, air-cooled, austenitized 1450°F 1 hour, quenched in salt bath 475°F, hold 6 hours, air-cooled.

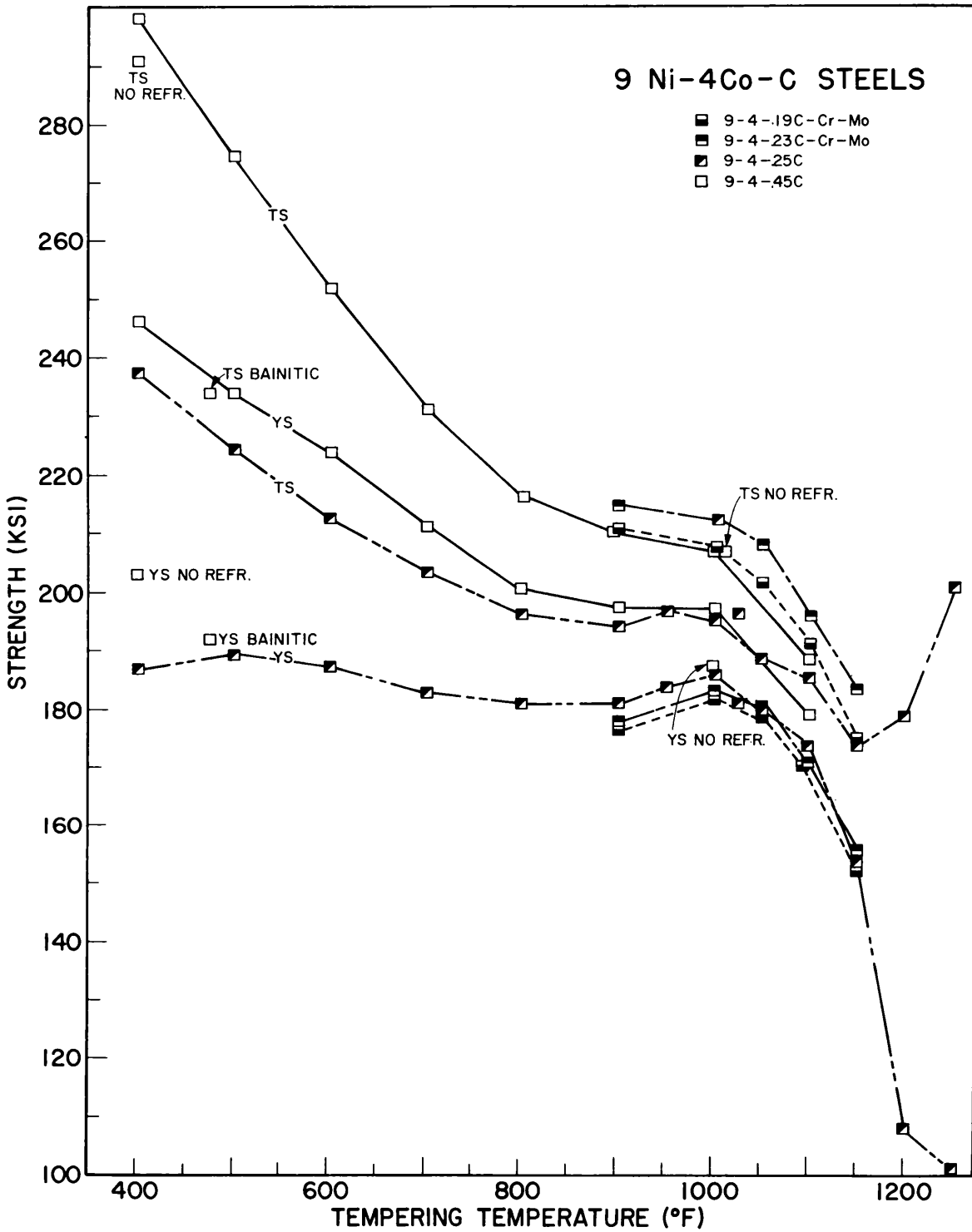


Fig. 4 - Yield and tensile strengths of 9Ni-4Co-.XXC steel plates as a function of tempering temperature

tempered at 900°F. Both UTS and YS values of the various 9-4-.XXC steels decrease continually with increasing temperatures from 1050° to 1150°F. The slight increase in UTS and large decrease in YS noted to be developed by the 9-4-.25 steel upon tempering at 1200° and 1250°F reflects the development and retention of untempered martensite as a result of exceeding the lower-equilibrium transformation temperature (reported to be approximately 1175° to 1200°F by the producer) for this steel.

The producer's recommendations for Q&T heat treatments of the 9-4-.XXC steels containing more than approximately 0.30% C require the use of refrigeration (to -100°F or lower) after quenching from the austenitizing temperature in order to achieve the maximum attainable strength levels. Such refrigeration treatments were employed to develop the data given in Fig. 4 for Q&T heat treatments of the 9-4-.45 steel. Q&T heat treatments of this steel without the refrigeration treatment were conducted for tempering temperatures of 400° and 1000°F. As noted in Fig. 4, the omission of the refrigeration treatment resulted in a greater loss in YS (approximately 45 and 10-ksi) than in UTS (approximately 8 and no change) for the 9-4-.45 steel tempered at 400° and 1000°F respectively.

For conventional Q&T steels, the maximum attainable as-quenched hardness (and consequently UTS) is dependent essentially upon carbon content. This general trend may also be expected for low tempering temperature conditions of 400°F, as noted in Fig. 4, where the UTS (and YS as well) of the basic 9-4-.45C steel exceeds that of the basic 9-4-.25C steel by approximately 60-ksi. At tempering temperatures ranging from 900° to 1100°F, however, the strength values of the basic high carbon 9-4 alloy are approximately 10-ksi higher than that of the basic 9-4-.25 steel. The general effects of the alloy additions made to promote secondary hardening characteristics in the 9-4 steels are noted for the strength values given in Fig. 4 for the 9-4-.19C-Cr-Mo steels and 9-4-.23C-Cr-Mo modified steels. Tempering of these steels in the range of 900° to 1100°F resulted in UTS values ranging slightly higher than that of the basic high carbon content (0.45%) alloy, however, the YS values are noted to be slightly lower than that of the basic low carbon content (0.25%) composition of the commercially-available 9-4-.XXC steels.

Figures 5 and 6 present a summary of the DWTT-YS and  $C_v$ -YS data given for the 9-4-.XXC steels in Tables 2 to 5, as referenced to the FTID-OMTL charts for 1-in.-thick steel plates presented in Figs.1 and 3. The high carbon content (9-4-.45C) alloy steel is noted to be capable of propagating fractures at elastic stress levels for all heat treatment conditions studied except that of Q&T 1100°F. For this heat treatment condition, however, the YS is noted to be below the 180-ksi minimum YS level developed by the basic 9-4-.25C alloy tempered as recommended by the producer at 1000°F. The apparently low DWTT values illustrated in Fig. 5 for the 9-4-.25C basic alloy (H-2) resulted from the thin section (13/16-in.) of this steel plate. The DWTT energy values obtained for this steel (No. H-2) are not included in the basic FTID chart for 1-in.-thick steels (Fig. 1). As noted from the  $C_v$ -YS data given in Fig. 6, the lower carbon content (0.19 and 0.23%), higher Cr-Mo content versions of the basic 9-4-.25C alloy exhibit slightly lower YS values and slightly lower  $C_v$  values than those obtained by the basic 9-4-.25C alloy at tempering temperatures of 1000°F and higher. The retention of untempered martensite as a result of tempering the basic 9-4-.25C alloy at temperatures of 1200°F and 1250°F is noted to result in significantly lower toughness levels as shown by the data given in Figs. 5 and 6.

#### DWTT OF 12% NICKEL MARAGING STEELS

The 12%Ni-5%Cr-3%Mo maraging steels comprise a new family of potentially high fracture toughness steel alloys capable of developing yield strengths ranging from approximately 150 to 200-ksi. The metallurgical characteristics of these steels have been described and test results for numerous 1-in.-thick plates, including exploratory explosion bulge tests of 180-ksi YS weldments, have been given in previous reports (11, 12, 13). These steels are virtually carbon-free compositions that may be strengthened by aging at temperatures up to 1000°F. The YS levels attained depend upon the alloy composition, aging time, and aging temperature. Additional 1 to 2-in.-thick maraging steel plates of compositions designed to develop nominal yield strengths of 160 and 180-ksi upon aging for 3 hours at 900°F were received for these studies. Some of these plates (Nos. H-83 and H-84) were from early air-melt heats of poor melting practice that resulted in relatively low  $C_v$  properties. These low fracture toughness plates were procured for special

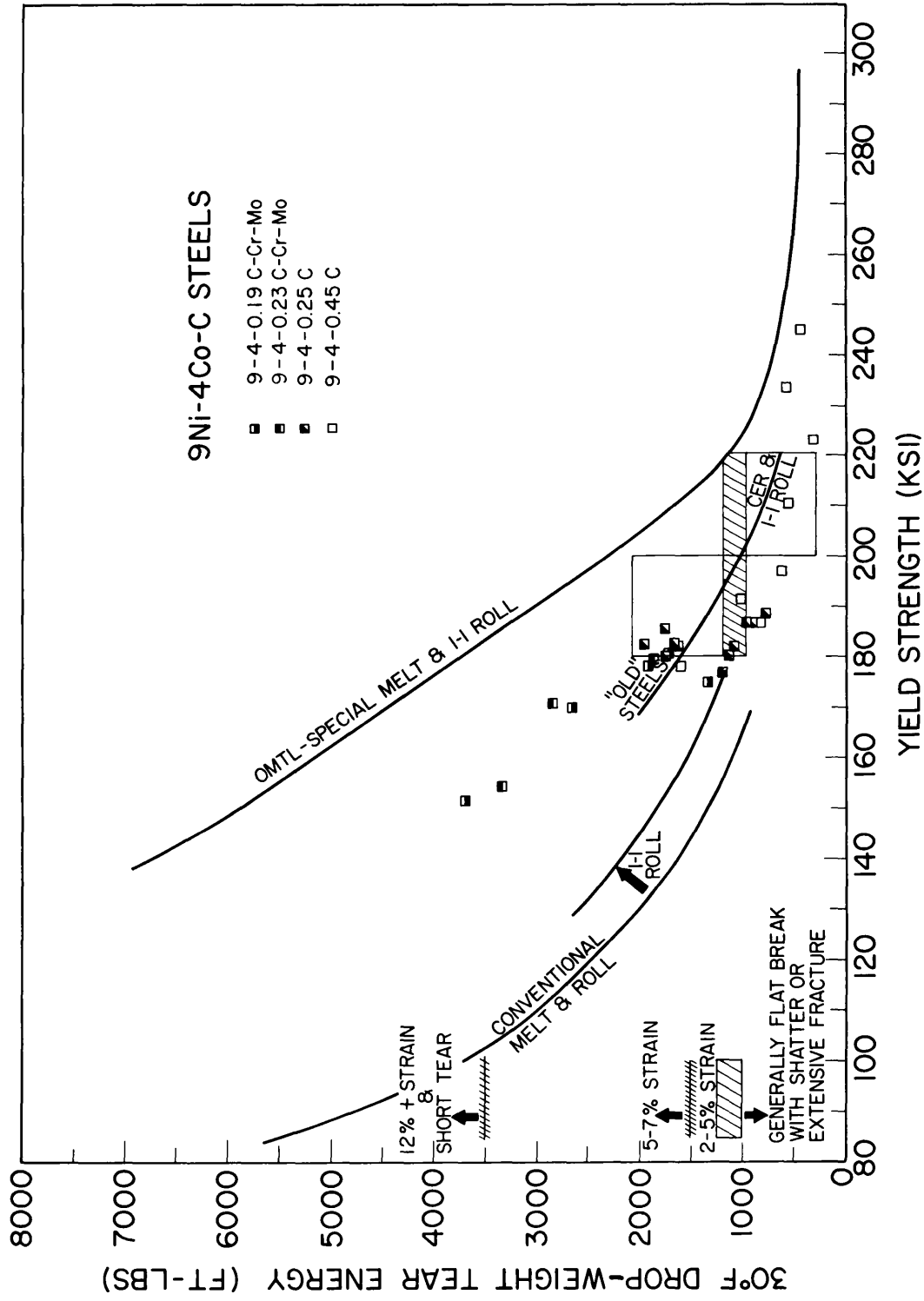


Fig. 5 - Drop-weight tear test energy relationship with Q&T yield strengths of 9Ni-4Co-.XXC steel plates. The OMTL of FTID charts are included for reference.

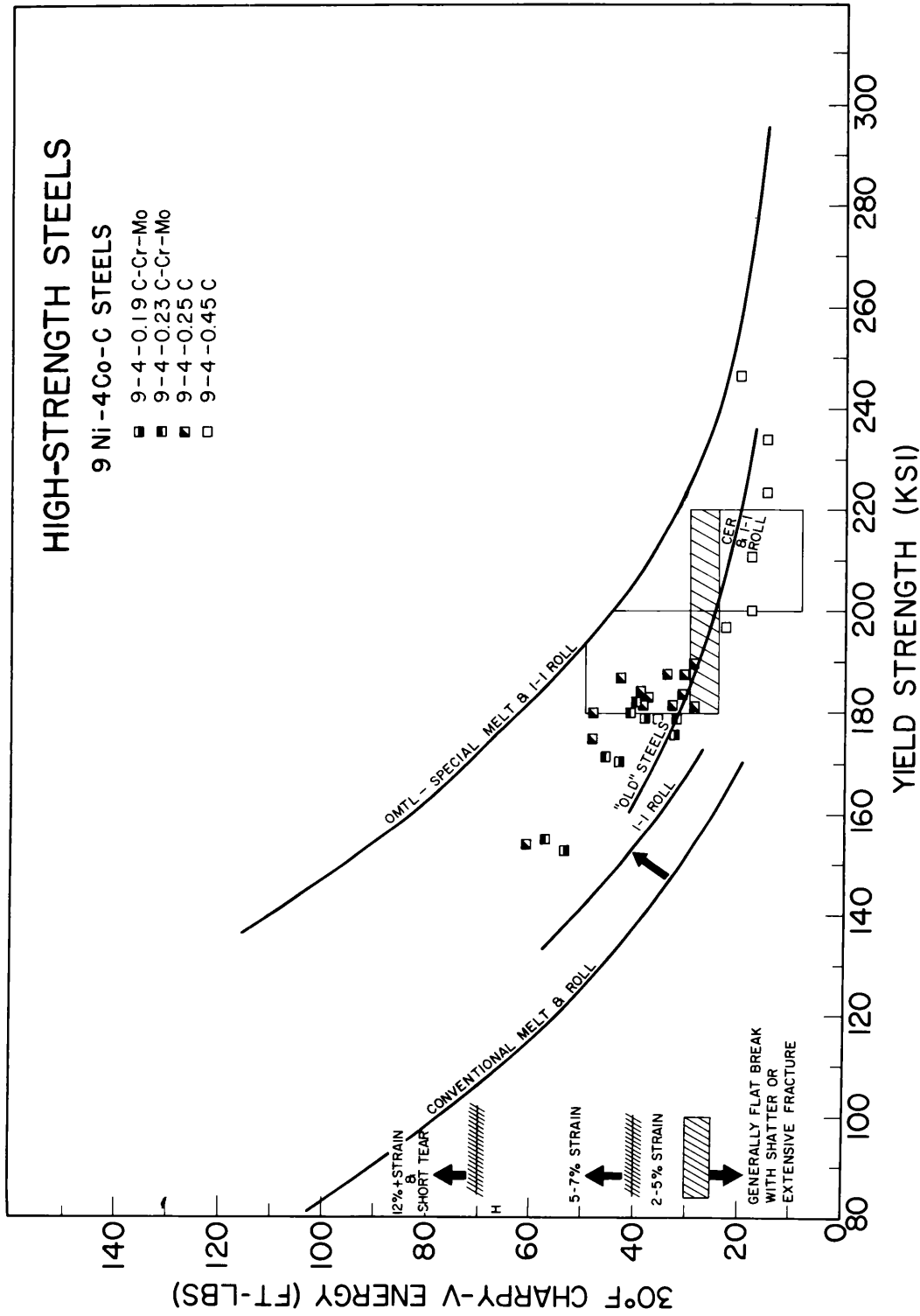


Fig. 6 - Charpy-V energy absorption relationships with Q&T yield strengths of 9Ni-4Co-.XXC steel plate material. The OMTL of FTID lines are included, as in Fig. 5.

studies of weld metal dilution effects and Robertson type crack-arrest tests to be conducted in cooperation with the Naval Construction Research Establishment Laboratories of the United Kingdom. Other plates (Nos. J-1 to J-10), expected to develop high fracture toughness properties, were from special melt practice heats consisting of vacuum-carbon deoxidation of vacuum-induction melts and consumable-electrode-remelting practices.

The chemical compositions and the test results obtained for these 12% Ni maraging steels are given in Tables 6 and 7. Figures 7 and 8 present a summary of the DWTT-YS and  $C_v$ -YS data for the 1-in.-thick maraging steels, as referenced to the FTID-OMTL charts for 1-in.-thick steels presented in Figs. 1 and 3. Similar data for the 2-in.-thick maraging steels are presented in Figs. 9 and 10. The latter steels were heat treated in full thickness but DWTT were conducted in 1-in.-thickness. The DWTT were conducted on material in the mill-aged condition or on material aged at 900°F for 3 hours at NRL. The numbered, connected points in Figs. 7 and 10 depict the changes in  $C_v$  energy and YS attained in aging these plates at 900°F for the number of hours shown. A data point for the recently developed 130/140 YS 5Ni-Cr-Mo-V steel is also included in Figs. 9 and 10 for comparison. It is noted that the special practice steels (Nos. J-1 to J-10) exhibit superior strength and toughness properties than those developed by similar steel compositions (Nos. H-88, H-94, and H-95) from air-induction melts. For YS levels ranging from approximately 160 to 185-ksi, the special melt practice steels develop properties that equal or exceed the best of the previously tested steels depicted by the limiting OMTL curve. In addition, the strength and toughness properties of the 2-in.-thick special melt practice steels are essentially identical to those of the best of the 1-in.-thick steels tested to date. Future tests are planned for full-thickness drop-weight tear tests of plate and weldments to be fabricated with these special melt practice maraging steels.

#### FRACTURE TOUGHNESS EVALUATION AND CONTROL OF HIGH STRENGTH WELD METALS

The DWTT provides a relatively simple method of assessing fracture toughness characteristics of full-thickness

Table 6  
Chemical Compositions of 12-5-3 Maraging Steel Plates

Steel	Mill Information	Composition (Wt.-%)									
		Ni	Cr	Mo	Ti	Al	C	Mn	P	S	Si
H83	1-1/2" Air Melt	12.0	3.94	3.22	.24	.30	.029	.05	.006	.006	.05
H84	1" Air Melt	12.1	3.87	3.05	.32	.35	.029	.10	.007	.010	.12
H88	2" Air Melt	12.1	4.31	3.05	.24	.42	.019	.04	.011	.007	.07
H94	1" Air Induct. Melt (150)	13.0	5.32	3.20	.12	.32	.019	.06	.006	.007	.11
H95	1" Air Induct. Melt (170)	12.5	5.47	3.35	.12	.32	.033	.08	.006	.007	.10
J1	2" VIMCD + CER (180)	12.1	4.83	3.00	.24	.24	.003	.03	.003	.007	.06
J2	2" VIMCD + CER (180)	12.1	4.83	3.00	.24	.24	.003	.03	.003	.007	.06
J3	2" VIMCD + CER (160)	12.1	4.96	3.10	.24	.24	.003	.03	.003	.007	.06
J4	2" VIMCD + CER (160)	12.1	4.83	3.10	.24	.24	.003	.03	.003	.007	.06
J5	1" VIMCD + CER (180)	12.1	4.83	3.10	.24	.21	.003	.03	.003	.007	.06
J6	1" VIMCD + CER (180)	11.8	5.08	3.30	.24	.14	.007	.04	.005	.007	.08
J7	1" VIMCD + CER (180)	12.1	4.83	3.10	.24	.22	.005	.03	.003	.007	.06
J8	1" VIMCD + CER (160)	11.8	5.16	3.30	.24	.13	.005	.04	.005	.007	.05
J9	1" VIMCD + CER (160)	12.1	4.77	3.10	.24	.22	.005	.03	.003	.007	.06
J10	1" VIMCD + CER (160)	12.1	4.80	3.10	.24	.21	.003	.03	.003	.007	.06

Table 7  
Test Data for 12-5-3 Maraging Steel

Steel No.	Anneal (° F)	Aged (° F-Hr)	Direction of test	0.505-in.-Diam. Tension Test				Charpy V at 30° F (ft-lb)	Drop-weight tear at 30° F (ft-lb)		
				0.2% YS (ksi)	UTS (ksi)	El. in 2 in. (%)	R.A. (%)				
H-84 1 in. Airmelt	Mill	900° - 3	Weak	177.7	183.4	14.3	53.7	28	-		
			Strong	-	-	-	-	34	-		
H-83 1-1/2 in. Airmelt	Mill	Mill 900° - 3	Weak	192.2	197.0	12.0	51.0	31	-		
	Mill	Mill+NRL 3-900°	Weak	192.9	198.6	12.0	51.9	29	-		
H-88 2 in. (180) Air IM	1500	900° - 1	Weak	158.0	164.6	15.5	61.5	63	-		
			Strong	157.7	163.8	16.5	63.6	63	-		
		900° - 3	Weak	162.7	169.4	15.8	60.4	56	3228		
			Strong	162.8	169.3	14.5	57.5	54	3228		
		900° - 7	Weak	167.4	173.4	15.0	61.4	57	-		
			Strong	167.1	173.1	14.5	59.3	57	-		
		900° - 15	Weak	172.7	177.9	15.0	61.5	56	-		
			Strong	172.2	179.1	15.0	61.4	53	-		
		900° - 30	Weak	179.5	184.9	15.3	61.4	49	-		
			Strong	177.8	184.0	15.0	61.0	48	-		
		900° - 50	Weak	179.2	187.2	15.3	60.1	43	-		
			Strong	180.5	188.8	15.5	60.0	44	-		
		H-94 1 in. (150)	1600	900° - 3	Weak	145.8	151.3	18.0	67.7	84	3964
					Strong	-	-	-	-	-	-
Weak	152.5				157.8	18.0	65.8	70	-		
H-95 1 in. (170)	1600	900° - 3	Weak	173.5	183.8	14.0	58.8	39	2384		
			Strong	173.2	183.6	14.8	60.3	47	-		
			Weak	178.7	187.0	14.5	59.6	39	-		
J-1 2 in. (180) VIMCD + CER	Mill	Mill	Weak	179.0	185.1	15.5	64.0	60	3436		
			Strong	-	-	-	-	67	-		
			Weak	187.2	190.4	15.5	63.5	62	3122		
J-2 2 in. (180)	Mill	Mill	Strong	-	-	-	-	65	-		
			Weak	170.5	175.5	16.3	66.0	72	3866		
J-3 2 in. (160)	Mill	Mill	Weak	162.8	170.9	16.0	64.4	67	3729		
J-4 2 in. (160)	Mill	Mill	Weak	176.2	185.3	13.5	58.3	67	3633		
			Strong	176.8	184.4	16.0	61.1	70	-		
J-5 1 in. (180)	Mill	Mill	Weak	184.4	190.0	13.5	55.7	58	3041		
			Strong	181.6	187.4	15.0	62.2	66	-		
J-6 1 in. (180)	Mill	Mill	Weak	181.5	188.5	14.5	62.3	66	3843		
			Strong	180.0	186.6	15.0	64.0	73	-		
J-7 1 in. (180)	Mill	Mill	Weak	162.6	170.6	15.8	64.1	84	4478		
			Strong	161.0	168.8	16.8	67.4	99	-		
J-8 1 in. (160)	Mill	Mill	Weak	162.5	170.9	16.0	64.5	77	-		
			Strong	162.0	170.2	17.0	66.5	94	-		
J-9 1 in. (160)	Mill	Mill	Weak	167.3	173.3	15.0	64.1	72	-		
			Strong	164.4	172.1	16.5	65.6	93	-		
J-10 1 in. (160)	Mill	Mill	Weak	-	-	-	-	-	-		
			Strong	-	-	-	-	-	-		



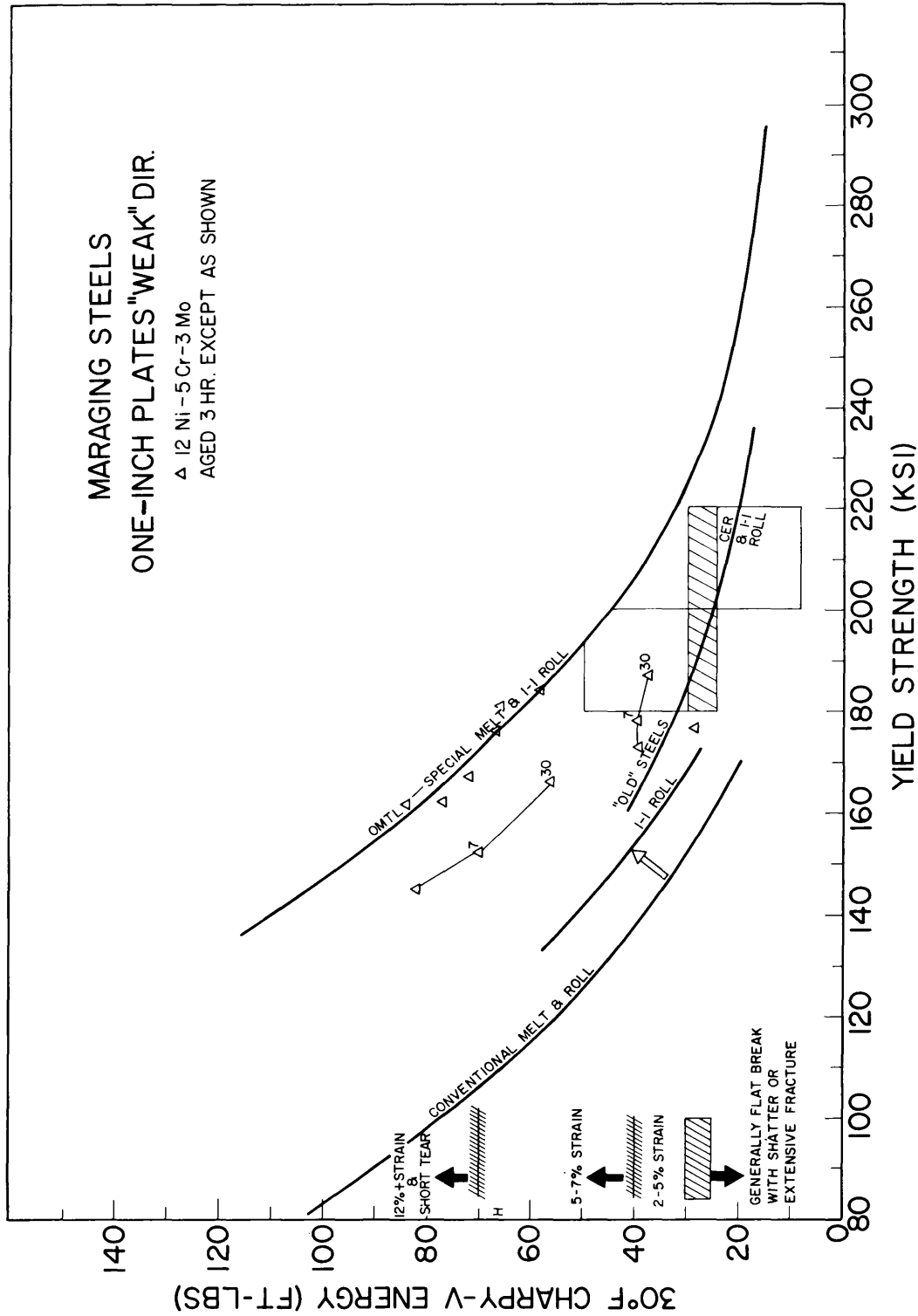


Fig. 8 - Charpy-V energy and YS relationships of 1-in. 12-5-3 maraging steel plates, mill heat-treated and further aged. The OMTL of FTID lines are included, as in Fig. 7.

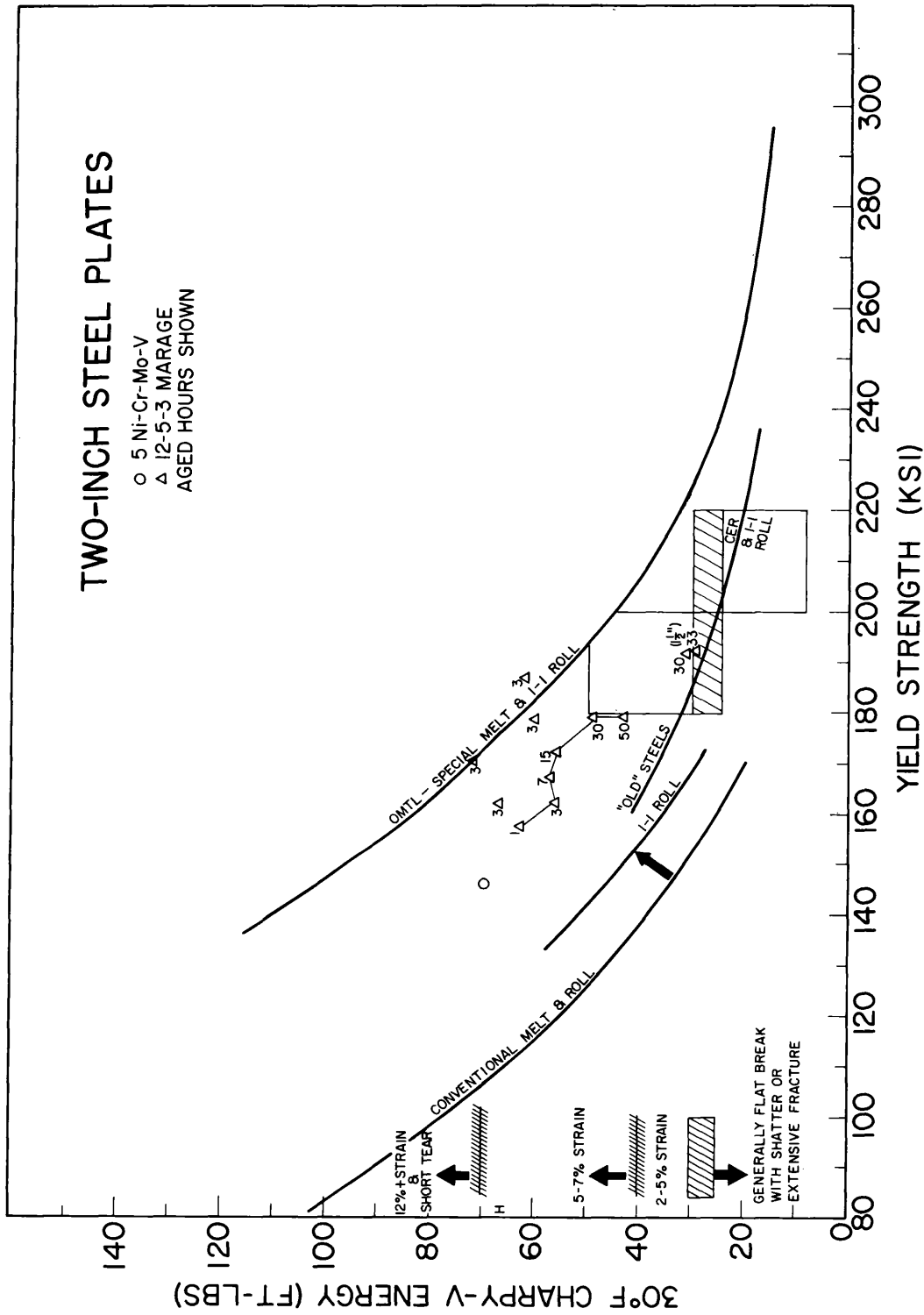


Fig. 9 - DWTT energy and YS relationships for 2-in. 12-5-3 maraging steel plates, mill heat-treated as 2-in. DWT. Tested in 1-in.-thickness for 1-in. steel plates. The OMTL of FTID lines and a similar 5Ni-Cr-Mo-V data point are included for reference.

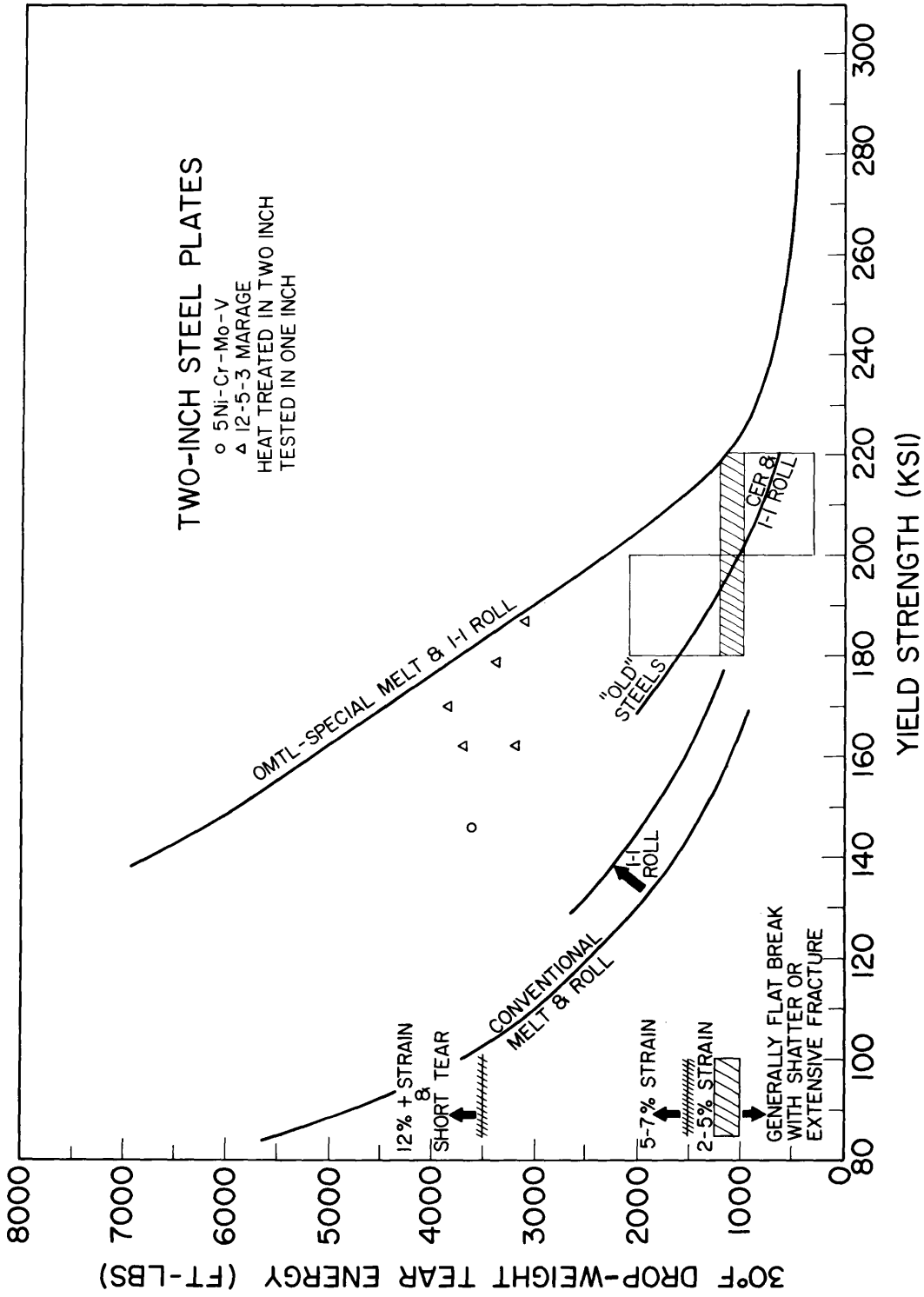


Fig. 10 - Charpy-V energy and YS relationships for 1-1/2 and 2-in. 12-5-3 maraging steel plates, mill heat-treated and further aged. The OMTL of FTID lines and a 5Ni-Cr-Mo-V point are included, as in Fig. 9.

weld deposits. Such tests were conducted and reported (8) for an experimental 1-in.-thick 130-ksi YS MIG weld metal of the type now used in the BuShips-USS HY-130/150 hull steel development program. The weld metal DWTT specimen is cut from a length of weldment prepared with specific welding procedures and alloys. An enlarged single "V" or single "U" joint preparation, back-chipped and rewelded uniformly to remove the root passes and base metal, is preferred in order to provide a width of weld metal sufficient to contain all of the fracture surface in the DWTT specimen. Double "V" joint preparation welds require a build-up of weld metal on the thickness faces of the steel plates prior to depositing the "test" weld to provide a similar width of weld. The brittle, crack-starter portion of the DWTT specimen, located on the central axis of the "test" weld, is confined to a narrow, embrittled, through-the-plate electron-beam weld, as shown in Fig. 11. An unalloyed titanium wire (1/16-in.-diameter  $\times$  2-in.-long), peened into a shallow groove (Fig. 11, top left), is diffused through the test weld by a single pass electron-beam weld, forming a hard and brittle alloy (Fig. 11, top right). The "V" notch side grooves (Fig. 11, bottom) are saw-cut along the embrittled weld to reduce initiation energy of the fracture to a reproducible low level similar to that required for plate DWTT specimens.

DWTT data for high strength steel welds are very limited at present because the weld wires have not been commercially available until very recently. Optimization studies (by the producers) of weld composition and procedures have invariably been based on results obtained with numerous small (approximately 30 to 100 lb) heats of different alloys that were produced in wire form only in quantities sufficient to evaluate conventional mechanical, toughness ( $C_v$ ), and bend test ductility properties of the weld deposits. Large tonnage heats of the optimized composition for MIG wire and stick electrodes developed for welding the 5Ni-Cr-Mo-V steel are reportedly available now as weld wire, and welding wire for the TIG process is being produced from 1/2-ton vacuum-melt heats of two new alloys developed for welding the 160-ksi and 180-ksi YS grades of the 12Ni-5Cr-3Mo maraging steels. Extensive drop-weight tear tests of weldments produced with these new electrodes are planned to evolve fracture toughness index diagrams (FTID) for the various weld metals in order to characterize the merits or disadvantages of different welding

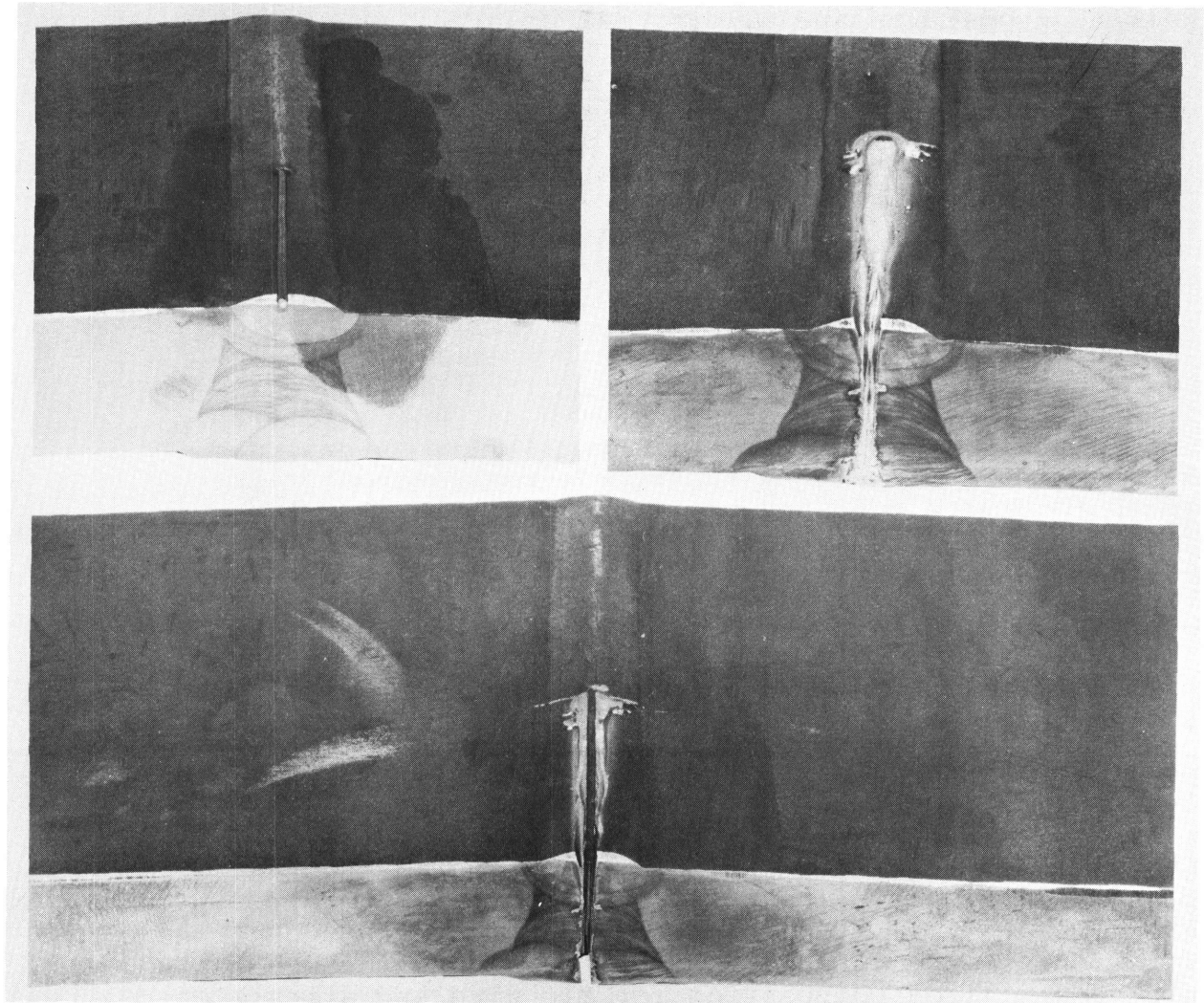


Fig. 11 - Electron-beam weld techniques for DWTT crack-starter in test TIG welds: above right, Ti wire peened into shaper groove; above left, electron-beam welded; lower, weld with sawed notches.

processes and procedures. The FTID charts for weld metals will then provide a frame-of-reference, or "yardstick", to evaluate the significance of  $C_v$  tests for welds in terms of whether elastic, or plastic, deformation is required for fracture propagation.

From limited DWTT data and fairly extensive  $C_v$  determinations for 1/2 to 1-in.-thick welds, it is possible to project preliminary weld metal FTID charts for the family of alloy compositions used for welding the 5Ni-Cr-Mo-V and the maraging steels. Figure 12 presents a summary of  $C_v$  energy values and YS relationships reported for the family of Ni-Cr-Mo and maraging weld metals (14,15,16) deposited in 1/2 to 1-in.-thick plates, as referenced to the FTID-OMTL chart for 1-in.-thick, high strength steel plates described in Fig. 3. The shaded areas in this figure were drawn to encompass the range of values developed by the best of the experimental weld metal compositions produced in each of the respectively designated families of weld metal alloys.

Generally, the data summarized in Fig. 12 indicate decreasing weld metal toughness with increasing weld metal strength. However, the strength level at which a given weld metal can be expected to sustain propagation of fracture at elastic stress levels is noted to vary for each characteristic family of weld metals within a generic alloy group. For example, the development of Ni-Cr-Mo MIG weld metals is noted to have progressed to a point where "as-deposited" weld with 130 to 140-ksi YS and high  $C_v$  values (approximately 100 ft-lb) at 30°F can be produced under laboratory conditions. A sharp change in fracture toughness with increasing strength level, denoted by the large arrow, for this weld metal family is indicated by the fact that "as-deposited" MIG welds of 150-ksi and higher YS values are reported to be highly brittle and highly susceptible to weld metal cracking. The "as-deposited" welds of the best of the covered "stick" electrode family of alloys are noted to be characterized by considerably lower  $C_v$  values at the 130 to 140-ksi YS level than that of the MIG process welds developed at this stage for joining the 5Ni-Cr-Mo-V steel plate. However, they are equally brittle and susceptible to weld cracking above 150-ksi YS. From the  $C_v$  data reported for "as-aged" TIG and MIG welds for the alloy compositions developed for welding the 12% Ni maraging steels, it is expected that 180 to 200+ ksi may prove to be the critical YS range in which these welds will change from a plastic to an elastic stress requirement for propagation of

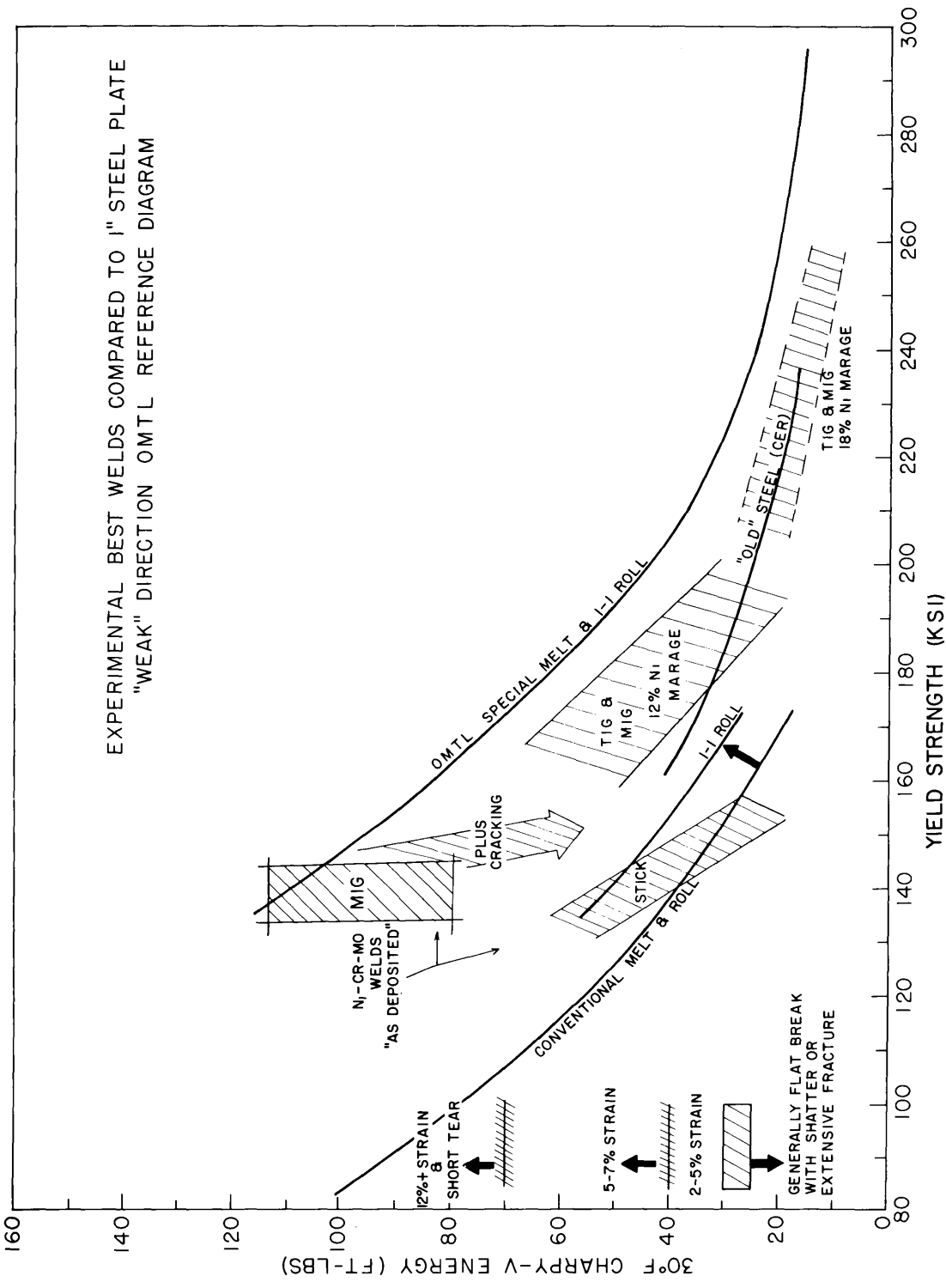


Fig. 12 - Summary of  $C_v$  energy value - yield strength relationships of experimental high-strength steel welds

fractures. The "as-aged" MIG and TIG welds developed for welding the higher strength level 18% Ni maraging steels apparently are all expected to sustain propagation of fractures at elastic stress levels.

The available  $C_v$  data for the 9-4-.XXC welds are not nearly as extensive as those reported above for the 5Ni-Cr-Mo-V and maraging steels, and projections of preliminary weld metal FTID charts for the 9-4-.XXC weld family are not considered warranted at this time. Intensive weld metal development studies for this alloy family are stated (by the producer) to involve evaluations principally of TIG process welds with wires produced from small (50 to 350-lb) vacuum-melt heats of alloys equivalent to or slightly modified from that of the basic 9-4-.25C alloy composition. Limited MIG process welds are stated to have shown lower strengths and  $C_v$  values than those obtained with the same wire compositions used for TIG welds. A summary of pertinent data reported for 9-4-.XXC welds by the producer (17) and the U.S. Naval Applied Science Laboratory (18), who received a small section ( $4 \times 8 \times 1-5/8$ -in.) of a producer-fabricated weldment of  $2-1/4$ -in. thickness, is given in Table 8.

Producer-fabricated TIG process weldments of 1-in.-thick 9-4-.20C + Cr-Mo modified plates were received by NRL for preliminary evaluation of DWTT,  $C_v$ , tensile, and stress-corrosion cracking (to be reported separately by Dr. B.F. Brown) tests. Details of the welding procedures and results obtained in this investigation are summarized in Table 9. The weld wire used for both weldments was stated to be the product of a 350-lb laboratory vacuum-melt heat of one of the more recently developed 9-4 weld metal compositions. As shown in Table 9, these welds were made with a large (37 to 38) number of passes. Although essentially identical conditions were reportedly used for all weld passes, significant differences were found between the hardness of the top surface (cover) beads from that of the center (filler) and bottom (back) weld passes. The lower hardness of the top surface passes (42/44  $R_C$  compared to 46/47  $R_C$  for filler and bottom weld beads) resulted in significantly higher  $C_v$  values (see Table 9) of specimens cut and prepared to evaluate  $C_v$  properties of the top and bottom sections of these welds. In essence, the lower hardness (and concomitantly lower strength) surface weld beads serve to act effectively as a high toughness

Table 8  
Properties of Gas Tungsten Arc (TIG) 9-4-.XXC Welds

Data Source	Wire type	Base plate (thick.)	Base plate (ksi)	Trans. Weld (ksi)	Charpy V temperature	Charpy V (ft-lb)	Remarks
Note (1)	9-4-.25C	1/2 in.	196.4	198.0	Room	25	Base metal fracture - adjacent to weld
Note (1)	9-4-.25C	1 in.	193.0	170.0	70° F	37	Single U joint
Note (1)	9-4-.25C	1 in.	189.4	171.6	70° F	41	Double U joint
Note (1)	9-4-.25C	1 in.	192.0	173.5	70° F	46	Single U joint
Note (1)	9-4-.20Cr-Mo	1/2 in.	184.0	177.3	70° F	64	
Note (1)	9-4-.20Cr-Mo	1/2 in.	195.9	182.4	70° F	46	
Note (2)	9-4-.20Cr-Mo	2-1/4 in.	-	189.5	32° F	54	
Note (2)	9-4-.25C	1 in.	-	~190.0*	32° F	26	

\*All weld metal tensile specimens from preliminary welds exhibiting porosity.

Note (1) "Welding of 9Ni-4Co Alloy Steels," 4th Maraging Steel Seminar, Dayton, Ohio, 1964.

Note (2) "Investigation of 9-4-.25 Weld Deposit," USNASL Memo No.8, Proj. 9300-1, 2 March 1965.

Table 9  
 Welding Conditions and Test Data for Producer  
 Fabricated 9-4-.20C-Cr-Mo TIG Welds

Process: TIG (Tungsten-arc, inert gas-shielded)  
 Shielding Gas: Argon  
 Filler Wire: 0.045-in.-diam.  
 Groove Design: Single U, 40° included angle, 3/16-in. radius and 1/8-in. land.  
 Amperage: 300  
 Voltage: 14.5 (J-18); 16.5-17.0 (J-17)  
 Speed: 4.5-ipm  
 Preheat: None  
 Interpass: 200° F  
 Passes: Filler 34; Cover 3; Back 3 (J-18)  
           Filler 35; Cover 3; Back 4 (J-17)

<u>No.</u>	<u>YS (ksi)</u>	<u>UTS (ksi)</u>	<u>% El.</u>	<u>R.A. (%)</u>	<u>30° Charpy V</u>	<u>Re</u>	<u>DWTT (ft-lb)</u>
J-17	197.9	220.0	18.0	54.1	Top 66 Bottom 41	42/44 46/47	2529

All weld metal 0.505-in.-diam. spec.

J-18					Top 63 Bottom 38	43/44 46/47	1935
------	--	--	--	--	---------------------	----------------	------

"cladding" on a lower toughness, higher hardness "core" material. The all-weld metal tensile data in Table 9 for weld No. J-17 are representative of the high hardness filler bead weld material. The relatively high DWTT values given for these welds in Table 9 depict an integrated energy absorption value for the full-thickness, "composite" weld metals. The enhanced toughness of the low hardness top surface weld beads are reflected in the DWTT fractures, Fig. 13, by the development of significantly wider shear lips than that developed by the higher hardness bottom (back) surface weld beads.

Figure 14 presents a summary of the  $C_v$  energy values and YS relationships given for 9-4-.XXC welds in Tables 8 and 9, as referenced to the FTID-OMTL chart for 1-in.-thick steel plates. The NRL data for weld Nos. J-17 and J-18 have been plotted to indicate the approximate  $C_v$ -YS relationships expected for the high hardness weld beads discussed above. Generally, the indicated properties of the more recently developed 9-4-.20C-Cr-Mo welds appear to be more promising for utilization in complex structures of the 9-4-.XXC high strength steels than is the case for the weld metals of the basic 9-4-.25C alloy composition.

It should be emphasized that essentially all of the data summarized in Figs. 12 and 14 represent properties developed for "experimental" weld wires in "laboratory" produced welds deposited in the most favorable "down-hand" position. These data should not be taken as necessarily representative of the expected properties in "out-of-position" (vertical or overhead) or "shop" produced welds. Weld metal properties are determined during the "act of welding" and retention of optimum characteristics of "laboratory" welds is expected to require a more exact duplication of controls and laboratory conditions for the high strength welds than has proved to be required in the past for low strength, structural steel welds. Such requirements point directly to the need for more rigorous control of welding procedures. This in turn points toward increased use of fully-automatic, positioned down-hand welding techniques for the high and ultrahigh strength steels. Additional tests to determine suitability and reproducibility with production lots of electrodes are required to establish fabrication confidence.

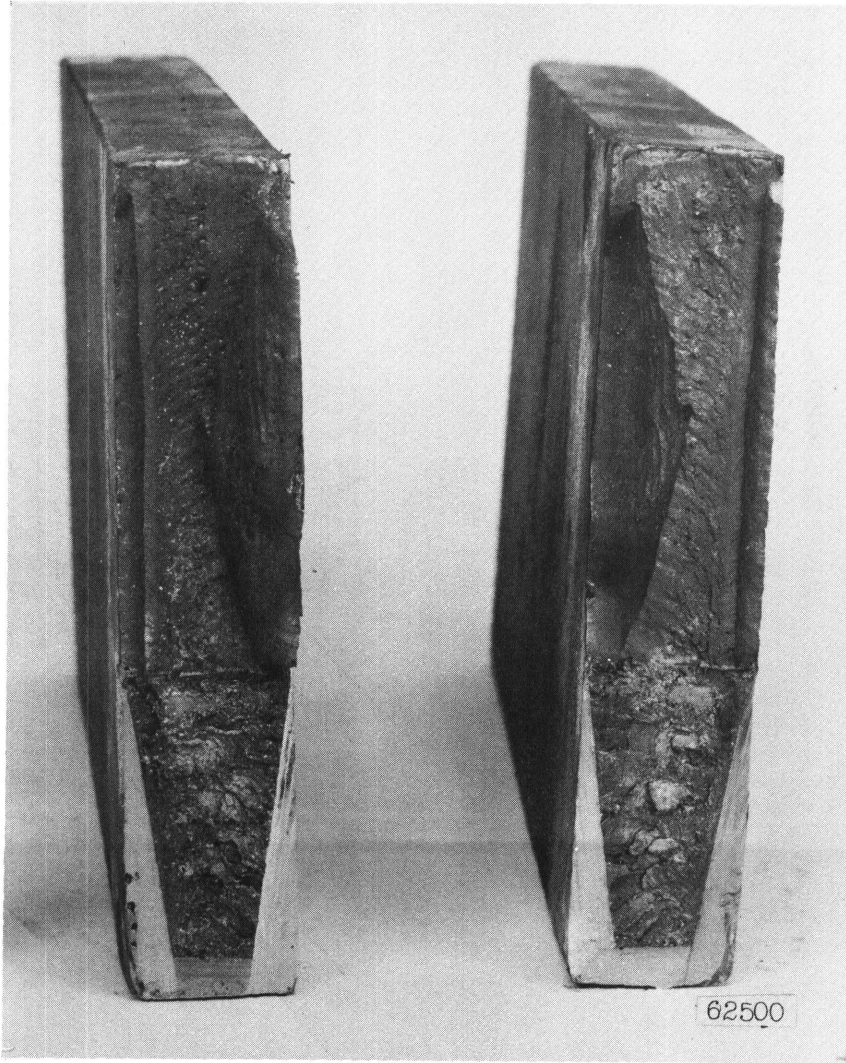


Fig. 13 - DWTT fracture faces of 9-4-.20C-Cr-Mo weld specimen illustrating significantly different amounts of shear lips developed on top (inside) and bottom (outside) surfaces of weld No. J-17

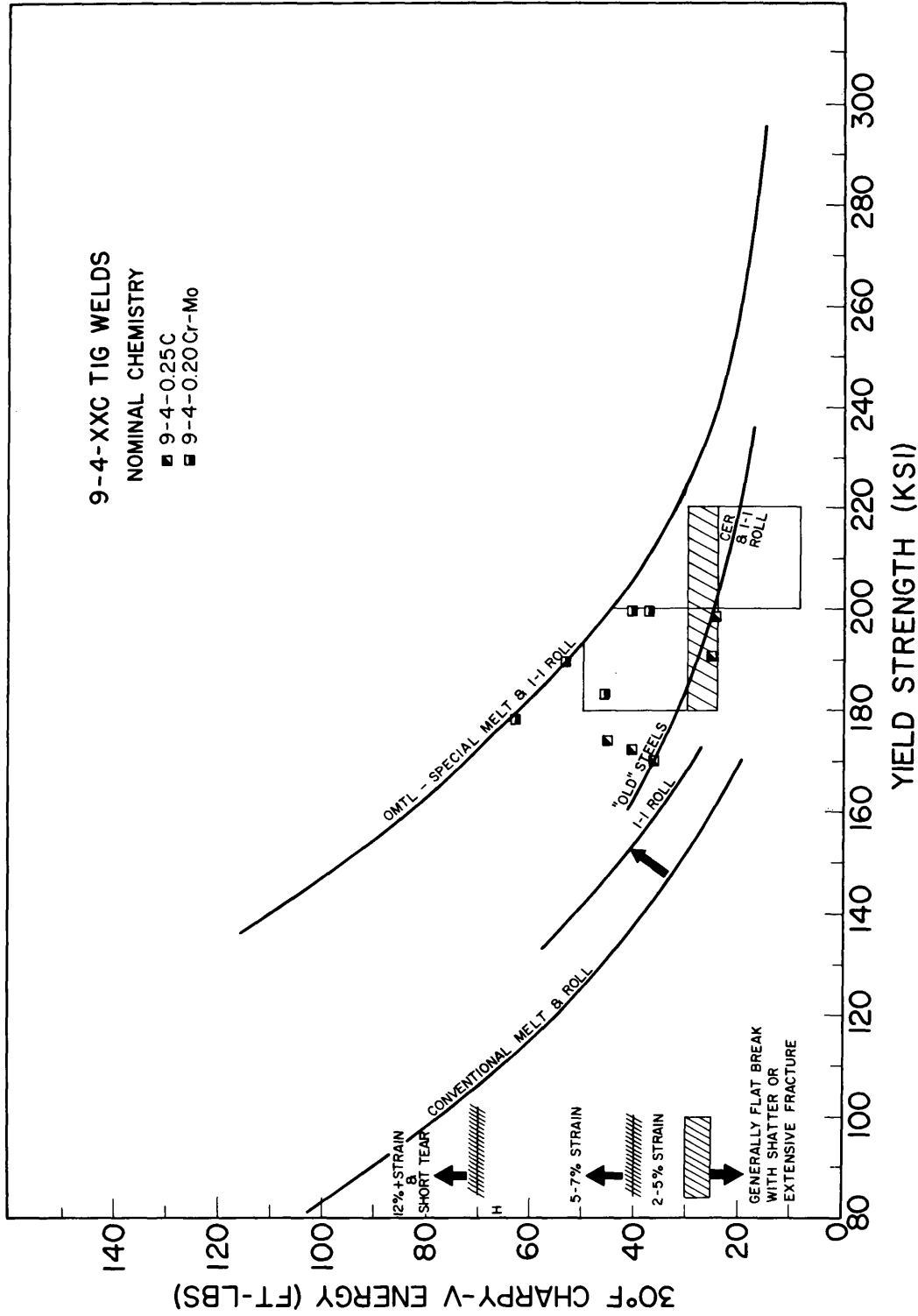


Fig. 14 - Summary of Cv energy value - yield strength relationships of 9-4-.XXC welds in plate

## TITANIUM ALLOYS

(R. J. Goode, R.W. Huber, D.G. Howe, and R.W. Judy, Jr.)

The broad scope investigation of titanium alloys in thick sections has included a wide variety of alloys. The program was begun in late 1962 and during this time the fracture toughness characteristics of thirty-one different alloys in 1-in.-thick plate have been determined. Many of them were studied in a variety of heat-treated conditions, interstitial levels (0.04-0.15+ oxygen), and in a few instances, under different conditions of processing. Also, a number of NRL special laboratory heats were studied in the "as-cast" condition as well as in the forged and rolled plate form. From these fracture toughness studies, a fracture toughness index diagram (FTID) for titanium has been developed which indexes the drop-weight tear test (DWTT) fracture toughness characteristics of the material in terms of the explosion tear test (ETT) performance. The ETT uses a large plate specimen incorporating a flaw, and as such, is considered a structural prototype element test. These tests are described in detail for titanium in reference 19.

### FRACTURE TOUGHNESS INDEX DIAGRAM FOR TITANIUM

The FTID for titanium is shown in Fig. 15. The spectrum of DWTT data, which has been the principle fracture toughness test used in evaluating titanium alloys, is presented for both the RW ("strong") and WR ("weak") fracture directions. Significance has been given to the DWTT energy values by indexing them to the ETT performance as indicated on the left side of the chart. As shown by the shaded band at 1500-1700 ft-lb DWTT energy, materials having DWTT energies below this level of fracture toughness are characterized by "flat breaks" and shattering in the ETT and thus would be expected to propagate fractures through elastic load regions. Above 1500-1700 ft-lb DWTT energy, plastic overloads are required for fractures to propagate; the relative level of DWTT energy is indicative of the relative level of plastic strain required to propagate fracture in the ETT. For example, above 2500 ft-lb DWTT energy over 5% plastic strain would be required and between 2000 and 2500 ft-lb DWTT energy, 3-5% plastic strain would be required.

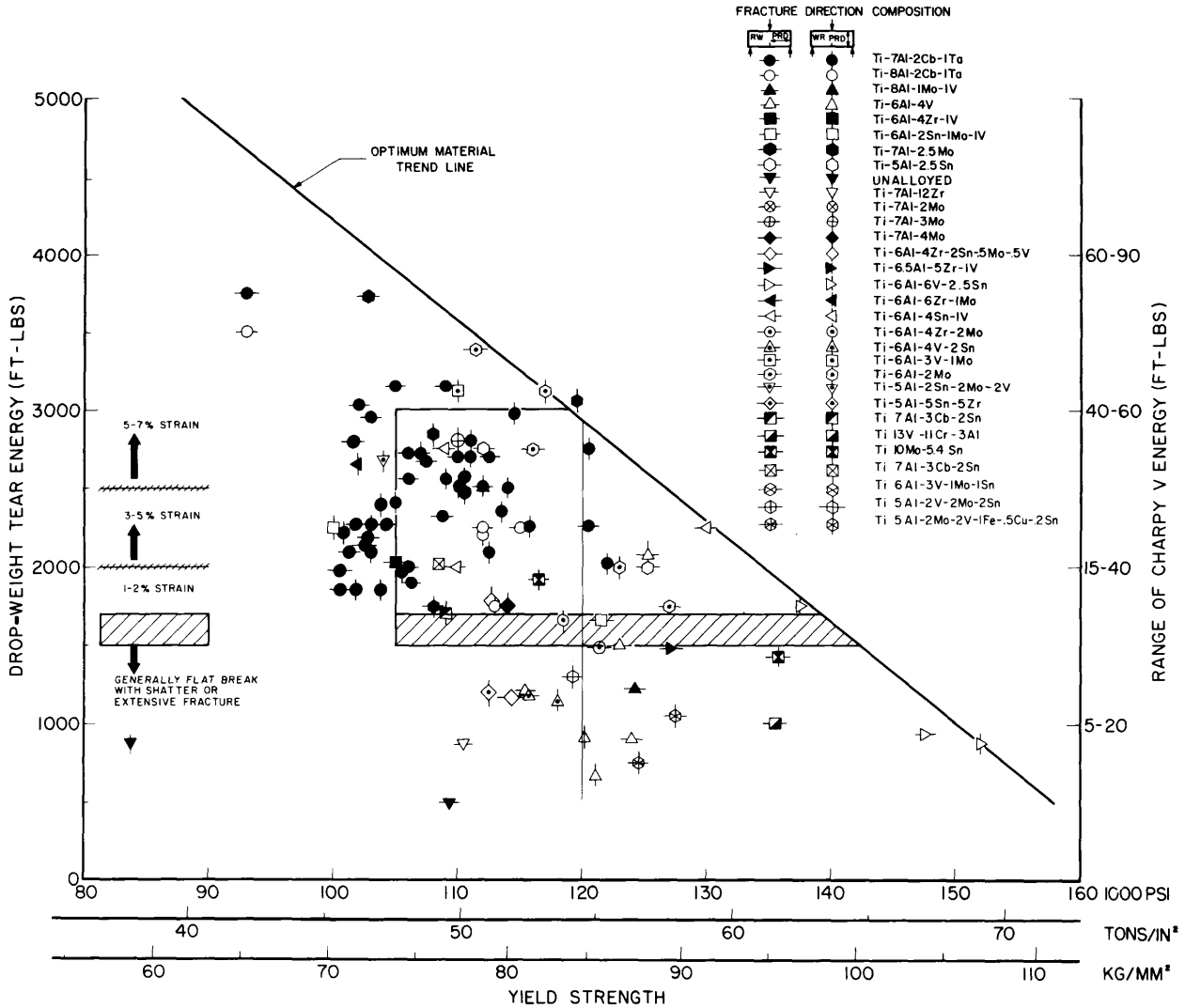


Fig. 15 - FTID for titanium alloys. 1-in.-thick titanium alloys showing correlation of DWTT, ETT, Cv, and YS. The OMTL indicates the highest level of strength for any given level of toughness.

The spectrum of DWTT data that has been obtained from the wide variety of titanium alloys in 1-in.-thick plate listed in Fig. 15, has also provided information concerning the expected maximum levels of toughness for different levels of yield strength (YS). This is shown by the optimum materials trend line (OMTL) in the FTID (Fig. 15) which is defined by both the RW and WR orientations. It is recognized that for titanium, processing variables play a very important role in developing whatever longitudinal and transverse properties the alloy plate may possess. For example, the FTID for steels (Fig. 1) clearly shows the significant movement of the OMTL to higher strength and toughness levels when 1 to 1 cross-rolling is employed instead of straightaway-rolling. The information necessary to "break out" effects of processing variables on the FTID chart have not generally been available; here we are concerned principally with ingot breakdown and rolling procedures since a special melt practice (vacuum-arc melting) is employed by the entire industry. Such a "break out" is needed if for no other reason than to provide a basis for determining the relative degree of improvement that new and different processing procedures may offer.

The cross-over of the elastic to plastic performance band with the OMTL indicates that above about 140-ksi YS, all materials should be expected to propagate fractures through elastic stress regions. However, as more data is obtained for materials above the 140-ksi YS and the OMTL established for the highest possible strengths, the YS limitation for fracture propagation requiring plastic overloads as presented in the FTID, may shift to a higher strength than the 140-ksi shown. Below 120-125-ksi YS, most alloys should be expected to require plastic overloads for fractures to propagate--provided they are of low interstitial content. Between 120-125-ksi and 140-ksi YS, the degree of optimization will determine whether elastic or plastic loads are required to propagate fractures.

#### ALLOY DEVELOPMENT STUDIES

Two double vacuum-arc melted titanium alloy ingots (9-in.-diameter × 12-in.-long, weight 115-lb) prepared at NRL using electro-refined titanium were forged and rolled into 1-in.-plate at a commercial concern. The alloy compositions 6Al-2Mo-2V-2Sn (T-80) and 6Al-3Mo-1V-2Sn (T-81) were aimed at the 130-ksi YS level in the

heat-treated condition. Forging breakdown temperatures were 2100-2200°F. The hot-rolling temperatures were 1900°F at the start of rolling and in the order of 1650°F for finishing at 1-in. gage.

The DWTT energy values of the as-rolled T-80 and T-81 plates were 1418 and 1326 ft-lb respectively. Water-quenching from 1625°F (approximately 150°F below  $\beta$  transus) followed by aging at 1400°F for 1-hr., then air-cooling, increased the respective DWTT energy values to 1540 and 1356 ft-lb. A solution heat treatment at a temperature just below the  $\beta$  transus, followed by oil-quenching and aging at 1200°F, resulted in severe embrittlement of both of these alloys as indicated by the low DWTT energy values of 455 (T-80) and 339 ft-lbs (T-81). Additional solution anneals and aging treatments will be conducted with these alloys in order to determine the heat treatments required to produce the optimum combinations of strength and toughness. Tensile properties resulting from the above heat treatments are in the process of being obtained and will be reported in a future report.

Drop-weight tear tests of a Ti-2.5Al-16V, all  $\beta$  alloy, in the as-received forged condition, showed this material to be of low fracture toughness (573 ft-lb DWTT energy). A 1400°F anneal followed by air-cooling resulted in an even lower DWTT energy value (310 ft-lb). Furnace-cooling instead of air-cooling from 1400°F did little to improve the DWTT energy (600 ft-lb) over that obtained for the as-received material. At these levels of DWTT energy, this material would be expected to propagate fractures through elastic stress regions; as such they would be considered of little use for heavy-wall structures.

#### WELDING STUDIES

As previously reported, the DWTT energy values obtained for two MIG welds in as-received Ti-6Al-2Mo (T-22) plate were 1500 and 1662 ft-lb (9). The fracture toughness of these welds were increased to 1966 ft-lb DWTT energy by a solution-anneal and aging treatment. This is comparable to the 2000 ft-lb DWTT energy of the as-received base plate. A similar heat treatment of the base plate increases its DWTT energy value to 2800 ft-lb, and an electron-beam weld in this plate had a DWTT energy of 2026 ft-lb. Previous electron-beam welds in the as-received Ti-6Al-2Mo plate had less than half this DWTT value.

The response of 1-in.-thick Ti-7Al-2.5Mo alloy to heat treatment and welding is being investigated. The as-received DWTT energy of 1800 ft-lb can be increased by a solution heat treatment below the  $\beta$  transus temperature. DWTT energy values between 2800 and 3000 ft-lb have been measured for plates heat treated between 1700-1800°F, followed by aging for 2 hrs. at 1100°F. Electron beam weldments of the as-received plate give DWTT energy values of 1400 ft-lb, indicating a slightly embrittled weld zone.

Through the cooperation and courtesy of the Linde, Newark Laboratories, "Plasmarc" welds were made in 1-in.-plate samples of the 7Al-2.5Mo and the 6Al-4V titanium alloys. A fusion pass through a 7/16-in. butt joint was followed by a filler pass in the remaining 60° included angle "V" joint. The bottom surface of the weld--shown in Fig. 16--is 3/16-in.-wide, has a slight crown, and displays excellent fusion characteristics. The top of the weld--Fig. 17--is quite smooth, has no undercutting at the edges, and also has a slight crown. DWTT energy values of 1540 and 1418 ft-lb were measured respectively for the 7Al-2.5Mo and the 6Al-4V titanium alloys as welded. Similar weld sections of both alloys annealed for 1 hr. at 1600°F and air-cooled resulted in a slight decrease in fracture toughness.

A systematic approach to study the effect of heat treatment towards improving the fracture toughness of welds in four titanium alloys of interest was completed. Through penetration electron beam welds 10-in.-long into back-up strips were prepared in the following 1/2-in.-thick titanium alloy plates: 6Al-4V, 5Al-2.5Sn, 7Al-2Cb-1Ta, and 6Al-2Mo. These plates were then sectioned and Charpy V ( $C_v$ ) specimens were prepared with the weld bead transverse to the bar and with the V-notch being centered along the top surface of the weld. Typical weld cross-sections are shown in Fig. 18.  $C_v$  test data at -80°F and +32°F are shown for the welds in Table 10 along with the  $C_v$  energy values for the base plate and the heat treatments given each alloy. The fracture toughness of the 6Al-4V weld section is improved by a short term annealing treatment at 1600°F, however, it does not respond as well as the base plate. The all alpha 5Al-2.5Sn alloy shows better weld fracture toughness properties than the base plate for the heat treatments employed.

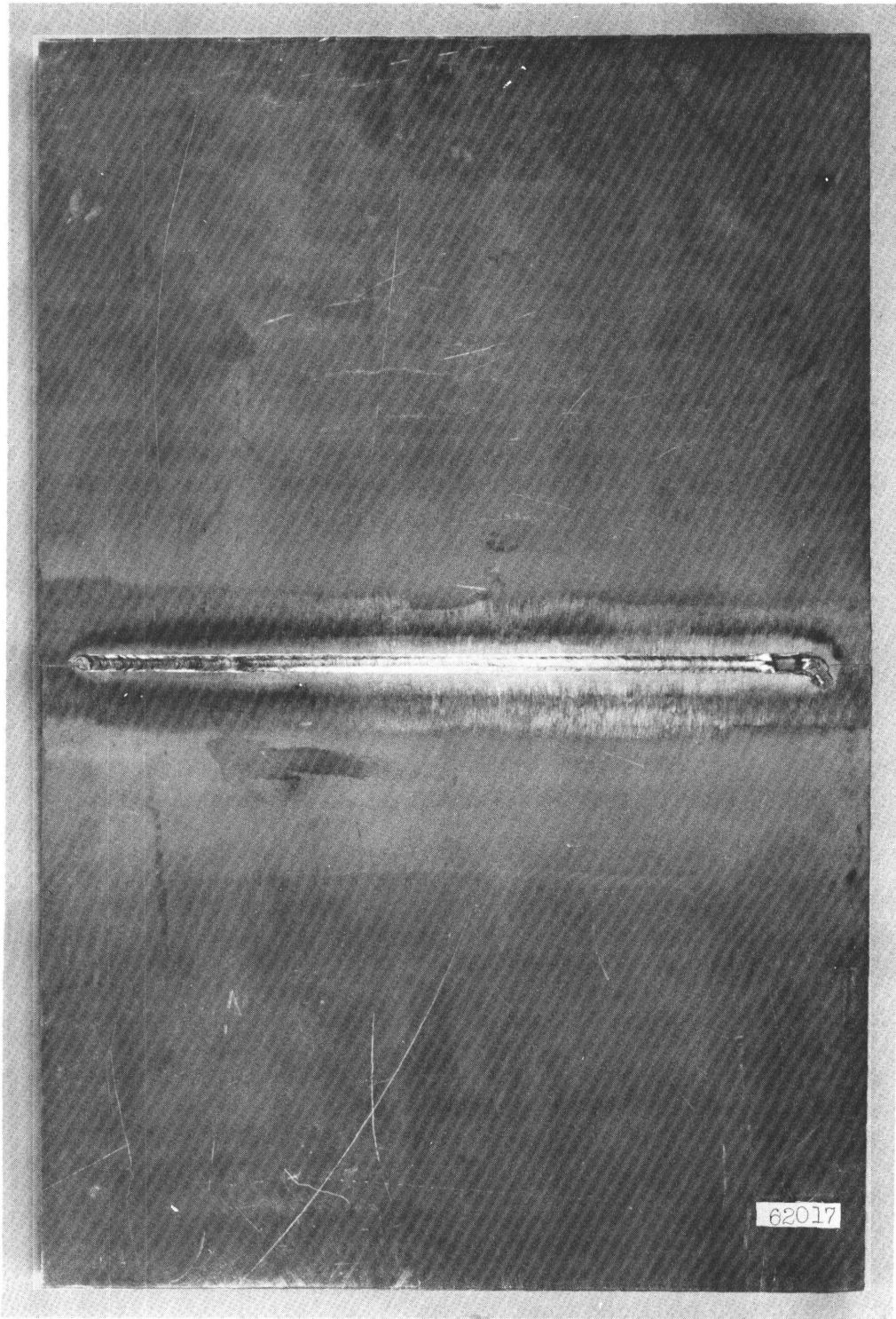


Fig. 16 - "Plasmarc" weld in a 1 x 11 x 17-in. Ti-7Al-2.5 Mo alloy plate; bottom view of fusion pass of the weld

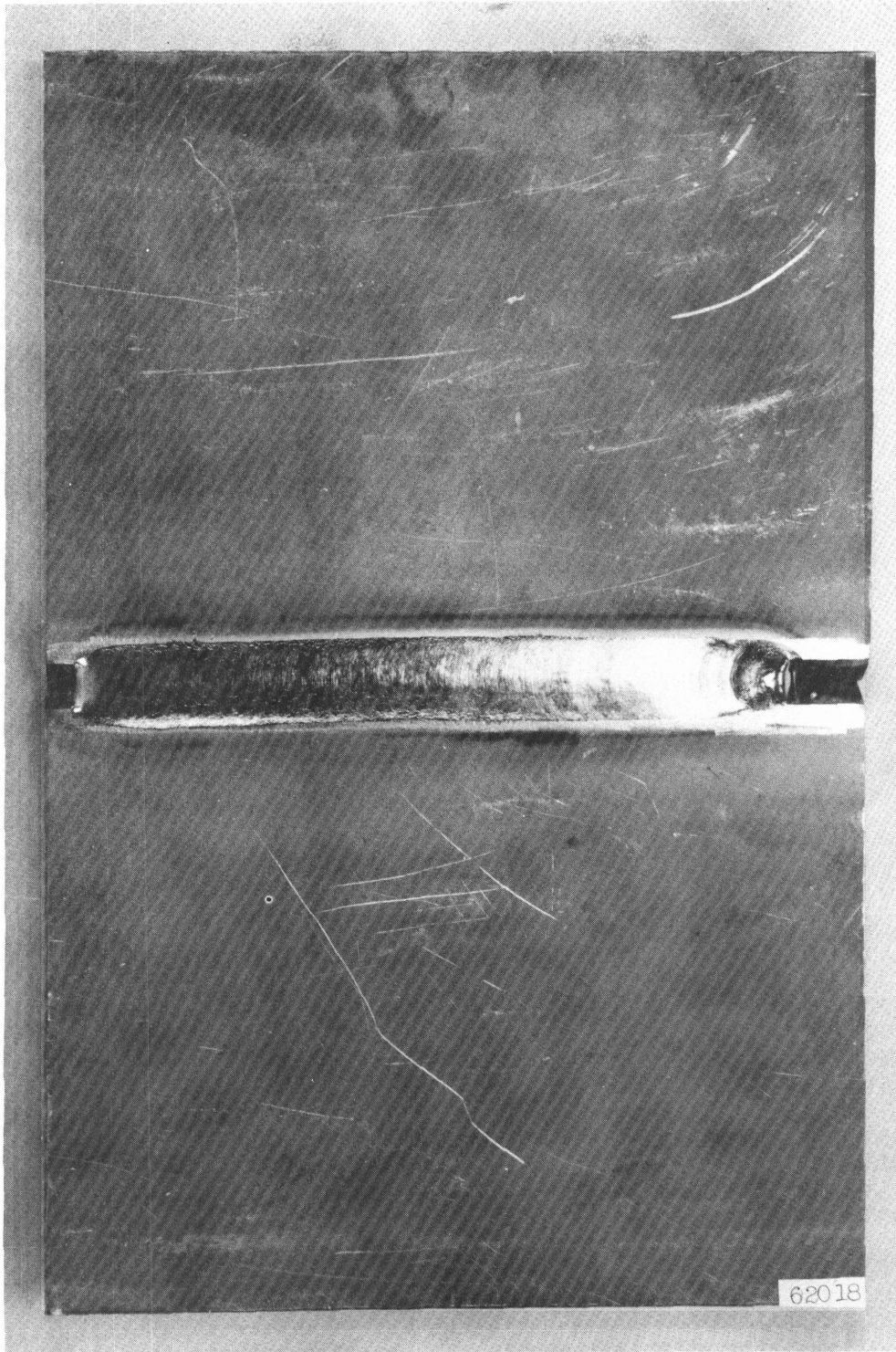


Fig. 17 - "Plasmarc" weld in a 1-in.-thick Ti-7Al-2.5Mo alloy plate; top view of surface of the weld

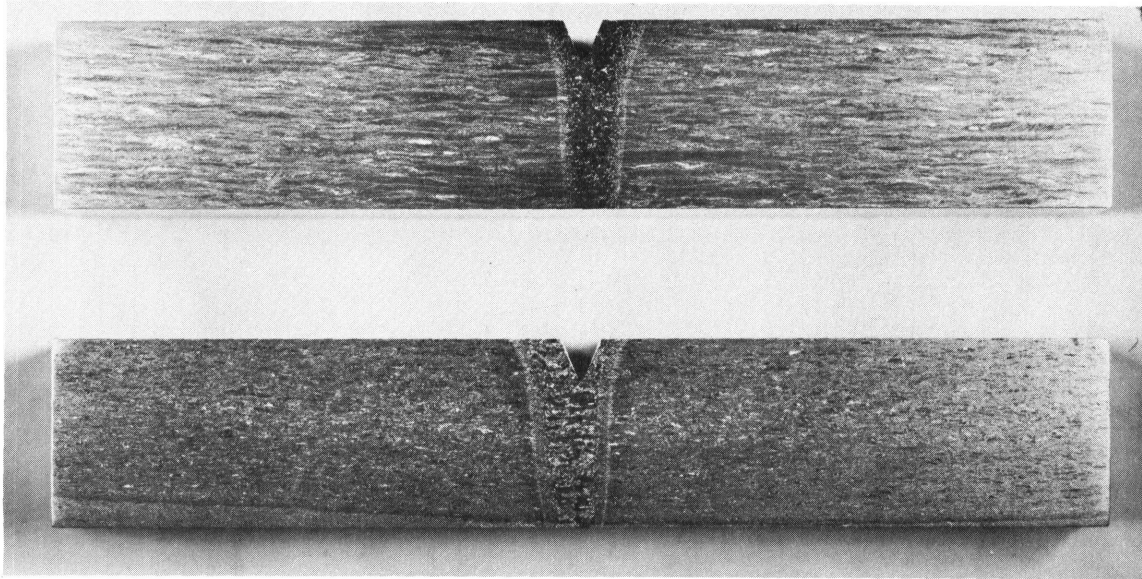


Fig. 18 - Examples of notch location in Charpy V specimen for determining the fracture toughness of electron-beam welds

Table 10  
Charpy V Data for 1/2-in. Titanium Alloy Electron Beam Welds

Alloy	Nominal Composition	Heat Treat Condition	E. B. Welds (ft-lb)		Base Plate (ft-lb)	
			-80° F	+32° F	-80° F	+32° F
T-56	Ti-6Al-4V	As-received plate	18	25	22	25
T-56	Ti-6Al-4V	Annealed 1500° F/1 hr/AC	17	22	22	28
T-56	Ti-6Al-4V	Annealed 1600° F/1 hr/AC	20	28	26	35
T-56	Ti-6Al-4V	Annealed 1650° F/1 hr/AC	20	28	-	-
T-57	Ti-5Al-2.5Sn	As received plate	34	44	20	28
T-57	Ti-5Al-2.5Sn	Annealed 1400° F/1 hr/AC	30	38	20	35
T-57	Ti-5Al-2.5Sn	Annealed 1400° F/1 hr/WQ	32	40	-	-
T-57	Ti-5Al-2.5Sn	Annealed 1500° F/1 hr/AC	30	41	25	27
T-58	Ti-7Al-2Cb-1Ta	As-received plate	36	46	45	58
T-58	Ti-7Al-2Cb-1Ta	Annealed 1500° F/1 hr/AC	22	33	47	64
T-58	Ti-7Al-2Cb-1Ta	Annealed 1600° F/1 hr/AC	25	36	65	77
T-58	Ti-7Al-2Cb-1Ta	Annealed 1600° F/1 hr/AC & aged 2 hr/1100° F	18	28	-	-
T-59	Ti-6Al-2Mo	As-received plate	30	38	26	32
T-59	Ti-6Al-2Mo	Annealed 1600° F/1 hr/AC	34	40	32	46
T-59	Ti-6Al-2Mo	Annealed 1750° F/1 hr/AC	31	36	-	-
T-59	Ti-6Al-2Mo	Annealed 1750° F/1 hr/AC & aged 2 hr/1100° F	27	32	-	-

The properties of the 7Al-2Cb-1Ta alloy welds are degraded by the selected heat treatments; however, the base plate shows some improvement.

Comparative weld and base plate improvements were noted for the 6Al-2Mo alloy.

Both of the last two alloys show a decrease in fracture toughness associated with the aging reaction at 1100°F.

Specimens of MIG spray and MIG short-circuit butt welds in 1-in.-thick Ti-7Al-2Cb-1Ta alloy plate, welded at the U.S. Naval Applied Science Laboratory, were subjected to the NRL DWTT. Energy absorption values of fractures running through the weld metal were as follows:

	<u>Spec. No.</u>	<u>DWTT</u>
Short Circuit MIG Weld. . .	SCW T-1 . . .	2958 ft-lb
	SCW T-2 . . .	3013 ft-lb
Spray Arc MIG Weld. . . .	SAW T-1 . . .	2958 ft-lb
	SAW T-2 . . .	2930 ft-lb

These values are equivalent to the 2800-3200 ft-lb DWTT of the base plate in the WR and RW directions. The fracture shear lips were within the weld metal but approach the area between the fusion and heat-affected-zones. Only scattered minor defects were discernible on the fracture surfaces.

Three high strength titanium experimental alloys (>135-ksi YS), prepared by New York University and submitted through the U.S. Naval Marine Engineering Laboratory, were tested at NRL for notch fracture toughness. The DWTT energy values, composition, heat treatments, and yield strengths, are listed in Table 11.

#### HEAT TREATMENT STUDIES ON SOME TITANIUM ALLOYS

Heat treatment studies have been continued on a number of titanium alloys in order to develop information on the stability of the alloys and to determine the heat treatments which will produce an optimum combination of strength and toughness.

The effects of the heat treatments studied to date on the tensile and fracture toughness (as measured by the  $C_v$  and

Table 11  
 Properties of Some NYU Experimental High-Strength Titanium Alloys

Alloy*	Nominal Composition	Solution Heat Treatment	Aging Heat Treatment	DWTT (ft-lb)	YS (0.2%) (ksi)
T-84	Ti-6Al-3V-1Mo-1Sn	1650° F/2-1/2 hr/WQ	1300° F/1 hr/AC	1052	128
T-84	Ti-6Al-3V-1Mo-1Sn	1650° F/2-1/2 hr/WQ	1300° F/1 hr/AC	1052	-
T-85	Ti-5Al-2V-2Mo-2Sn	1675° F/2 hr/WQ	1350° F/1 hr/AC	1478	119
T-85	Ti-5Al-2V-2Mo-2Sn	1675° F/2 hr/WQ	1350° F/1 hr/AC	1296	-
T-86	Ti-5Al-2V-2Mo-2Sn-1Fe-.5Cu	1400° F/4 hr/AC		750	125
T-86	Ti-5Al-2V-2Mo-2Sn-1Fe-.5Cu	1400° F/4 hr/AC		750	-

\*The composition of two of these alloys is similar to NRL heats T-80 and T-81.

DWTT) properties of the alloys Ti-6Al-2Mo (T-22) and Ti-7Al-2.5Mo (T-71) are shown in Table 12. The Ti-6Al-2Mo alloy is capable of developing a high level of fracture toughness, around 120-ksi YS. This is seen in Table 12 from both the  $C_v$  and DWTT data obtained for the 1750°F solution anneal and 1100°F aging treatment on the DWTT specimens. The DWTT energies of well over 3000-ft-lb indicate that a plastic strain of over 5% would be expected for fracture propagation (9). It can also be seen that the properties obtained for the Ti-6Al-2Mo alloy are somewhat dependent upon specimen size. The tensile and  $C_v$  specimens are considerably smaller than the DWTT specimens (1 x 5 x 17-in.) and the lower  $C_v$  energy accompanied by the slightly higher YS values obtained for the smaller heat-treated specimens, compared to the properties obtained for the heat-treated DWTT specimens, could possibly be the result of faster cooling during quenching.

The  $C_v$  data indicate that the same level of fracture toughness that was developed in the Ti-6Al-2Mo alloy can also be developed in the Ti-7Al-2.5Mo alloy, using similar heat treatments. Also, it appears that the Ti-7Al-2.5Mo alloy may be relatively insensitive to section size compared to the Ti-6Al-2Mo alloy. This is indicated by the 1700°F/1 hr/AC solution anneal, 1100°F/2 hr/WQ data.

An effect common to both the Ti-6Al-2Mo and Ti-7Al-2.5Mo alloys is the considerably lower fracture toughness which develops when given a solution anneal above the beta transition temperature. The severity of this effect can be seen for the Ti-7Al-2.5Mo alloy by comparing the  $C_v$  values obtained for solution anneals above the  $\beta$  transus temperature (1850°F) against those values obtained for the solution anneals approximately 50°F below the transus. [Data for the Ti-6Al-2Mo (T-22) alloy was presented in an earlier report (20).] The DWTT energy values increased about 100% when the alloy was heat treated 50°F or more below the  $\beta$  transus.

Figures 19-25 illustrate the  $C_v$  notch properties of RS-70--unalloyed titanium (T-17)--and the alloys Ti-5Al-2.5Sn (T-18), Ti-6Al-4Sn-1V (T-20), Ti-6Al-6V-2.5Sn (T-21), Ti-8Al-2Cb-1Ta (T-23), Ti-6Al-4V (T-27), and Ti-7Al-2Cb-1Ta (T-74) in the conditions specified. It should be noted that the data for several of these alloys are for heat treatments that resulted in very high yield strengths.

Table 12  
The Effect of Heat Treatments on the Mechanical Properties of the Alloys Ti-6Al-2Mo (T-22) and Ti-7Al-2.5Mo (T-71)

Nominal Composition	Solution Heat Treatment	Aging Heat Treatment	Cv Notch Energy (32° F) (ft-lb)		Yield Strength (0.2% offset) (psi)	Ultimate Tensile Strength (psi)	Elong. (%)	R.A. (%)	DWTT Energy (+30° F) (ft-lb)
			(RW)	(WR)					
T-22 (Ti-6Al-2Mo)	1750° F/1 hr/AC	1100° F/2 hr/WQ	58.0	60.0	122,000(L)(est)	124,000(T)	13.6	38.1	3729(RW)†
	1750° F/1 hr/AC	1100° F/2 hr/WQ			118,800(T)	124,000(T)			
	1750° F/1 hr/AC	1100° F/4 hr/WQ	57.5	52.5	119,000(L)	123,200(L)	13.6	42.2	3333(RW)†
	1750° F/1 hr/AC	1100° F/4 hr/WQ			116,100(T)	123,400(T)	14.6	42.8	
	1750° F/1 hr/AC	1100° F/2 hr/WQ	40.0	35.5	125,900(L)	131,700(L)	12.5	35.7	†
	1750° F/1 hr/AC	1100° F/2 hr/WQ			123,000(T)	131,200(T)	12.9	32.7	†
	1750° F/1 hr/AC	1100° F/4 hr/WQ	31.5*	35.0	127,300(L)	131,600(L)	12.9	41.5	
	1750° F/1 hr/AC	1100° F/4 hr/WQ			122,400(T)	129,000(T)	13.2	35.0	
T-71 (Ti-7Al-2.5Mo)	1850° F/1 hr/AC	1100° F/2 hr/WQ	27.0	28.5	123,500(T)	135,700(T)	7.5	9.9	1263(WR)†
	1800° F/1 hr/AC	1100° F/2 hr/WQ	52.0	49.0	120,000(L)	132,400(L)	11.1	24.6	2846(RW)†
	1800° F/1 hr/AC	1100° F/2 hr/WQ	51.0	42.0	116,500(T)	130,200(T)	14.0	25.2	2560(WR)†
	1700° F/1 hr/AC	1100° F/2 hr/WQ	45.5	46.0	121,600(T)	134,800(T)	11.8	27.0	3013(WR)
	1850° F/1 hr/AC	1100° F/2 hr/WQ	28.0	28.5	123,700(L)	136,300(L)	10.7	19.0	†
	1850° F/1 hr/AC	1100° F/2 hr/WQ			122,000(T)	138,600(T)	10.0	17.8	
	1850° F/1 hr/AC	1200° F/2 hr/WQ	26.5	-	120,000(L)	131,300(L)	8.6	21.8	†
	1850° F/1 hr/AC	1200° F/2 hr/WQ			123,300(T)	134,300(T)	10.7	21.2	
	1800° F/1 hr/AC	1100° F/2 hr/WQ	52.5	47.5					
	1800° F/1 hr/AC	1200° F/2 hr/WQ	44.0	-					
	1750° F/1 hr/AC	1100° F/2 hr/WQ	51.0	-					
	1750° F/1 hr/AC	1200° F/2 hr/WQ	49.0	-					
1700° F/1 hr/AC	1100° F/2 hr/WQ	42.5	43.5	123,200(L)	137,900(L)	11.4	16.0	†	
1700° F/1 hr/AC	1100° F/2 hr/WQ			120,700(T)	135,300(T)	10.7	22.3		
1700° F/1 hr/AC	1200° F/2 hr/WQ	38.0		122,800(L)	134,500(L)	10.0	16.0	†	

\*Single sample - value appears low.

†Charpy V and tensile specimens premachined and then heat-treated.

‡Charpy V and tensile specimens taken from heat-treated 1-in.-plate materials (values are average of two).

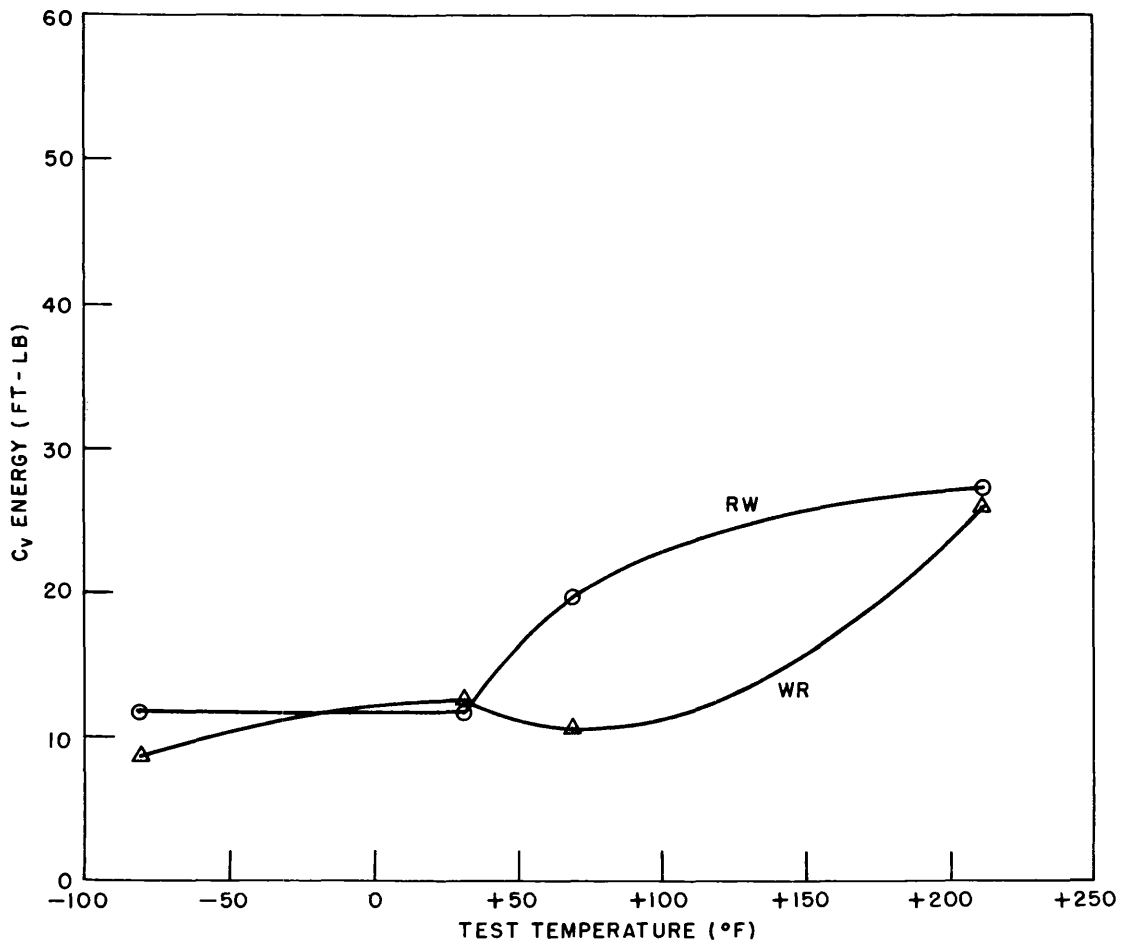


Fig. 19 - Charpy V curves for 1-in.-thick RS-70 unalloyed titanium (T17) plate in the as-received condition

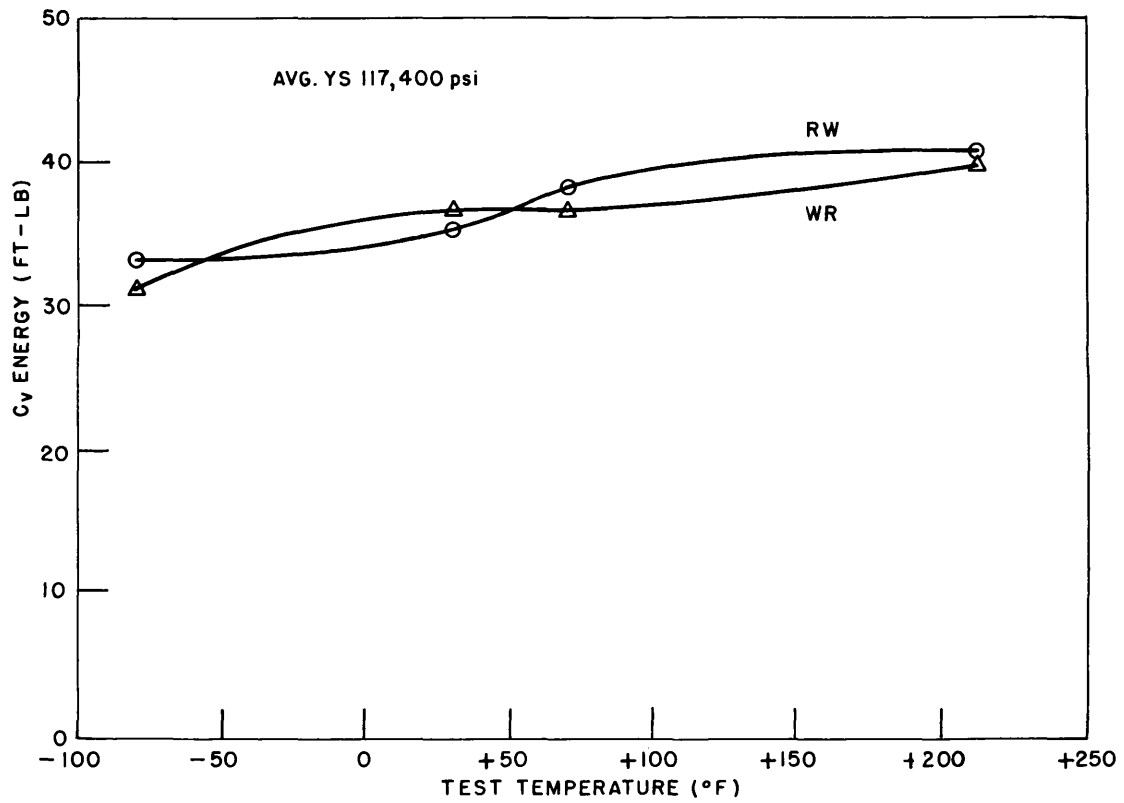


Fig. 20 - Charpy V curves for 1-in.-thick Ti-5Al-2.5Sn (T-18) alloy plate in the as-received condition

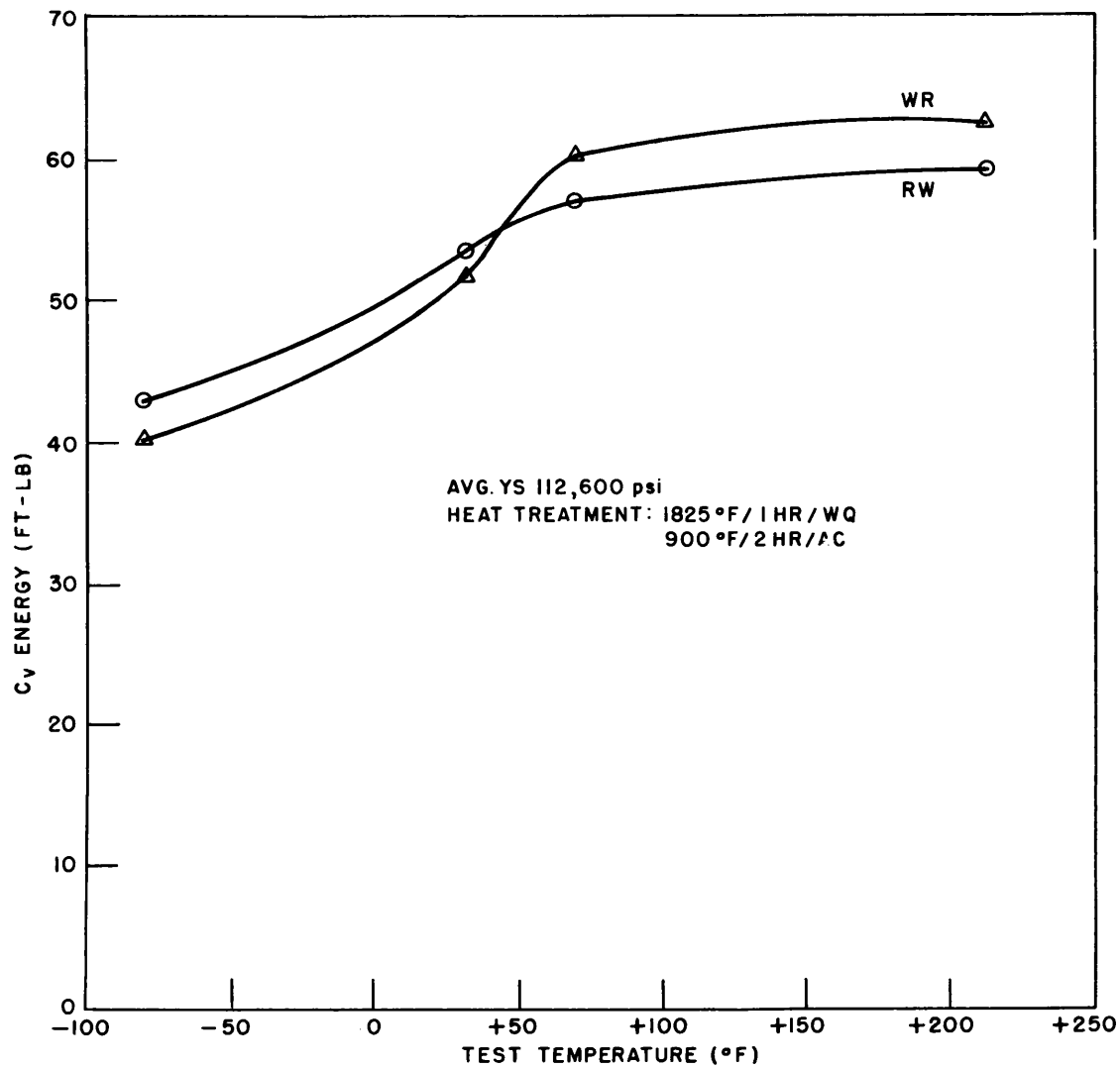


Fig. 21 - Charpy V curves for 1-in.-thick  
Ti-6Al-4Sn-1V (T-20) alloy plate

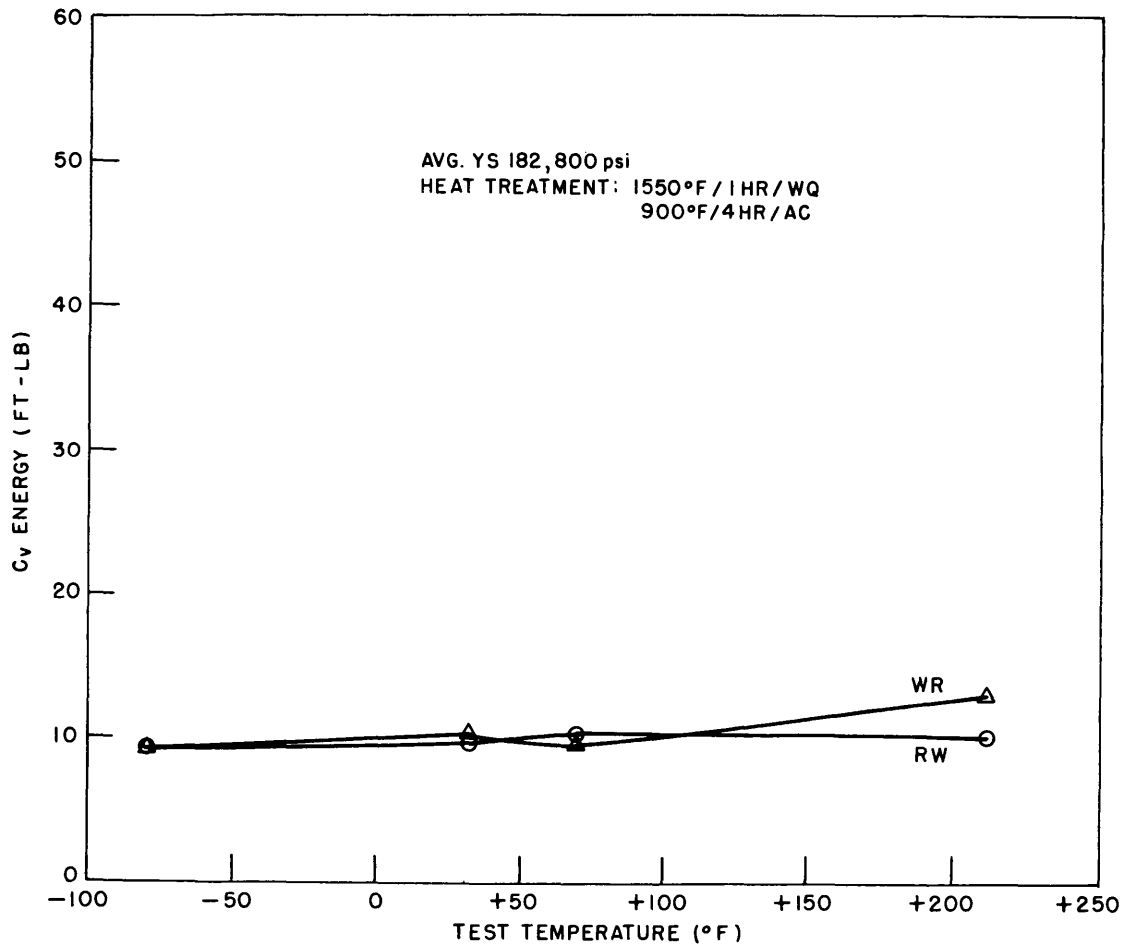


Fig. 22 - Charpy V curves for 1-in.-thick Ti-6Al-6V-2.5Sn (T-21) alloy plate

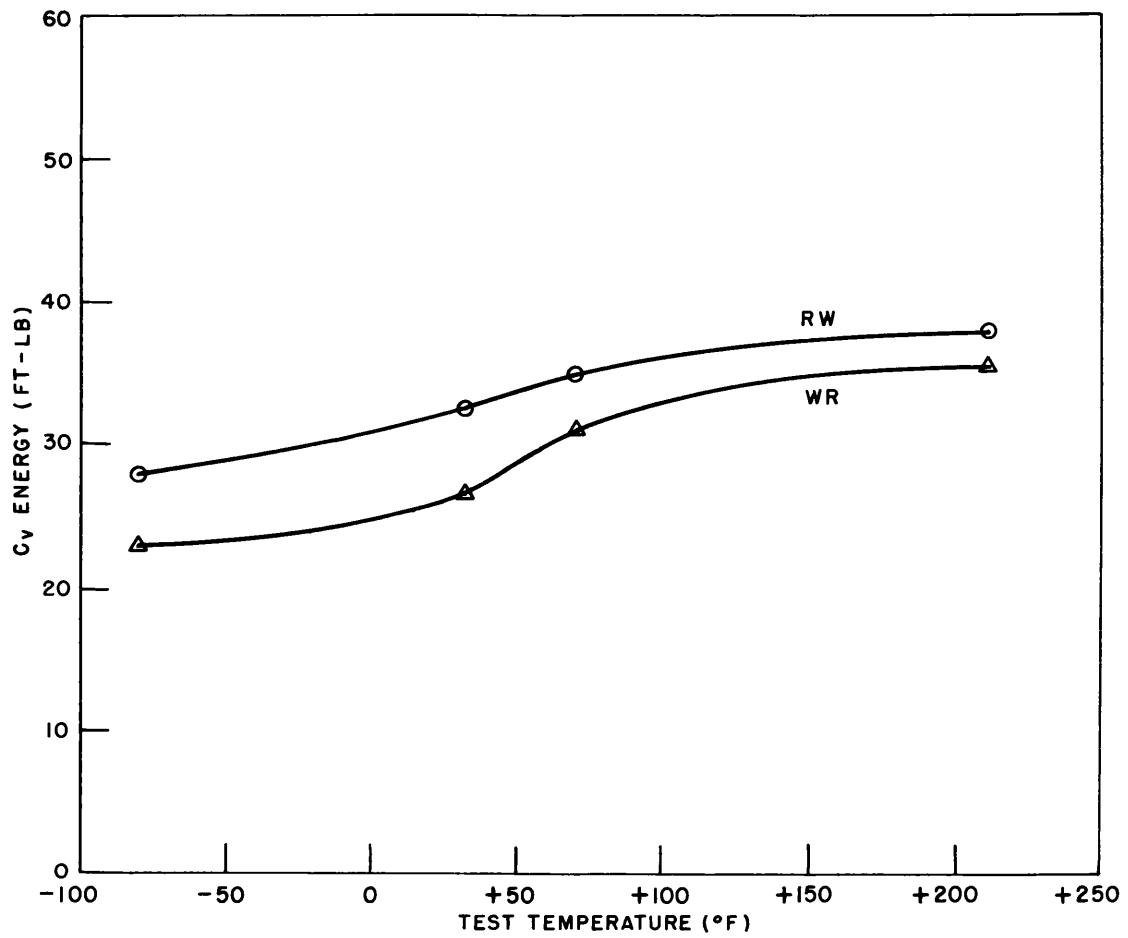


Fig. 23 - Charpy V curves for 1-in.-thick Ti-8Al-2Cb-1Ta (T-23) alloy plate in the as-received condition

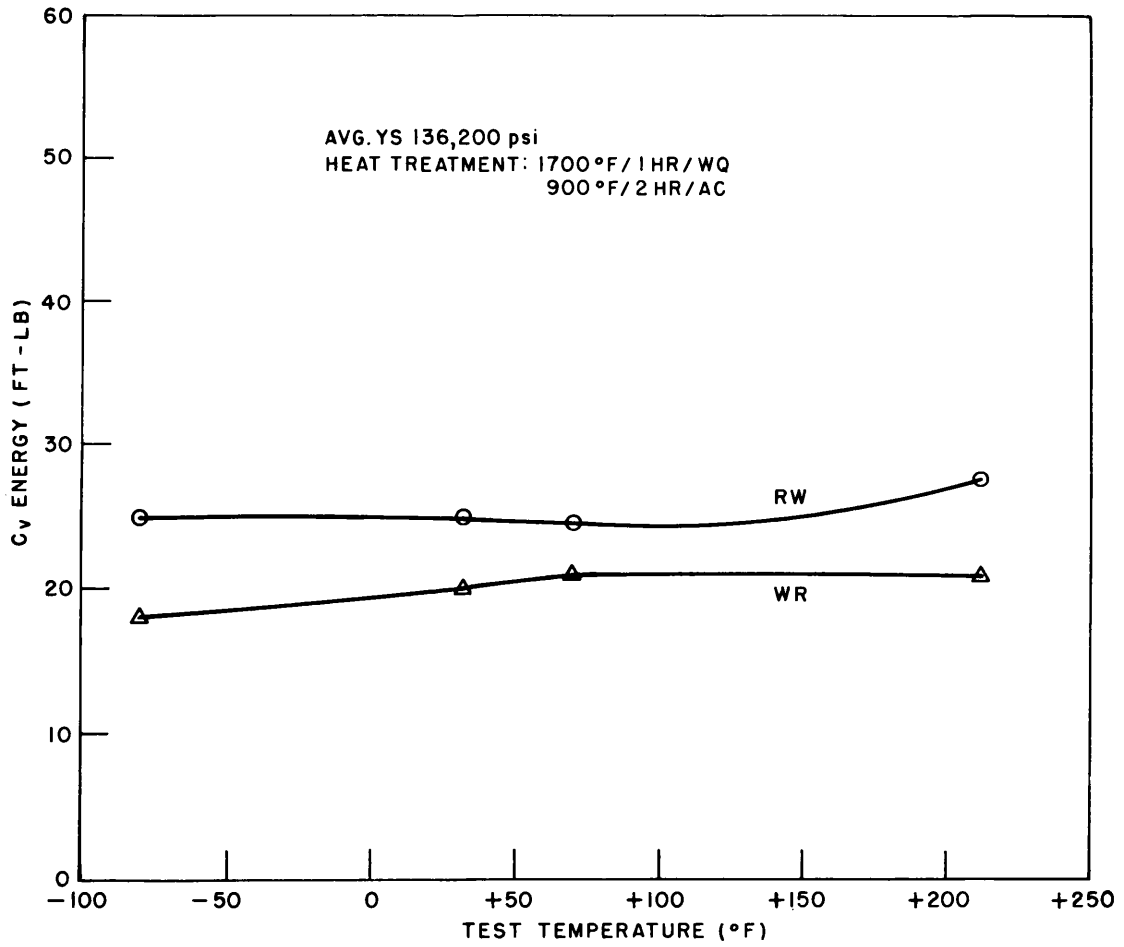


Fig. 24 - Charpy V curves for 1-in.-thick Ti-6Al-4V (T-27) alloy plate

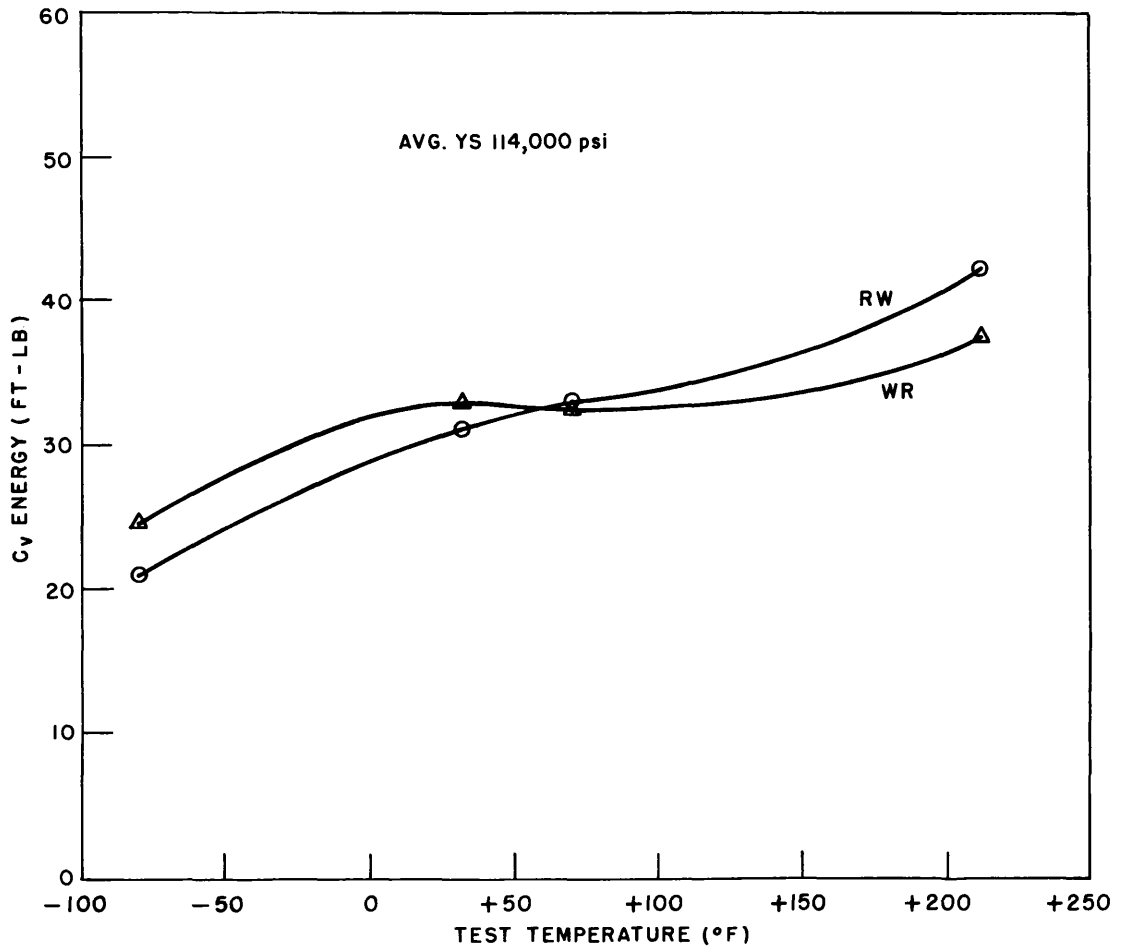


Fig. 25 - Charpy V curves for 1-in.-thick Ti-7Al-2Cb-1Ta (T-74) alloy plate in the as-received condition

Tables 13 and 14 show the data obtained to date for the alloys Ti-6Al-4V-2Sn (T-67) and Ti-6Al-6V-2.5Sn (T-21). It can be seen in Table 14 that by selected heat treatments, a very high YS can be obtained in the Ti-6Al-6V-2.5Sn alloy. The fracture toughness properties of these types of materials are being determined by plane-strain fracture toughness ( $K_{Ic}$ ) techniques.

Of all the alloys investigated to date in the heat-treatment studies, the alloys Ti-8Al-1Mo-1V (T-19), Ti-6Al-4Sn-1V (T-20), Ti-6Al-2Mo (T-22), Ti-6Al-4Zr-2Mo (T-55), Ti-6Al-4Zr-2Sn-.5Mo-.5V (T-68), and Ti-7Al-2.5Mo (T-71), have shown the best combinations of strength and toughness. However, the matching of plate and weld metal properties of some of these alloys may be difficult; further work will be required to determine if reasonable post-weld heat treatments can provide satisfactory weldment performance of the particular problem alloys which may be of interest.

#### ALUMINUM ALLOYS

(R.W. Judy, Jr., and R.J. Goode)

Aluminum alloys are being studied to determine their fracture toughness characteristics and to determine the significance of small laboratory fracture toughness tests in providing engineering criteria to predict service performance of the material in large, complex structures. A major portion of the work to date has been concerned with indexing the drop-weight tear test (DWTT) results in terms of explosion tear test (ETT) performance. From these studies, a very preliminary fracture toughness index diagram (FTID) for 1-in.-thick, commercially-produced, aluminum plate has been developed. As for the steels and titanium alloys, the diagram relates DWTT energy to ETT performance over a wide range of yield strength (YS).

#### EXPLOSION TEAR TEST RESULTS

A previous ETT test demonstrated that the alloy 6061-T651 could develop 8.2% plastic strain in the ETT with only limited fracture propagation (13). Since the YS and fracture toughness of this alloy were reasonably high (YS 38-ksi, DWTT 750 ft-lb), ETT studies were continued at higher strain levels to determine its maximum level of plastic strain capability. In this manner, an ETT performance index of 12% plastic strain was determined for a DWTT energy of 750 ft-lbs.

Table 13  
Test Data for Solution Annealing and Aging Treatments  
on the Alloy Ti-6Al-4V-2Sn (T-67)

Solution Heat Treatment	Aging Heat Treatment	Charpy V Notch Energy (ft-lb)				YS (0.2%) (ksi)	UTS (ksi)	Elong. (%)	R.A. (%)
		(-80° F)		( +32° F)					
		RW	WR	RW	WR				
As-received		17.5	18.5	21.0	20.5	115.8(L)	127.6(L)	13.1	35.3
As-received						123.4(T)	133.2(T)	12.1	24.6
1750° F/1 hr/WQ		16.0	14.5	17.0	16.0	129.8(L)	154.5(L)	9.3	25.7
1750° F/1 hr/WQ						129.3(T)	153.5(T)	7.1	25.7
1750° F/1 hr/WQ	1100° F/2 hr/AC					150.5(L)	161.1(L)	5.0	11.8
1750° F/1 hr/WQ	1100° F/2 hr/AC					153.8(T)	161.5(T)	5.7	13.0
1750° F/1 hr/WQ	1200° F/2 hr/AC					143.9(L)	152.2(L)	6.4	13.6
1750° F/1 hr/WQ	1200° F/2 hr/AC					140.9(T)	150.5(T)	6.4	14.9
1700° F/1 hr/WQ						125.2(L)	154.2(L)	10.0	23.6
1700° F/1 hr/WQ						123.3(T)	151.5(T)	10.0	28.5
1700° F/1 hr/WQ	1100° F/2 hr/AC					152.2(L)	161.8(L)	7.1	19.0
1700° F/1 hr/WQ	1100° F/2 hr/AC					148.2(T)	159.2(T)	6.4	15.0
1700° F/1 hr/WQ	1200° F/2 hr/AC					142.6(L)	154.2(L)	10.0	25.7
1700° F/1 hr/WQ	1200° F/2 hr/AC					145.9(T)	156.2(T)	9.3	19.6
1650° F/1 hr/WQ						99.8(L)	135.8(L)	13.6	36.6
1650° F/1 hr/WQ						108.4(T)	138.3(T)	12.9	36.4
1650° F/1 hr/WQ	1100° F/2 hr/AC					134.8(L)	145.6(L)	7.9	20.0
1650° F/1 hr/WQ	1100° F/2 hr/AC					138.6(T)	148.5(T)	7.9	14.2
1650° F/1 hr/WQ	1200° F/2 hr/AC					130.3(L)	139.6(L)	12.1	22.4
1650° F/1 hr/WQ	1200° F/2 hr/AC					130.6(T)	139.9(T)	10.0	22.9
1550° F/1 hr/WQ						93.5(L)	135.5(L)	13.6	36.0
1550° F/1 hr/WQ						92.1(T)	136.5(T)	14.3	39.7
1550° F/1 hr/WQ	1100° F/2 hr/AC					134.8(L)	143.5(L)	10.0	11.2
1550° F/1 hr/WQ	1100° F/2 hr/AC					133.8(T)	141.9(T)	12.1	23.1
1550° F/1 hr/WQ	1200° F/2 hr/AC					125.7(L)	134.6(L)	11.4	30.6
1550° F/1 hr/WQ	1200° F/2 hr/AC					131.2(T)	139.5(T)	12.9	28.6
1750° F/1 hr/AC		19.5	18.5	25.0	26.5	113.7(L)	130.0(L)	10.7	24.7
1750° F/1 hr/AC						112.7(T)	128.6(T)	10.0	26.8
1750° F/1 hr/AC	1100° F/2 hr/WQ	19.0	18.5	24.5	24.5	119.5(L)	129.5(L)	10.7	34.4
1750° F/1 hr/AC	1100° F/2 hr/WQ					120.6(T)	130.4(T)	11.4	31.6
1750° F/1 hr/AC	1200° F/2 hr/WQ	17.5	17.0	24.5	23.0	118.6(L)	126.5(L)	10.7	26.7
1750° F/1 hr/AC	1200° F/2 hr/WQ					125.0(T)	131.0(T)	11.4	24.3
1700° F/1 hr/AC		20.0	19.5	25.0	24.5	110.1(L)	128.0(L)	12.1	30.2
1700° F/1 hr/AC						115.4(T)	131.3(T)	12.1	27.5
1700° F/1 hr/AC	1100° F/2 hr/WQ	23.0	22.0	26.5	24.5	119.2(L)	129.5(L)	12.1	33.5
1700° F/1 hr/AC	1100° F/2 hr/WQ					121.4(T)	130.3(T)	11.4	28.0
1700° F/1 hr/AC	1200° F/2 hr/WQ	17.5	17.0	22.5	21.5	120.2(L)	128.2(L)	14.3	34.6
1700° F/1 hr/AC	1200° F/2 hr/WQ					121.7(T)	129.0(T)	11.4	39.7
1650° F/1 hr/AC		22.0	20.0	28.5	25.0	109.4(L)	127.1(L)	12.9	31.8
1650° F/1 hr/AC						113.1(T)	130.0(T)	12.9	32.9
1650° F/1 hr/AC	1100° F/2 hr/WQ					117.8(L)	128.5(L)	10.7	24.2
1650° F/1 hr/AC	1100° F/2 hr/WQ					123.7(T)	132.3(T)	11.4	33.4
1650° F/1 hr/AC	1200° F/2 hr/WQ	19.5	17.5	23.0	21.0	121.4(L)	129.0(L)	12.1	28.0
1650° F/1 hr/AC	1200° F/2 hr/WQ					121.8(T)	130.5(T)	12.1	33.5
1550° F/1 hr/AC						111.8(L)	127.5(L)	14.3	26.4
1550° F/1 hr/AC						116.4(T)	130.0(T)	11.4	32.4
1550° F/1 hr/AC	1100° F/2 hr/WQ					123.3(L)	131.0(L)	14.3	39.7
1550° F/1 hr/AC	1100° F/2 hr/WQ					127.2(T)	134.8(T)	11.4	30.3
1550° F/1 hr/AC	1200° F/2 hr/WQ					123.8(L)	130.8(L)	11.4	25.9
1550° F/1 hr/AC	1200° F/2 hr/WQ					125.7(T)	132.0(T)	10.0	29.7

Table 14  
 Test Data for Solution Annealing and Aging Treatments  
 on the Alloy Ti-6Al-6V-2.5Sn (T-21)

Solution Heat Treatment	Aging Heat Treatment	YS (0.2%) (ksi)	UTS (ksi)	Elong. (%)	R. A. (%)
As-received		147.5(L)	150.5(L)	10.0	42.0
As-received		152.0(T)	154.5(T)	9.5	41.5
1700° F/1 hr/WQ	1100° F/2 hr/AC	194.9(L)	201.3(L)	3.6	6.9
1700° F/1 hr/WQ	1100° F/2 hr/AC	188.7(T)	194.3(T)	3.6	3.8
1700° F/1 hr/WQ	1200° F/2 hr/AC	175.4(L)	181.7(L)	3.6	10.6
1700° F/1 hr/WQ	1200° F/2 hr/AC	172.9(T)	179.2(T)	3.6	6.9
1550° F/1 hr/WQ	1100° F/2 hr/AC	171.4(L)	173.4(L)	7.9	22.9
1550° F/1 hr/WQ	1100° F/2 hr/AC	166.9(T)	168.2(T)	8.6	21.9
1550° F/1 hr/WQ	1200° F/2 hr/AC	154.8(L)	155.8(L)	12.1	37.7
1700° F/1 hr/AC	1100° F/2 hr/WQ	149.9(L)	156.8(L)	6.4	10.6
1700° F/1 hr/AC	1100° F/2 hr/WQ	145.9(T)	154.8(T)	10.7	25.2
1700° F/1 hr/AC	1200° F/2 hr/WQ	146.2(L)	154.5(L)	9.3	24.1
1650° F/1 hr/AC	1100° F/2 hr/WQ	153.8(L)	157.8(L)	10.7	30.2
1650° F/1 hr/AC	1100° F/2 hr/WQ	151.9(T)	155.2(T)	12.1	31.3
1650° F/1 hr/AC	1200° F/2 hr/WQ	148.6(L)	151.2(L)	11.4	36.4
1650° F/1 hr/AC	1200° F/2 hr/WQ	145.5(T)	148.5(T)	12.1	36.6
1550° F/1 hr/AC	1100° F/2 hr/WQ	154.8(L)	158.4(L)	12.9	44.7
1550° F/1 hr/AC	1200° F/2 hr/WQ	147.6(T)	149.9(T)	13.6	40.1

Explosion tear test specimens of the 6061-T651 alloy were tested at 12% and 14% plastic strain. The specimen tested at 12% plastic strain propagated a fracture completely across the test section (Fig. 26). The change in the shear fracture from that of 45° to the plate surface in the center portion of the specimen to a plane normal to the plate surface near the cut slots indicates that the explosive load intensity was barely enough to cause the specimen to fail. This is also indicated by the lack of separation of the fracture surfaces at the cut slots of the specimen. The specimen tested at a 14% plastic strain level failed with the fracture surface limited exclusively to the 45° shear plane and with considerable separation of the fracture surfaces at the cut slots (Fig. 27). This is indicative of an explosive load intensity considerably in excess of that necessary for failure.

An ETT plate of the alloy 5086-H112, having a YS of 24-ksi and DWTT energy of 2000 ft-lb, had previously been tested to 10.4% plastic strain with practically no crack extension (13). The same plate was subjected to a second explosive loading using the same test conditions. The total plastic strain in the plate was not measured but was estimated to be 16-18%. Even at this high level of plastic strain, the total crack extension was about 1-in. on either side of the brittle weld flaw. A second ETT plate of the same alloy was tested at 16.8% plastic strain and developed a short tear of about 2-in. on each side of the flaw (Fig. 28). These results demonstrate not only the high fracture toughness of the 5068 alloy in the H112 temper, but then also indicate that alloys having similarly high DWTT energy values, will probably require plastic strains in the ETT of 20% or more for fracture propagation: i.e., the material literally has to be pulled apart to cause failure.

A plate specimen of the alloy 5083 was also tested in the ETT. This material had a YS of 11-ksi and a DWTT energy value of 2200 ft-lb. It was subjected to 10% plastic strain and, as can be seen in Fig. 29, only short tears developed at each end of the brittle weld flaw.

#### FRACTURE TOUGHNESS INDEX DIAGRAM

The FTID for aluminum is shown in Fig. 30. The ETT results obtained with the alloy 6061-T651 have provided a modification of the ETT performance index of the DWTT energy at



Fig. 26 - Explosion tear test of alloy 6061-T651 at 12-percent plastic strain. The crack which extends completely across test section was almost arrested, as indicated by the change of orientation of the fracture plane relative to the plate surface. Also, near-arrest is indicated by the absence of fracture surface separation near the cut slot.



Fig. 27 - Explosion tear test of alloy 6061-T651 at 14.3-percent plastic strain. The complete separation of the fracture surface indicates that the explosion load intensity of the plastic overload was in excess of that necessary for fracture propagation through the test plate.

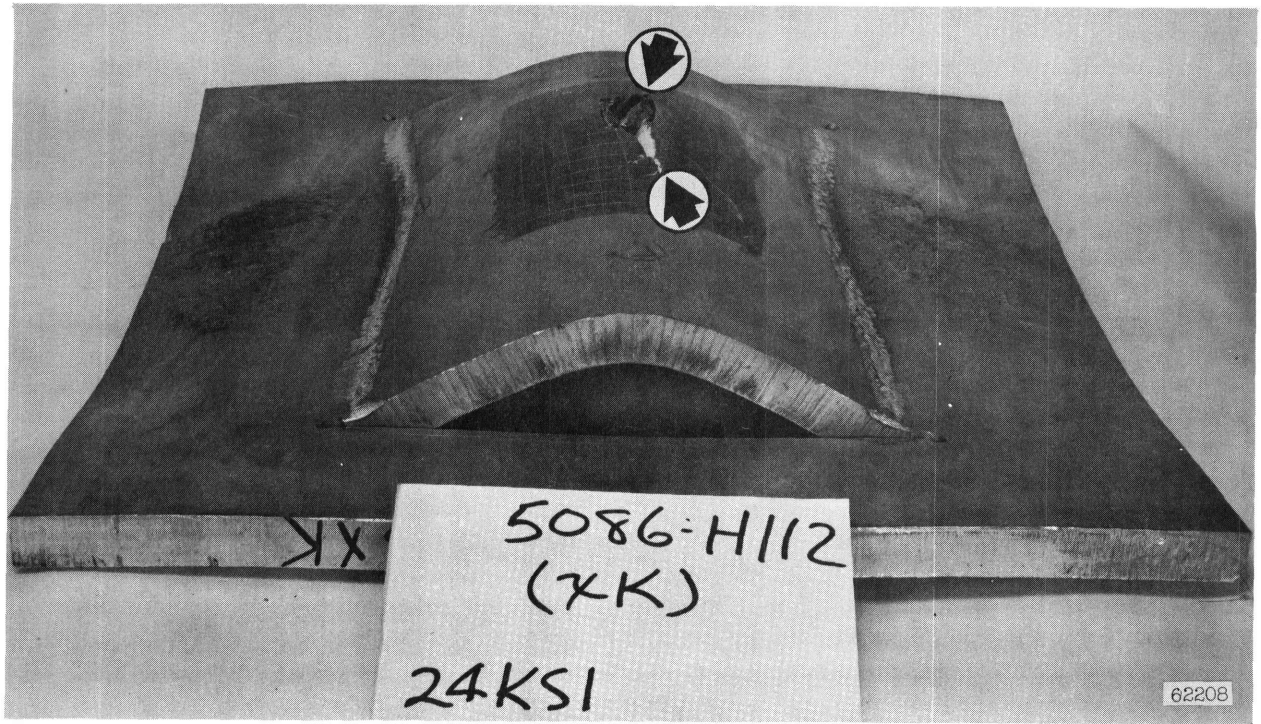


Fig. 28 - Explosion tear test of alloy 5086-H112 at 16.8-percent plastic strain. Arrows indicate limits of crack extension.

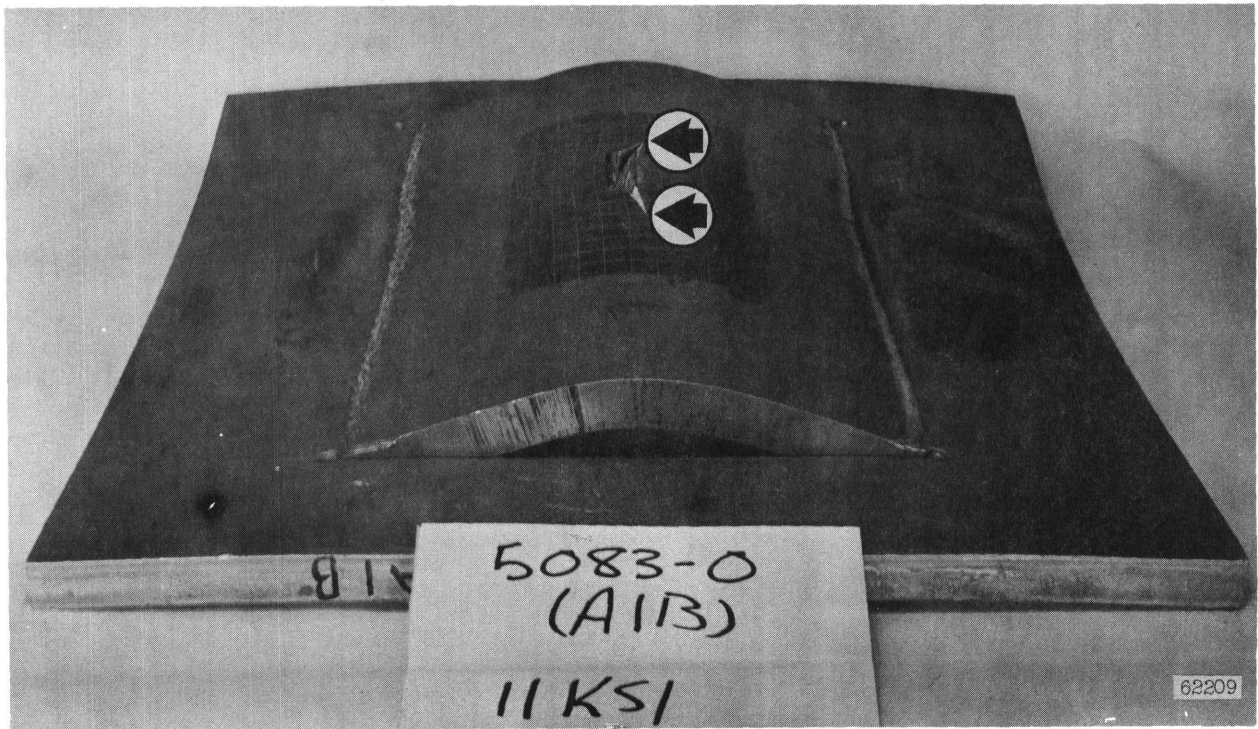


Fig. 29 - Explosion tear test of alloy 5083-0 at 10-percent plastic strain. Arrows indicate limits of crack extension.

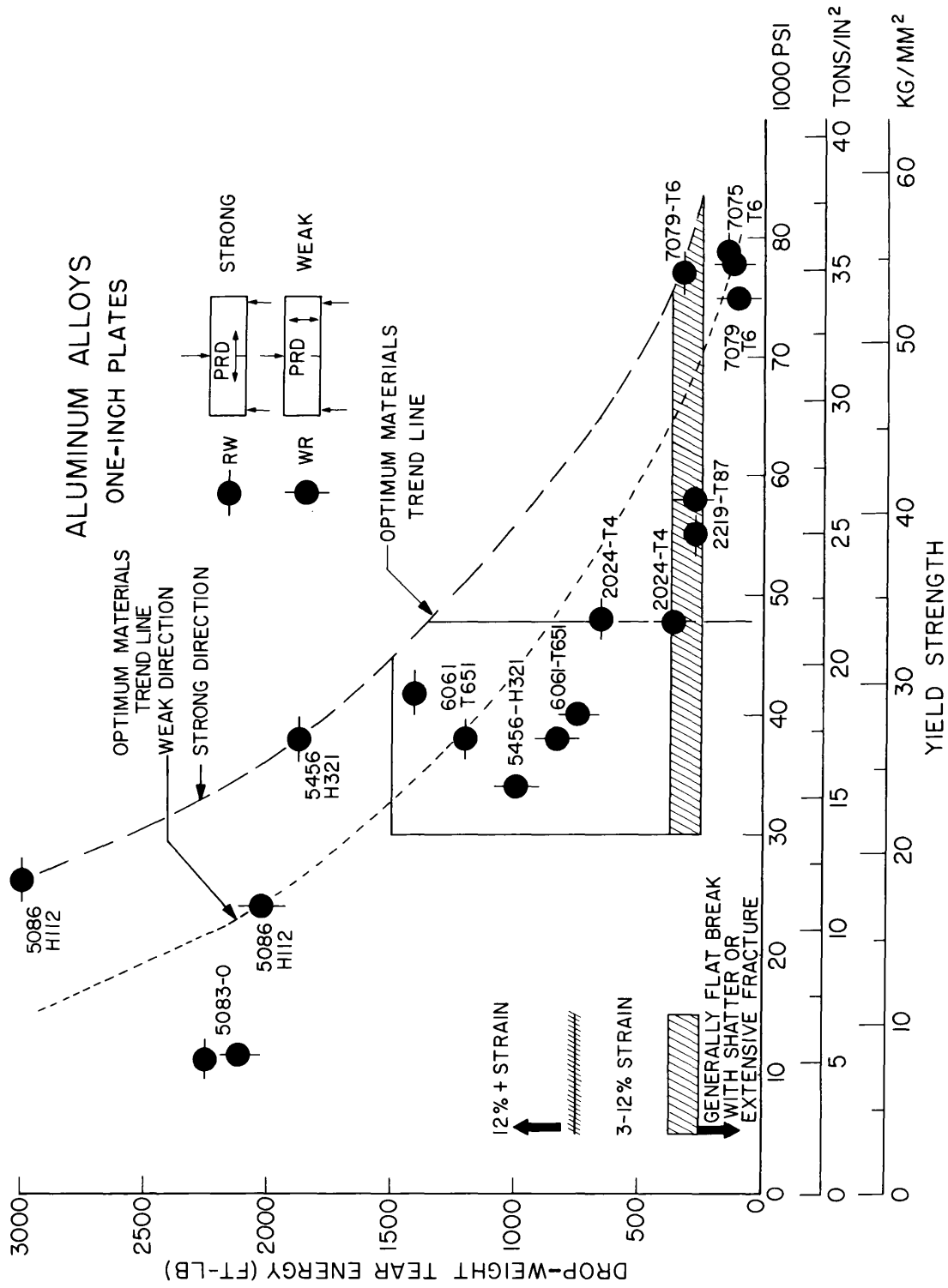


Fig. 30 - Preliminary fracture-toughness index diagram (FTID) for 1-in.-thick aluminum alloy plate. Alloy designations and tempers are indicated with data points.

750 ft-lb. This is shown by the hashed line on the left side of the chart. It indicates that materials having DWTT energies above 750 ft-lb will require over 12% plastic strain for fracture propagation. The shaded band at 200-300 ft-lb DWTT energy indicates the transition from elastic strains required for crack propagation --less than 200-300 ft-lb DWTT energy--to plastic overloads required for fractures to propagate--above 200-300 ft-lb DWTT energy. The optimum materials trend lines (OMTL) are shown for both the RW ("strong") and the WR ("weak") fracture directions (21). Comparison of the OMTL for both fracture directions indicate considerable anisotropy in the commercially-produced 1-in.-thick aluminum alloy plates at all but the highest strengths. The cross-over point of the elastic to plastic performance band for fracture propagation with the "weak" direction OMTL indicates that alloys above 50-ksi YS should propagate fracture at elastic stress levels. Below this strength level, practically all alloys should require plastic deformation overload for fracture propagation. The cross-over of the elastic-to-plastic performance band with the "strong" direction OMTL indicates that above the range of 60-ksi YS most alloys should be expected to propagate fracture at elastic stress levels, and below 60-ksi YS plastic deformation overload will be required for fracture propagation. However, it must be remembered that in practically all large complex structures, the "weak" direction fracture toughness properties are the most critical. Unless the material is optimized --highly cross-rolled--so that the "weak" direction fracture toughness properties approach those obtained in the "strong" direction, the limitations indicated for the "weak" direction OMTL are the most significant.

A COMPARATIVE EVALUATION OF LOW CYCLE  
FATIGUE CRACK PROPAGATION IN 5Ni-Cr-Mo-V STEELS

(T.W. Crooker, R.E. Morey, and E.A. Lange)

The determination of the low cycle fatigue characteristics of a wide variety of high strength metals is part of the Metallurgy Division's high strength structural materials program. Recently, a series of tests were conducted on two 130-140-ksi yield strength (YS) 5Ni-Cr-Mo-V quenched and tempered (Q&T) steels (22) to determine their resistance to the slow growth of cracks from low cycle fatigue. These steels are currently under evaluation for application in large welded Naval structures. One necessary characteristic of a high strength structural material is the ability

to resist the growth of crack-like flaws under cyclic loading. Small flaws invariably are formed during fabrication and manufacture of a large welded structure, despite the use of the best current processing and inspection techniques. Since fabrication flaws are unavoidable, the only available recourse is to provide design criteria for preventing the growth of flaws to a critical size from repeated service loads.

This investigation evaluated the low cycle fatigue performance of 5Ni-Cr-Mo-V steels in relation to similarly measured performance of HY-80 steel--the current Naval hull material. The results of these tests were obtained from studies of fatigue crack propagation in center-notched plate bend specimens. This testing procedure has been previously employed on a wide variety of materials, both ferrous and nonferrous (10, 11, 13, 14, 20, 23-28).

Specific studies of HY-80 (10, 11, 20, 24) provide a broad background for comparison of the effects of the various factors which control the growth rate of fatigue cracks.

Analytical procedures are based on the observation that, in the plate bend fatigue specimen, the growth rate of a low cycle fatigue crack is a function of the applied total strain range, as expressed by the relationship

$$\frac{dL}{dN} = C(\epsilon_T)^m$$

where L = total length of fatigue crack, N = cycle of load application,  $\epsilon_T$  = total strain range, and C and m are constants. This relationship has been found to exist for all materials tested to date. It provides a common basis for comparing the fatigue performance of materials of various YS levels and elastic moduli. In addition, it serves as a basis for estimating the effect of mean strain and environment on fatigue performance.

#### MATERIALS AND EXPERIMENTAL PROCEDURE

Tests were conducted on two samples of 5Ni-Cr-Mo-V steel which differed slightly in chemical composition and yield strength (YS) level, as indicated in Tables 15 and 16

respectively. Although these two steels possess important differences in fracture toughness properties for structural applications involving welded joints, no significant difference was found to exist in their respective fatigue crack propagation properties. Hence this report will consider the effects of strain range and environment on their common fatigue properties, except with regard to certain observations of crack initiation where significant differences were observed. These differences are discussed in a later section under the subheading "Microcrack Formation and Growth".

The strain range-deflection characteristics of these materials in the plate bend specimen are shown in Fig. 31. The total strain range at which the plastic strain range reaches 500  $\mu\text{in./in.}$  is arbitrarily defined as the proportional limit in the plate bend specimen and this proportional limit is indicated on Fig. 31 for each material. The plastic strain level of 500  $\mu\text{in./in.}$  is the smallest value of plastic strain which can be measured with consistent accuracy and is employed as the "benchmark" for indicating the onset of nominal plastic loading. For the two 5Ni-Cr-Mo-V steels tested, the measured proportional limits were 11,500 and 12,000  $\mu\text{in./in.}$ , and an average value of 11,750 is used for purposes of discussion. The amplitude of this average proportional limit strain range equals approximately 90% of the strain at the 0.2% offset yield strength for these materials.

Plate bend test specimens were machined from 1-in.-thick rolled plate stock. Specimen orientations were chosen so that the fatigue crack propagation was either perpendicular ( $\perp$ ) or parallel (P) to the principal rolling direction. These orientations are respectively equivalent to the ASTM designated RW and WR orientations (21).

The experimental procedure employed for this series of tests is the same as that described in references 10, 11, 13, 14, 20, 23-28. Experimental data are based on the observed macroscopic growth of fatigue cracks across the surface of center-notched plate bend specimens. The specimens are cantilever loaded in full-reverse strain cycling. Specimens were tested in three environments: room-temperature air, distilled water, and 3.5% salt water. Nominal surface strains across the test section are measured with electrical resistance strain gages. Constant total strain range loading conditions are maintained by adjusting specimen deflection, and the resulting

Table 15  
Chemical Compositions of 5Ni-Cr-Mo-V Steels\*

NRL Code	USS Heat No.	Element (Weight-Percent)									
		C	Mn	P	S	Si	Ni	Cr	Mo	V	Al
H13	x53588	.11	.86	.005	.008	.20	5.19	.54	.57	.08	.015
H98	3P0074	.11	.76	.007	.004	.25	4.90	.60	.49	.06	.021

\*NRL data.

Table 16  
Tensile Properties of 5Ni-Cr-Mo-V Steels\*

NRL Code	USS Heat No.	Yield Strength (0.2%)(ksi)	Ultimate Tensile Strength (ksi)	Elongation (%)	Reduction in Area (%)
H13	x53588	145	153	19	63
H98	3P0074	134	141	19	65

\*NRL data.

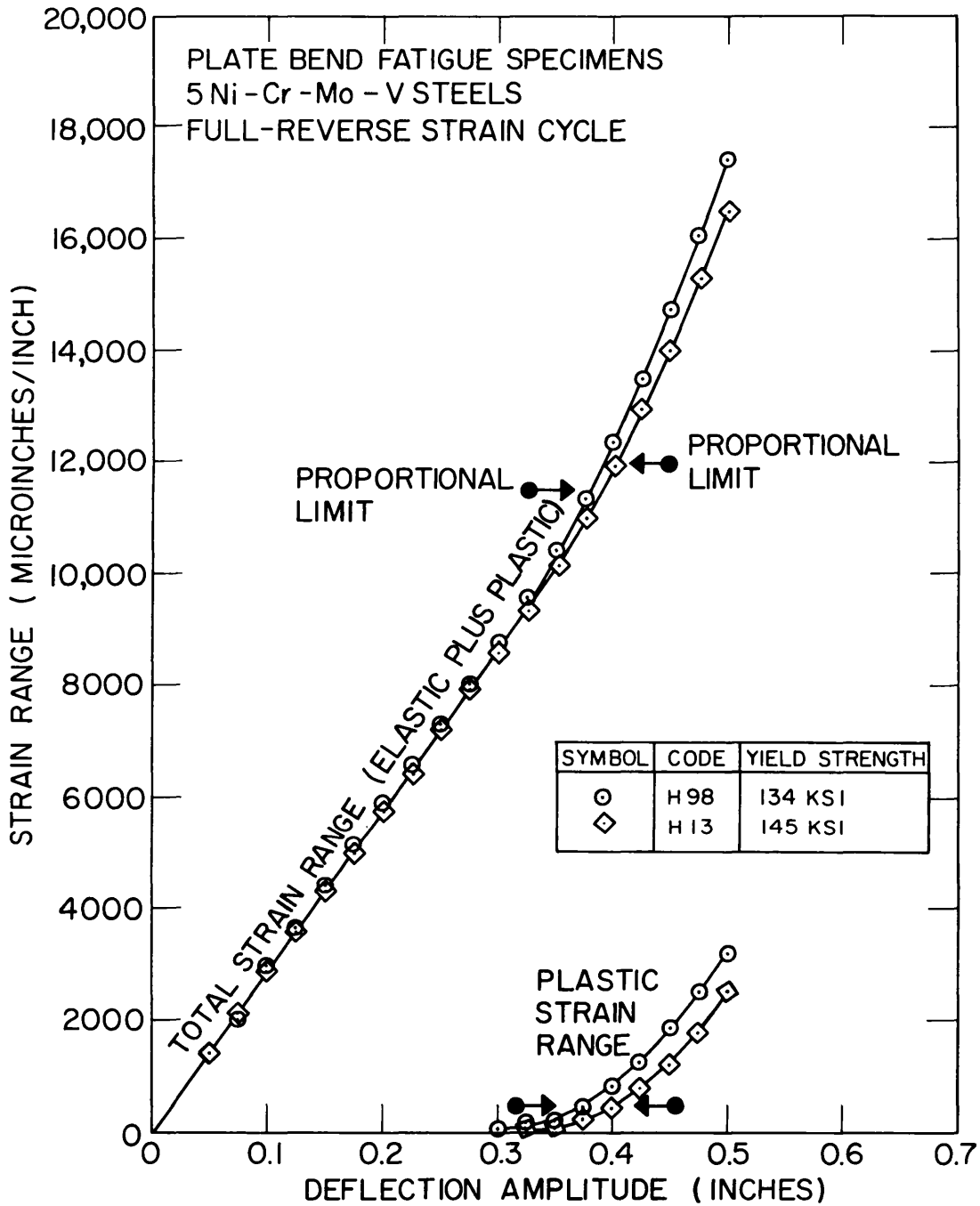


Fig. 31 - Strain-range deflection characteristics of 5Ni-Cr-Mo-V steel plate bend fatigue specimens at two strength levels - 134-ksi and 145-ksi YS. The proportional limits corresponding to 500  $\mu$ in./in. plastic strain range are indicated for each steel.

crack growth rate is recorded. Each specimen is tested at a specific total strain range value for an interval of several hundred to several thousand cycles until the crack growth rate can be established; then it is successively loaded to a higher strain level and the procedure repeated. In this manner, a series of crack growth rate versus total strain range data points are obtained from each specimen. For tests conducted under a wet environment, a corrosion cell is added to the specimen, allowing the controlled aqueous solutions to flow over the fatigue-cracked surface from a reservoir during testing.

## TEST RESULTS

### Crack Growth Rates in Air

Fatigue crack growth rates in air as a function of total strain range are shown plotted on log-log coordinates in Fig. 32. Data points from both samples of 5Ni-Cr-Mo-V steel are plotted together. The resulting best fit curve is linear when plotted on log-log coordinates and has a 4:1 slope. Both the slope and intercept values of this crack growth rate-strain range curve are in very close agreement with the slope and intercept values of the crack growth rate-strain range curve generated from HY-80 steel data (10, 11, 20).

The curve shown in Fig. 32 for the 5Ni-Cr-Mo-V steels describes the intrinsic resistance of this material to the slow growth of fatigue cracks under cyclic loading. Previous studies on HY-80 have shown that this basic relationship for a given steel chemistry is not significantly affected by changes in YS or fracture toughness resulting from heat treatment or specimen orientation with respect to rolling direction. The data summarized in Fig. 32 support such observations. In addition, the data on which this curve is based are highly reproducible, as evidenced in the data summary (Table 17) and in references 11, 14, and 20 on the HY-80, and are presented with a high degree of confidence.

Consequently, Fig. 32 serves as a starting point from which comparison with other materials and estimates of the effect of environment and mean strain can be made in engineering terms which are of direct significance to structural applications.

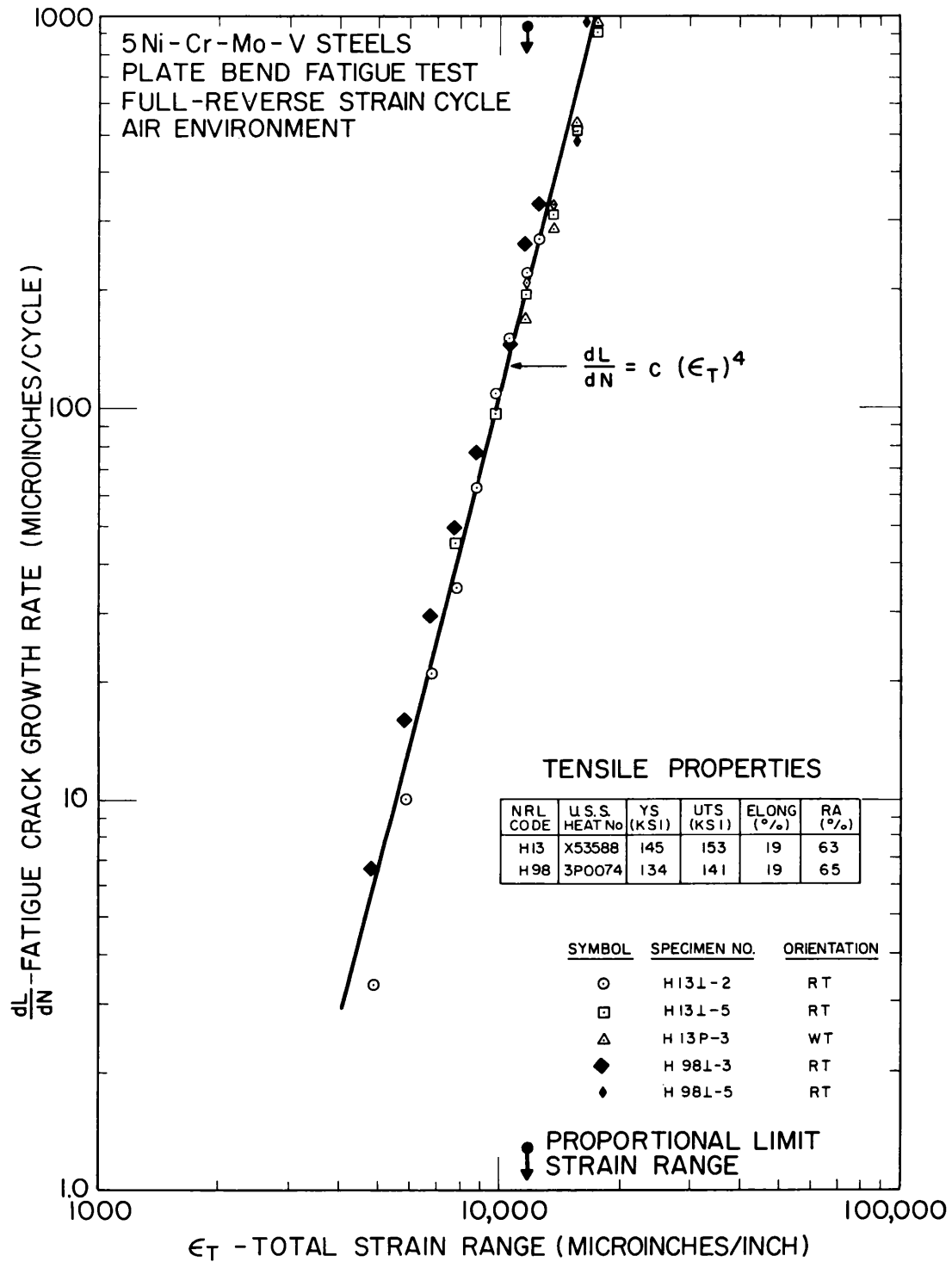


Fig. 32 - Log-log plot of fatigue crack growth rate data vs total strain range for 5Ni-Cr-Mo-V steels in an air environment

Table 17  
Data Summary – Air Environment

$\epsilon_T$ ( $\mu$ in./in.)	dL/dN ( $\mu$ in./cycle)					Average
	Specimen H131-2	Specimen H131-5	Specimen H13P-2	Specimen H981-3	Specimen H981-5	
4,850	3.33	-	-	6.50	-	4.92
5,850	10.0	-	-	15.7	-	12.8
6,800	21.0	-	-	29.0	-	25.0
7,800	34.5	45.0	-	48.7	-	42.7
8,800	62.5	-	-	75.5	-	69.0
9,800	108.	96.0	-	-	-	102.
10,700	150.	-	-	148.	-	149.
11,700	220.	193.	169.	261.	210.	211.
12,600	270.	-	-	330.	-	300.
13,600	-	310.	286.	-	315.	304.
15,600	-	518.	520.	-	484.	507.
17,600	-	915.	1080.	-	1033.	1010.

## Wet Fatigue

Fatigue crack growth rate versus total strain range data in a 3.5% salt water environment are shown plotted on log-log coordinates in Fig. 33. The best fit curve is denoted by the solid line and the plot of similar data obtained in air from Fig. 32 is shown in dashed lines for comparison.

The introduction of a salt water environment causes an increase in the rate of fatigue crack growth, as indicated by the vertical displacement of the two curves. This displacement varies over the range of cyclic strain values examined and, at the maximum displacement, shows an approximate fivefold increase in crack growth rate due to the salt water environment. An examination of the experimental data (Table 18) from which the best fit curve is derived reveals that the spread of all the data points lie below an order of magnitude increase. The steel was most sensitive to the salt water environment at a strain range corresponding to 50% of the YS.

It is significant to note that the salt water curve is nonlinear and deflects toward the air curve at high strain values near the proportional limit. Such behavior is in sharp contrast to materials that are susceptible to stress corrosion cracking. Stress corrosion cracking sensitive materials, such as the alloy Ti-7Al-2Cb-1Ta (14, 25) or 4335 steel (13), exhibit distinctly different behavior under the same test conditions in that the wet fatigue data diverge from corresponding air data at high strain levels.

In addition to tests in salt water, one specimen was tested in distilled water. The results of this test were very similar to distilled water tests on HY-80, shown in Fig. 33 of reference 20. At strain levels below 50% of yield strength, distilled water is a less hostile environment than salt water, and the data approach the air curve. However, at high strain levels, the deleterious effect of the distilled water environment increases, and at strain levels near the proportional limit the data approach the salt water curve.

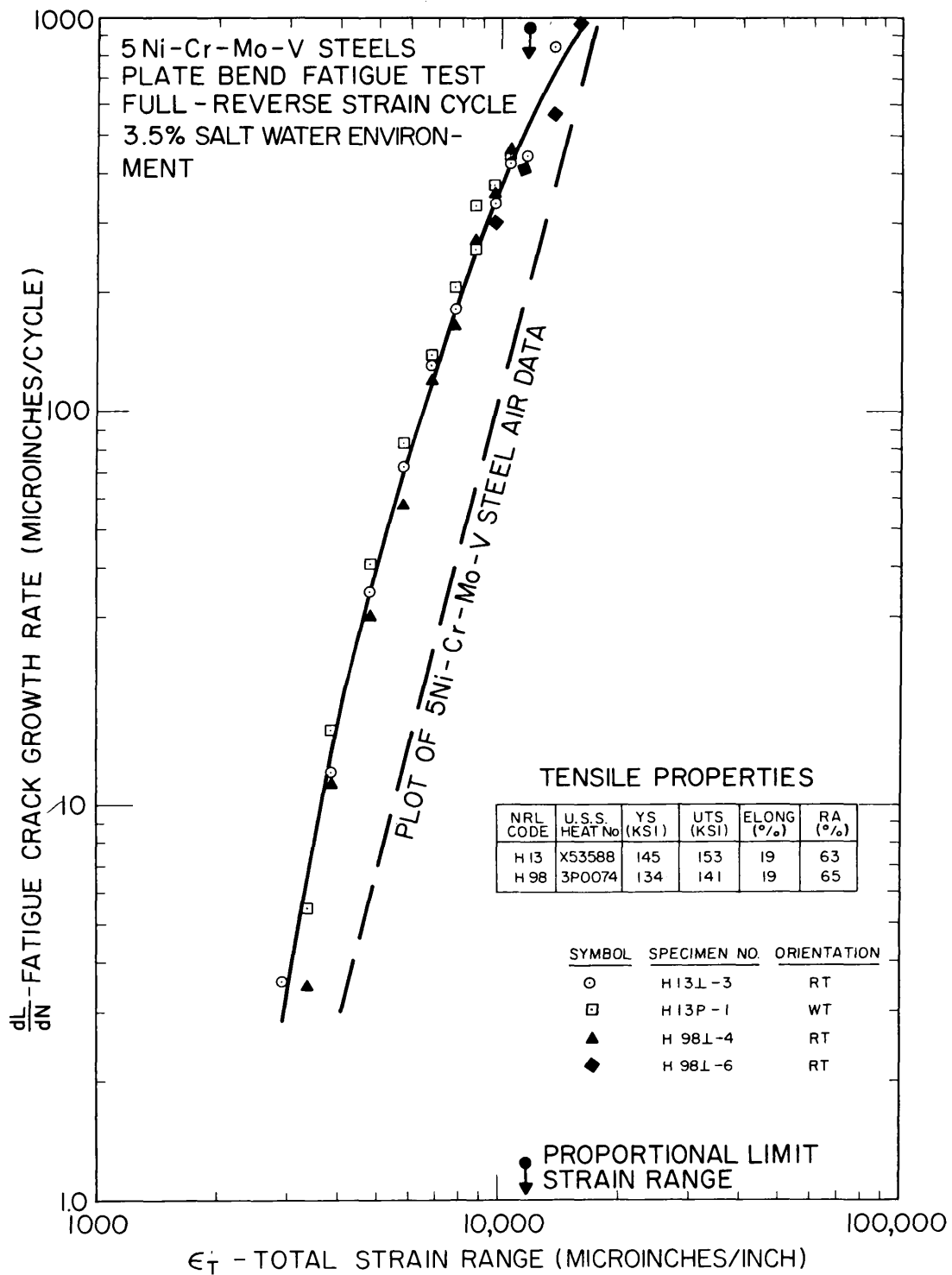


Fig. 33 - Log-log plot of fatigue crack growth rate data vs total strain range for 5Ni-Cr-Mo-V steels in a 3.5-percent salt water environment. The plot of similar data in an air environment is shown in dashed lines for comparison.

Table 18  
Data Summary – 3.5 Percent Salt Water Environment

$\epsilon_T$ ( $\mu$ in./in.)	dL/dN (microinches/cycle)				
	Specimen H131-3	Specimen H13P-1	Specimen H981-4	Specimen H981-6	Average
2,925	3.60	-	-	-	3.60
3,400	-	5.50	3.50	-	4.50
3,900	12.0	15.5	11.6	-	13.0
4,850	34.5	40.7	30.0	-	35.1
5,850	72.5	83.5	57.5	-	71.2
6,800	132.	132.	120.	-	128.
7,800	179.	206.	164.	-	183.
8,800	259.	332.	262.	-	284.
9,750	340.	375.	352.	301.	342.
10,700	423.	436.	431.	-	430.
11,600	444.	-	-	425.	435.
13,600	843.	-	-	565.	704.
15,500	-	-	-	1000.	1000.

## Microcrack Formation and Growth

The formation and growth of microcracks along the test surface was an important side effect noted while making measurements of the main fatigue crack in the 5Ni-Cr-Mo-V steel. Observations of these microcracks are limited to qualitative photographs such as shown in Figs. 34-36. The occurrence of the microcracks was considered important because they were not observed during extensive fatigue testing of HY-80 composition steels which had been heat treated to comparable 130-150 ksi YS levels (10, 11, 20, 24). Extensive quantitative studies of fatigue crack initiation in smooth (unnotched) plate bend specimens have been carried out by Gross (28); however, it is of interest here to note the appearance of the 5Ni-Cr-Mo-V steel specimens with the microcracks, and to discuss the interaction of the microcracks with the main fatigue crack.

Microcracks appeared to form more easily in the 5Ni-Cr-Mo-V steel sample having the lower (135-ksi) YS--NRL Code H-98--than in the higher (145-ksi) YS sample--NRL Code H-13. The introduction of a wet environment hastened the initiation process and reduced the strain level necessary to produce the microcracks. Microcrack formation occurred in both samples within a few thousand cycles, regardless of environment, at cyclic strain levels near YS, as might occur at points of strain intensification in a large welded structure.

Under the test conditions employed (a small crack in a bending plate), the initial effect of microcrack formation was to retard the fatigue crack growth rate of the primary crack. This phenomenon is attributed to the inability to maintain a high strain concentration at the crack tip as the material becomes honeycombed with a multitude of tiny surface microcracks. However, as these microcracks grow and link up with the advancing main fatigue crack, a rapid jump in the overall fatigue crack growth rate occurs and rapid weakening of the test specimen results.

Although the formation of microcracks can no doubt influence the performance of a structure, their occurrence is a separate phenomenon, and the fatigue crack growth data reported in Figs. 32 and 33 were obtained prior to the appearance and influence of microcracks.

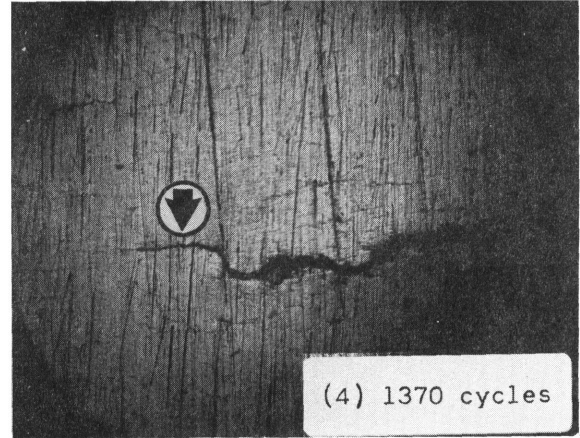
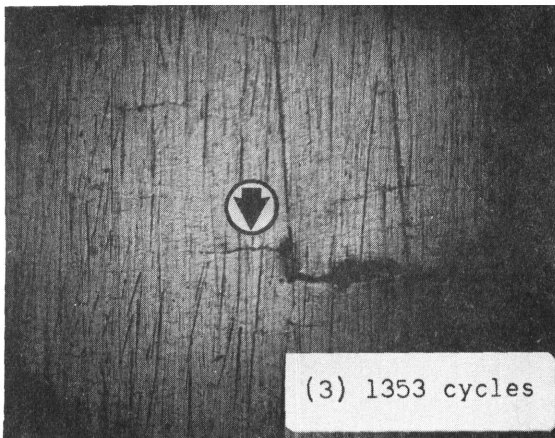
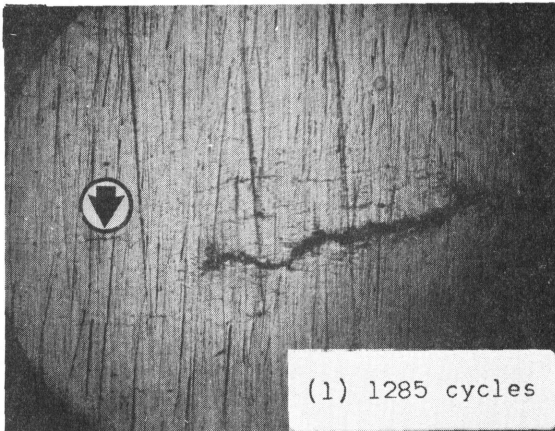


Fig. 34 - Sequence of photos showing microcrack growth ahead of advancing fatigue crack in 140-ksi YS 5Ni-Cr-Mo-V steel (Code H-13). Total strain range equals 18,000  $\mu$ in./in. (approximately 150 percent of yield strength). Air environment (14x).

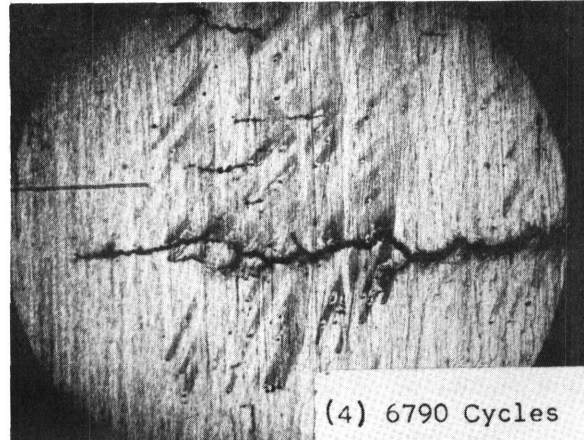
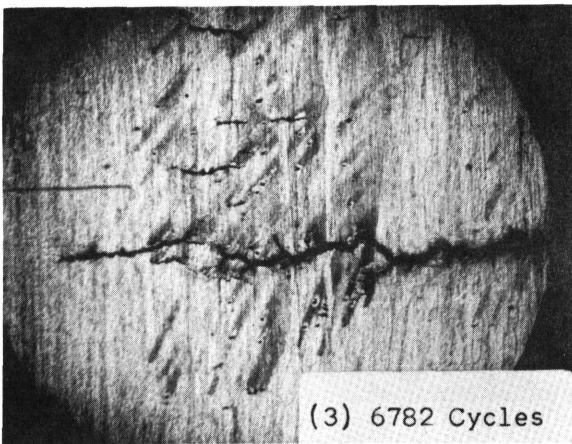
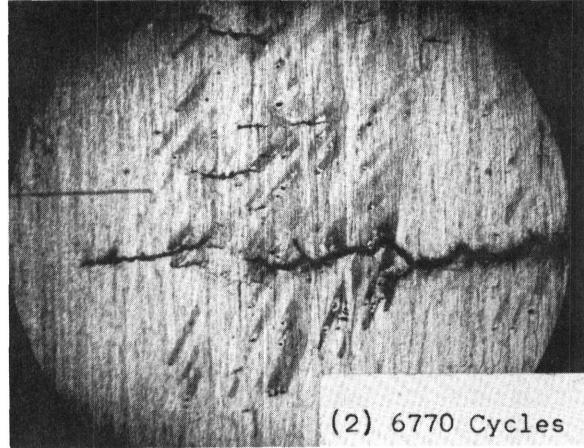
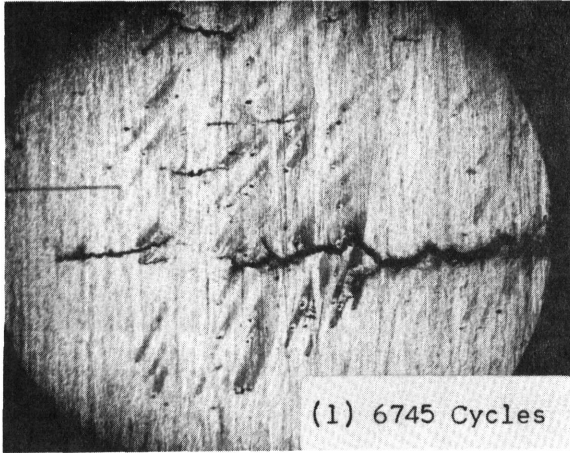
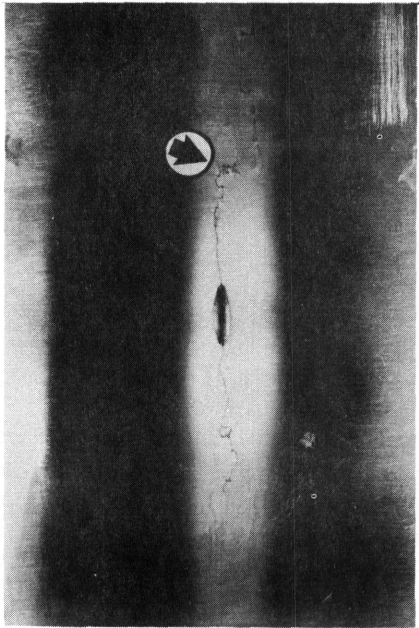


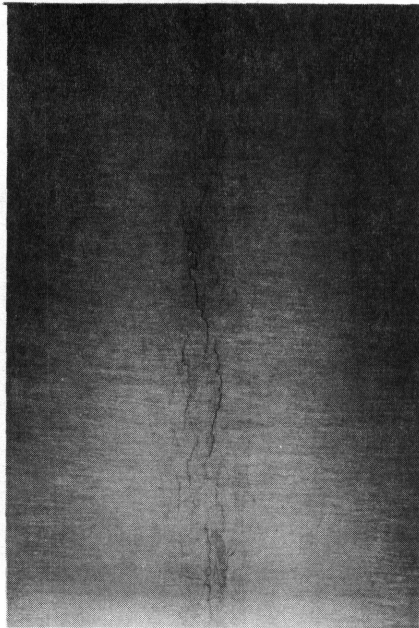
Fig. 35 - Sequence of photos showing microcrack growth ahead of advancing fatigue crack in 140-ksi YS 5Ni-Cr-Mo-V steel (Code H-13). Total strain range equals  $12,000 \mu\text{in.}-\text{in.}$  (approximately 90 percent of yield strength). Distilled water environment (14x).



1. UPPER SURFACE WITH PRINCIPAL FATIGUE CRACK INITIATED AT MECHANICAL NOTCH (1.7X).



2. DETAIL OF UPPER SURFACE SHOWING EXTENSIVE MICROCRACK DAMAGE (18X).



3. UNNOTCHED LOWER SURFACE SHOWING EXTENSIVE FATIGUE CRACK INITIATION (1.9X).



4. DETAIL OF FATIGUE CRACKS INITIATED ON LOWER SURFACE (18X).

Fig. 36 - Photos of 140-ksi yield strength 5Ni-Cr-Mo-V steel (Code H-13) plate bend fatigue specimen tested in an air environment for 3400 cycles full-reverse loading. Minimum total strain range was 8,000  $\mu$ in./in. (approximately 60 percent of yield strength). Maximum total strain range was 18,000  $\mu$ in./in. (approximately 130 percent of yield strength).

## COMPARATIVE FATIGUE PERFORMANCE

A comparison of low cycle fatigue crack growth rates in 5Ni-Cr-Mo-V steel (135-145 ksi YS) versus crack growth rates in HY-80 steel (88-ksi YS) is illustrated in Fig. 37. This figure is a log-log plot of fatigue crack growth rates versus the ratio of applied total strain range to proportional limit strain range for each material in an air environment. These curves are derived from the data in Fig. 32 and a similar plot for HY-80.

The comparison in Fig. 37 is based on the fatigue crack growth rates measured in the two materials at cyclic strain levels which are a fixed percentage of their respective elastic strengths. Under these conditions the higher strength 5Ni-Cr-Mo-V steel will propagate fatigue cracks at a rate 4 to 5 times faster than the lower strength HY-80 steel.

This brings to light a very important fact: increasing the elastic YS of a Q&T structural steel through alloy composition and heat treatment does not automatically result in a corresponding increase in fatigue crack propagation resistance, even though the high strength material may possess a high degree of fracture toughness. The intrinsic resistance of 5Ni-Cr-Mo-V steel to fatigue crack propagation is about the same as it is for HY-80 steel. Therefore, when the new, higher strength material is used at higher design stresses, there will be corresponding increase in fatigue crack growth rates which will be proportional to the fourth power of the increase in applied cyclic strain.

## CONCLUSIONS

1. The intrinsic fatigue crack propagation resistance of 130-140 ksi YS 5Ni-Cr-Mo-V steel, as measured on a strain range basis, is essentially the same as that of lower strength HY-80 steel.
2. Fatigue cracks propagate 4 to 5 times faster in 5Ni-Cr-Mo-V steel than in HY-80 steel when the steels are cycled at load levels corresponding to identical percentages of their respective elastic strengths, i.e., 80% YS.

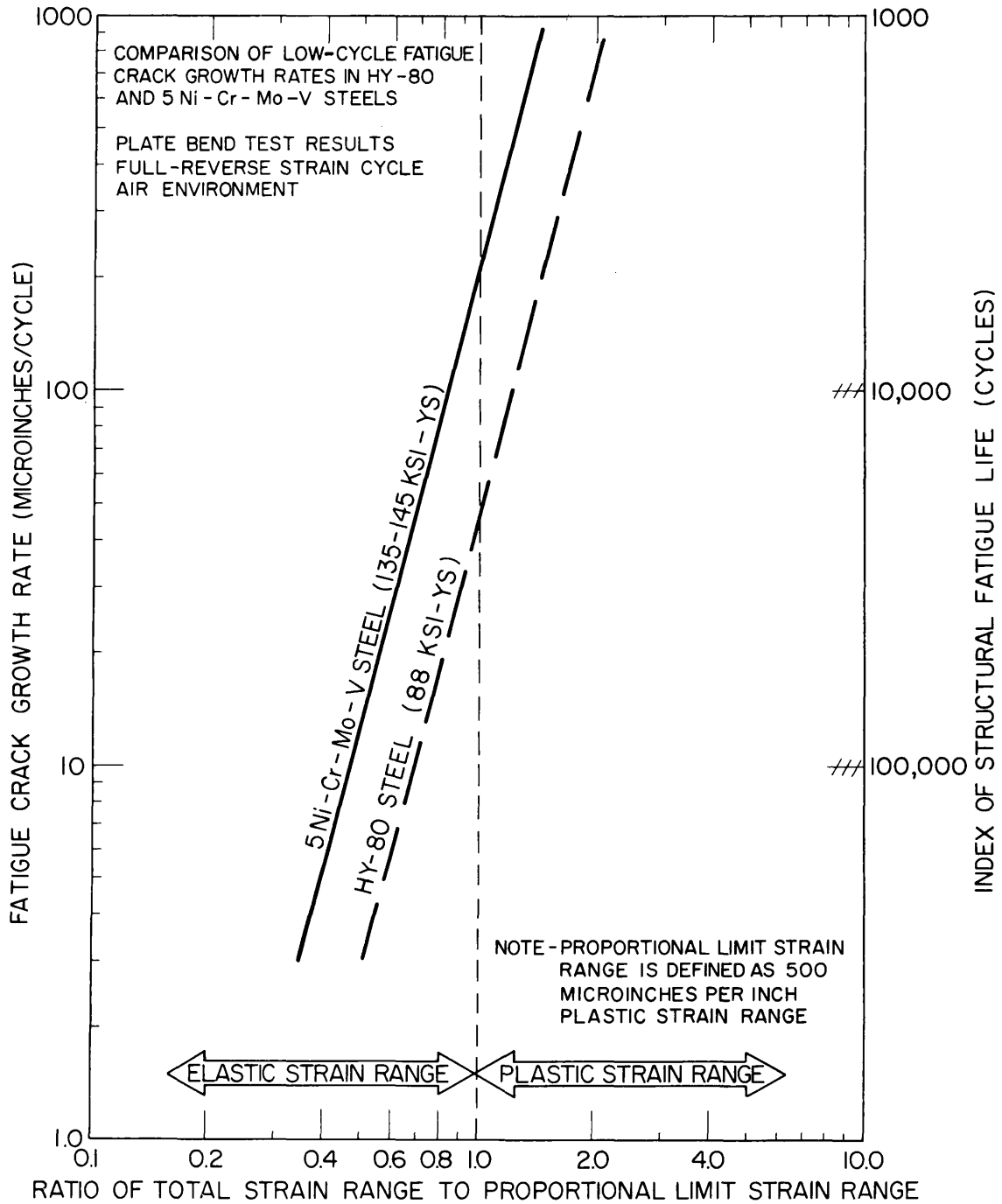


Fig. 37 - Log-log plot of fatigue crack growth rate vs the ratio of total strain range to proportional limit strain range for 5Ni-Cr-Mo-V steel (135 to 145-ksi yield strength) and HY-80 steel (88-ksi yield strength)

3. The fatigue performance of 5Ni-Cr-Mo-V steel was not seriously impaired by the presence of distilled water or salt water environments. No evidence of instability due to stress corrosion cracking under cyclic loading was observed.

4. The formation and growth of microcracks in advance of the main fatigue crack tip was of sufficient severity to recommend additional study of this phenomenon.

PLANE-STRAIN FRACTURE TOUGHNESS OF THE HIGH  
STRENGTH TITANIUM ALLOYS Ti-6Al-4V AND Ti-6Al-6V-2.5Sn

(C.N. Freed and R.J. Goode)

The plane-strain fracture toughness has been determined for the titanium alloys Ti-6Al-4V (T-27) and Ti-6Al-6V-2.5Sn (T-21). The Ti-6Al-4V alloy was studied in a single heat-treated condition. Specimens of the alloy Ti-6Al-6V-2.5Sn were heat treated to several different strength levels to determine the effect of yield strength (YS) on the plane-strain fracture toughness ( $K_{Ic}$ ). Single-edge-notch (SEN) specimens were used throughout the tests; a detailed description of the specimen dimensions is presented in the Seventh Quarterly Report (13). All of the test results tabulated in Tables 19 and 20 were obtained with "smooth" specimens, i.e., side-grooving was not employed. Detection of the load at which plane-strain instability occurred was made with a beam displacement gage instrumented with a strain gage circuit. This crack instability detection technique is described in reference 29.

TEST RESULTS ON 1-IN.-THICK Ti-6Al-4V PLATE

Test data for the Ti-6Al-4V alloy are given in Table 19. Three 1-in.-thick specimens were solution annealed at 1700°F for one hour, water-quenched, and then aged at 900°F for two hours, followed by an air-cool. Two specimens were tested at room temperature in the WR direction and one in the RW direction (Fig. 38). No significant difference in the  $K_{Ic}$  was found for either fracture direction ( $K_{Ic} = 104,500$  and  $106,000$  psi $\sqrt{\text{in.}}$ , for WR and RW respectively). The tensile and Charpy V data in Table 19 indicates a higher yield strength and slightly lower fracture toughness in the WR direction compared to the RW values. The plastic zone was well contained within the specimen and met the criteria necessary for a valid  $K_{Ic}$  test (13).

Table 19  
Plane-Strain Fracture-Toughness Test Data for Ti-6Al-4V Titanium (T-27)

Fracture Direction	Test Temperature (° F)	Type of *, † Specimen	Specimen Width W (in.)	Specimen Thickness B (in.)	Crack Length a (in.)	a/W	Load at $K_{Ic}$ (lbs)	$K_{Ic}$ (psi $\sqrt{\text{in.}}$ )	Plastic Zone $r_y$ (in.)	Percent Shear (%)
WR	82	SEN	5.002	0.946	1.520	0.304	128,000	104,000	0.088	38
WR	86	SEN	5.001	0.952	1.530	0.306	129,000	105,000	0.089	46
RW	86	SEN	4.500	0.961	1.495	0.332	113,000	106,000	0.102	39

85

Heat Treatment and Mechanical Properties of the Tested Specimens

Fracture Direction	YS (0.2%) (ksi)	UTS (ksi)	R.A. (%)	Elongation (%)	Charpy-V Impact Energy ‡ (ft-lb)			Heat Treatment ¶		
					-80° F	32° F	70° F	212° F	Solution-anneal	Aging
WR**	140.1	155.9	23.1	10.0	17.7	19.8	21.3	21.3	1700° F/1 hr/WQ	900° F/2 hr/AC
RW**	132.5	150.5	25.2	10.6	24.7	25.0	24.5	27.5	1700° F/1 hr/WQ	900° F/2 hr/AC

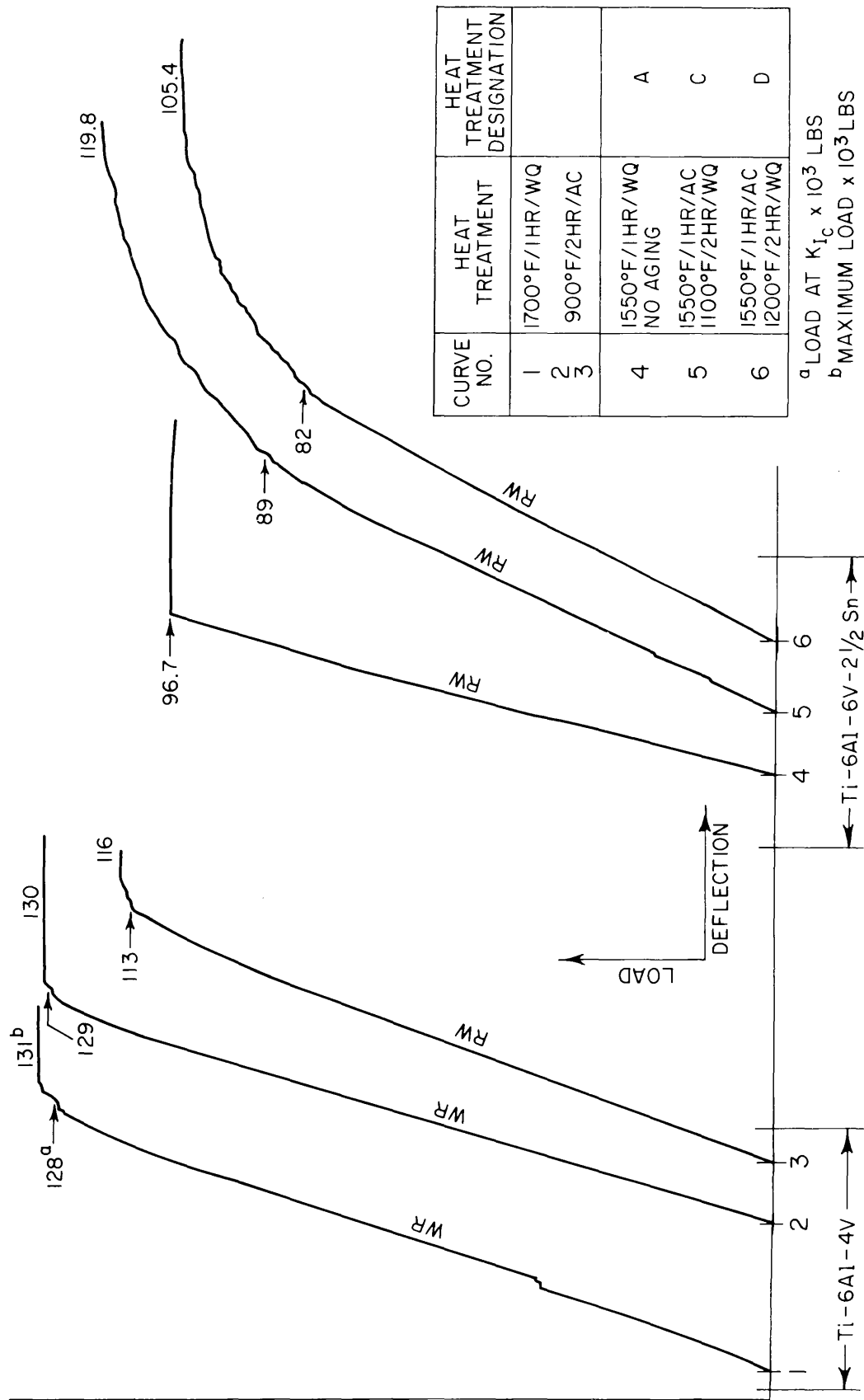
\*Specimen lengths were 12-in. and were cut from a 1-in.-thick plate.

†Fatigue cracks of approximately 0.1-in. in length were formed at the tip of the edge-notch.

‡Drop-weight tear data are being obtained.

¶  $\beta$  transus is 1820±25° F.

\*\*All mechanical test results are averages of two values.



<sup>a</sup> LOAD AT  $K_{Ic}$  x  $10^3$  LBS  
<sup>b</sup> MAXIMUM LOAD x  $10^3$  LBS

Fig. 38 - Representative load-deflection curves for Ti-6Al-4V and Ti-6Al-6V-2.5Sn

## TEST RESULTS ON 1-IN.-THICK Ti-6Al-6V-2.5Sn

The test data for the Ti-6Al-6V-2.5Sn alloy are presented in Table 20. One-inch-thick specimens were tested in five different heat-treated conditions and in the "as-received" condition. All  $K_{IC}$  tests were performed at the indicated room temperature.

Two specimens were tested in the "as-received" condition with the fracture propagating in the WR direction. The  $K_{IC}$  values obtained were 59,000 and 63,000 psi/in. at 152.0-ksi YS.

A RW specimen was solution-annealed at 1550°F for one hour, followed by a water-quench (heat-treatment "A"). The  $K_{IC}$  value for this heat-treatment was determined to be 81,000 psi/in. The tensile properties have yet to be determined. A second RW specimen was given the same solution anneal but was aged at 900°F for four hours and air-cooled (heat-treatment "B"). This treatment resulted in a low  $K_{IC}$  of 32,000 psi/in. at 186.0-ksi YS.

Heat treatments "C" and "D" consisted of a solution anneal at 1550°F for one hour, followed by an air-cool, then aging for two hours at 1100° and 1200°F respectively. The purpose was to determine the effect of different aging temperatures on  $K_{IC}$ . Specimens for each aging treatment were tested in both the RW and WR fracture directions. The  $K_{IC}$  values for a given fracture direction were essentially the same for the two aging temperatures studied. The  $K_{IC}$  values for the RW fracture direction were 88,000 and 84,000 psi/in. for "C" and "D" heat treatments respectively. For the WR fracture direction, they were 91,000 and 95,000 psi/in. for the same respective heat treatments. The YS values which have been determined only for the RW specimens were 154.8 and 147.6-ksi for the "C" and "D" heat treatments respectively.

In order to produce strength and toughness properties between those obtained for heat treatments "B" and "C" or "D", a RW specimen was solution-annealed at 1625°F for one hour and water-quenched, followed by aging at 1200°F for two hours and air-cooled (heat-treatment "E"). This heat treatment produced a  $K_{IC}$  of 62,000 psi/in. The yield strength has not yet been determined but it is expected to be between that produced by the "B" and "C" or "D" heat treatments.

Table 20  
Plane-Strain Fracture-Toughness Test Data for 1-in.-Thick Ti-6Al-6V-2.5Sn Titanium (T-21)

Heat Treatment	Solution Heat Treatment*	Aging Heat Treatment (°F)	Fracture Direction	YS† (0.2%) (ksi)	UTS (ksi)	R.A. EL. (%) calculated at fracture	K <sub>Ic</sub> Test Temp. (°F)	Specimen Width W (in.)	Specimen Thickness B‡ (in.)	Crack Length a (in.)	a/W	Load at K <sub>Ic</sub> (lb)	K <sub>Ic</sub> (psi√in.)	Plastic Zone Radius r <sub>p</sub> (in.)	Percent Shear (%)
A	As-received	As-received	WR	152.0	154.5	41.5	88	5.00	1.06	1.63	0.325	75,500	59,000	0.024	~39
	As-received	As-received	WR	152.0	154.5	41.5	88	5.00	1.07	1.73	0.345	76,000	63,000	0.027	~44
B	1550° F/1 hr/WQ	-	RW	-	-	-	86	4.51	1.06	1.49	0.330	96,700	81,000	-	10
	1550° F/1 hr/WQ	900/4 hr/AC	RW	186.0	202.0	18.3	90	4.50	1.07	1.48	0.328	38,400	32,000	0.005	6
C	1550° F/1 hr/AC	1100/2 hr/WQ	RW	154.8	158.4	44.7	85	4.50	1.04	1.64	0.365	89,000	88,000	0.052	63
	1550° F/1 hr/AC	1100/2 hr/WQ	WR	-	-	-	85	4.49	1.03	1.69	0.375	88,000	91,000	-	54
D	1550° F/1 hr/AC	1200/2 hr/WQ	RW	147.6	149.9	40.1	85	4.50	1.04	1.68	0.374	82,000	84,000	0.052	61
	1550° F/1 hr/AC	1200/2 hr/WQ	WR	-	-	-	85	4.50	1.03	1.80	0.401	83,000	95,000	-	44
E	1625° F/1 hr/WQ	1200/2 hr/AC	RW	-	-	-	87	4.51	1.06	1.66	0.368	64,000	62,000	-	10

\*βtransus is 1735±25°F.

†Additional tensile C<sub>v</sub> and DWT data are being obtained.

‡All specimens are SEN.

§Specimens were cut from a 1-in.-thick plate.

## EFFECT OF THICKNESS ON $K_{Ic}$

An additional experiment was conducted to determine the effect of thickness on the plane-strain fracture toughness. The test data and results are shown in Table 21.

A 1-in.-thick Ti-6Al-6V-2.5Sn plate was sawed into three equal thicknesses, identified, and machined into specimens 1/4-in.-thick. These three specimens were given heat treatment "B" and tested to determine the respective  $K_{Ic}$  values. These values, which represented the properties of two surface-cut specimens and one center-section specimen, were compared with the plane-strain fracture toughness of a 1-in.-thick (full-plate-thickness) specimen that had received heat treatment "B". The full-thickness specimen had a  $K_{Ic}$  value of 32,000 psi/in., Table 20, as compared to an average  $K_{Ic}$  value of 28,000 psi/in. for the 1/4-in.-thick specimens, Table 21. The slight difference in  $K_{Ic}$  values is probably due to the faster cooling rate of the thinner specimens.

A second set of three specimens was cut in the same manner as those mentioned above, and given heat treatment "F". Whereas in the first case the specimen from the center of the plate indicated a slightly lower  $K_{Ic}$  value (26,000 psi/in.) than the surface specimens (an average of 29,000 psi/in.), these specimens displayed no significant difference in  $K_{Ic}$  values across the thickness. An interesting sidelight, however, is that although the YS of the specimens given heat treatment "F" (194.9-ksi) is higher than the YS obtained from similar specimens given heat treatment "B" (186.0-ksi), the "B" treatment results in material of appreciably lower fracture toughness than that of the "F" treatment.

Table 21  
Plane-Strain Fracture-Toughness Test Data for 1/4-in.-Thick Ti-6Al-6V-2.5Sn Titanium

Heat Treatment	Solution Heat Treatment* (°F)	Aging Heat Treatment (°F)	Fracture Direction	YS† (0.2%) (ksi)	UTS (ksi)	R.A. EL. (%) (calculated at fracture)	K <sub>Ic</sub> Test Temp. (°F)	Specimen Width W (in.)	Specimen Thickness B‡ (in.)	Crack Length a (in.)	a/W	Load at K <sub>Ic</sub> (lb)	K <sub>Ic</sub> (psi√in.)	Plastic Zone Radius (in.)	Percent Shear (%)
B	1550/1 hr/WQ	900/4 hr/AC	RW	186.0**	202.0	18.3	80	1.50	0.247††	0.512	0.342	4240	28,000	0.004	13
B	1550/1 hr/WQ	900/4 hr/AC	RW	186.0	202.0	18.3	80	1.50	0.247††	0.500	0.334	4700	30,000	0.004	19
B	1550/1 hr/WQ	900/4 hr/AC	RW	186.0	202.0	18.3	80	1.50	0.249††	0.510	0.340	4000	26,000	0.003	22
F	1700/1 hr/WQ	1100/2 hr/AC	RW	194.9**	201.3	6.9	80	1.50	0.247††	0.500	0.333	6400	41,000	0.007	23
F	1700/1 hr/WQ	1100/2 hr/AC	RW	194.9	201.3	6.9	80	1.50	0.246††	0.500	0.333	6400	41,000	0.007	23
F	1700/1 hr/WQ	1100/2 hr/AC	RW	194.9	201.3	6.9	80	1.50	0.246††	0.512	0.340	6500	42,000	0.007	40

\* βtransus is 1735±25°F.

†Additional tensile C<sub>v</sub> and DWT data are being obtained.

‡All specimens are SEN.

§Specimens were cut from a 1-in.-thick plate.

\*\*Tensile data obtained from 0.505-in.-diam. specimen cut from 1-in.-thick plate.

††Thickness represents top or bottom quarter of 1-in.-thick plate.

‡‡Thickness represents center of 1-in.-thick plate.

## REFERENCES

1. Puzak, P.P., Eschbacher, E.W., and Pellini, W.S., "Initiation and Propagation of Brittle Fracture in Structural Steels," *Welding Journal*, December 1952
2. Puzak, P.P., and Pellini, W.S., "Standard Method for NRL Drop-Weight Test," *NRL Report 5831*, August 21, 1962; issued by BuShips as NAVSHIPS 250-634-3; and ASTM Standards Designation E208-63T, 1963
3. Pellini, W.S., and Puzak, P.P., "Fracture Analysis Diagram Procedures for the Fracture-Safe Engineering Design of Steel Structures," *NRL Report 5920*, March 15, 1963, and *Welding Research Council Bulletin Series No. 88*, May 1963
4. Pellini, W.S., and Puzak, P.P., "Practical Considerations in Applying Laboratory Fracture Test Criteria to the Fracture-Safe Design of Pressure Vessels," *NRL Report 6030*, November 5, 1963; also, *Trans. of the ASME, Series A, Journal of Engineering for Power*, October 1964, pp. 429-443
5. Babecki, A.J., Puzak, P.P., and Pellini, W.S., "Report of Anomalous 'Brittle' Failures of Heavy Steel Forgings at Elevated Temperatures," *ASME Paper No. 59-MET-6*, May 1959
6. Puzak, P.P., and Babecki, A.J., "Explosion Tear Test Studies of High Strength Q&T Steels," *NRL Memorandum Report 1333*, June 19, 1962
7. Puzak, P.P., and Babecki, A.J., "Explosion Tear Test Studies of High-Strength Q&T Steels," *NRL Report 5836*, September 6, 1962
8. Pellini, W.S., and Puzak, P.P., "Factors that Determine the Applicability of High Strength Quenched and Tempered Steels to Submarine Hull Construction," *NRL Report 5892*, December 5, 1962; and *Proceedings, Navy Workshop of Deep-Submergence Hulls, DTMB*, December 1962
9. Pellini, W.S., Goode, R.J., Puzak, P.P., Lange, E.A., and Huber, R.W., "Review of Concepts and Status of Procedures for Fracture-Safe Design of Complex Welded Structures Involving Metals of Low to Ultra-High Strength Levels," *NRL Report 6300*, June 1965

10. Puzak, P.P., et al., "Metallurgical Characteristics of High Strength Structural Materials (Third Quarterly Report)," NRL Report 6086, January 1964
11. Goode, R.J., et al., "Metallurgical Characteristics of High Strength Structural Materials (Fourth Quarterly Report)," NRL Report 6137, June 1964
12. Puzak, P.P., et al., "Metallurgical Characteristics of High Strength Structural Materials (Second Quarterly Report)," NRL Memorandum Report 1461, September 30, 1962
13. Goode, R.J., et al., "Metallurgical Characteristics of High Strength Structural Materials (Seventh Quarterly Report)," NRL Report 6327, May 1965
14. Pellini, W.S., et al., "Metallurgical Characteristics of High Strength Structural Materials (Sixth Quarterly Report)," NRL Report 6258, December 1964
15. Welding Journal, Vol. 43, December 1964, pp. 564s-576s
16. Welding Journal, Vol. 44, January 1965, pp. 21s-26s
17. "Welding of 9Ni-4Co Alloy Steels," 4th Maraging Steel Seminar, Dayton, Ohio, 1964
18. "Investigation of 9-4-25 Weld Deposit," USNASL Memorandum #8, Proj 9300-1, 2 March 1964
19. Goode, R.J., and Huber, R.W., "Fracture Toughness Characteristics of Some Titanium Alloys for Deep-Diving Vehicles," Journal of Metals, Vol. 17, No. 8, August 1965, pp. 841-846
20. Crooker, T.W., et al., "Metallurgical Characteristics of High Strength Structural Materials (Fifth Quarterly Report)," NRL Report 6196, September 1964
21. ASTM Materials and Research Standards, Vol. 1, No. 5, May 1961
22. Rathbone, A.M., Gross, J.H., and Dorsch, K.E., "A Tough Weldable Steel with a 140,000 Psi Yield Strength," Metal Progress, May 1965

23. Crooker, T.W., Morey, R.E., and Lange, E.A., "Low Cycle Fatigue Crack Propagation," Report of NRL Progress, pp. 30-33, June 1964
24. Crooker, T.W., Morey, R.E., and Lange, E.A., "Low Cycle Fatigue Crack Propagation," Report of NRL Progress, pp. 31-33, August 1964
25. Crooker, T.W., Judy, Jr., R.W., Morey, R.E., and Lange, E.A., "Low Cycle Fatigue Crack Propagation," Report of NRL Progress, pp. 41-44, March 1965
26. Crooker, T.W., Morey, R.E., and Lange, E.A., "Low Cycle Fatigue Crack Propagation," Report of NRL Progress, pp. 37-40, June 1965
27. Crooker, T.W., Morey, R.E., and Lange, E.A., "Low Cycle Fatigue Crack Propagation Characteristics of Monel 400 and Monel K-500 Alloys," NRL Report 6218, March 10, 1965
28. Gross, M.R., "Low-Cycle Fatigue of Materials for Submarine Construction," Naval Engineers Journal, Vol. 75, No. 4, October 1963
29. Krafft, J.M., "Fracture Toughness of Metals," Report of NRL Progress, pp. 4-16, November 1963

**This page intentionally blank.**

## DOCUMENT CONTROL DATA - R&amp;D

(Security classification of title, body of abstract and indexing annotation must be entered when the overall report is classified)

1. ORIGINATING ACTIVITY (Corporate author) U.S. Naval Research Laboratory Washington, D.C. 20390		2 a. REPORT SECURITY CLASSIFICATION Unclassified	
		2 b. GROUP	
3. REPORT TITLE METALLURGICAL CHARACTERISTICS OF HIGH-STRENGTH STRUCTURAL MATERIALS [Eight Quarterly Report]			
4. DESCRIPTIVE NOTES (Type of report and inclusive dates) A progress report on various problems.			
5. AUTHOR(S) (Last name, first name, initial) Puzak, P.P., Lloyd, K.B., Goode, R.J., Huber, R.W., Howe, D.G., Judy, R.W. Jr., Morey, R.E., Lange, E.A., Crooker, T.W., and Freed, C.N.			
6. REPORT DATE August 1965		7 a. TOTAL NO. OF PAGES 99	7 b. NO. OF REFS 29
8 a. CONTRACT OR GRANT NO. NRL Problems: F01-17, M01-05, M01-18, M03-01 b. PROJECT NO. SP-01426, RR 007-01-46- 5405, SR 007-01-02-0704, RR 007-01- c. 46-5420, SF 020-01-05-0731, MIPR- ENG-NAV-66-2, RR 007-01-46-5414, d. SF 020-01-01-0850		9 a. ORIGINATOR'S REPORT NUMBER(S) NRL Report 6364	
		9 b. OTHER REPORT NO(S) (Any other numbers that may be assigned this report) None	
10. AVAILABILITY/LIMITATION NOTICES Distribution of this document is unlimited Available from CFSTI - \$3.00			
11. SUPPLEMENTARY NOTES None		12. SPONSORING MILITARY ACTIVITY Dept. of the Navy (Office of Naval Research, BuShips, and Special Projects Office) and Dept. Army (Office of Chief of Engineers)	
13. ABSTRACT  A progress report covering research studies in high-strength structural materials conducted in the period May 1965 to July 1965 is presented. The report includes fracture-toughness studies on the 12 percent Ni maraging and 9Ni-4Co-.XXC steels, a variety of titanium alloy MIG, EB, and plasmarc weldments, and some aluminum alloys. The current fracture-toughness index diagrams are presented for steels, titanium alloys, and aluminum alloys. Results are presented of (a) a study of the plane-strain fracture toughness of the alloys Ti-6Al-4V and Ti-6Al-6V-2.5Sn over respective yield strength ranges of 130-140 ksi and 147-186 ksi, (b) heat-treatment studies on several titanium alloys, and (c) a low-cycle fatigue crack propagation study of 5Ni-Cr-Mo-V steel in dry and wet environments in which considerable microcrack formation and growth was encountered.			

14. KEY WORDS	LINK A		LINK B		LINK C	
	ROLE	WT	ROLE	WT	ROLE	WT
Engineering principles						
Titanium alloys						
Aluminum alloys						
High-strength steels						
Fracture toughness						
Low-cycle fractures						
Corrosion fatigues						
Mechanical properties						
Explosion tear test						
Explosion bulge test						
Drop-weight tear test						
Processing variables						
Heat treatment						
High-strength steel welds						
Maraging steel welds						
Weld testing						

INSTRUCTIONS

1. **ORIGINATING ACTIVITY:** Enter the name and address of the contractor, subcontractor, grantee, Department of Defense activity or other organization (*corporate author*) issuing the report.
- 2a. **REPORT SECURITY CLASSIFICATION:** Enter the overall security classification of the report. Indicate whether "Restricted Data" is included. Marking is to be in accordance with appropriate security regulations.
- 2b. **GROUP:** Automatic downgrading is specified in DoD Directive 5200.10 and Armed Forces Industrial Manual. Enter the group number. Also, when applicable, show that optional markings have been used for Group 3 and Group 4 as authorized.
3. **REPORT TITLE:** Enter the complete report title in all capital letters. Titles in all cases should be unclassified. If a meaningful title cannot be selected without classification, show title classification in all capitals in parenthesis immediately following the title.
4. **DESCRIPTIVE NOTES:** If appropriate, enter the type of report, e.g., interim, progress, summary, annual, or final. Give the inclusive dates when a specific reporting period is covered.
5. **AUTHOR(S):** Enter the name(s) of author(s) as shown on or in the report. Enter last name, first name, middle initial. If military, show rank and branch of service. The name of the principal author is an absolute minimum requirement.
6. **REPORT DATE:** Enter the date of the report as day, month, year; or month, year. If more than one date appears on the report, use date of publication.
- 7a. **TOTAL NUMBER OF PAGES:** The total page count should follow normal pagination procedures, i.e., enter the number of pages containing information.
- 7b. **NUMBER OF REFERENCES:** Enter the total number of references cited in the report.
- 8a. **CONTRACT OR GRANT NUMBER:** If appropriate, enter the applicable number of the contract or grant under which the report was written.
- 8b, 8c, & 8d. **PROJECT NUMBER:** Enter the appropriate military department identification, such as project number, subproject number, system numbers, task number, etc.
- 9a. **ORIGINATOR'S REPORT NUMBER(S):** Enter the official report number by which the document will be identified and controlled by the originating activity. This number must be unique to this report.
- 9b. **OTHER REPORT NUMBER(S):** If the report has been assigned any other report numbers (*either by the originator or by the sponsor*), also enter this number(s).
10. **AVAILABILITY/LIMITATION NOTICES:** Enter any limitations on further dissemination of the report, other than those

imposed by security classification, using standard statements such as:

- (1) "Qualified requesters may obtain copies of this report from DDC."
- (2) "Foreign announcement and dissemination of this report by DDC is not authorized."
- (3) "U. S. Government agencies may obtain copies of this report directly from DDC. Other qualified DDC users shall request through \_\_\_\_\_."
- (4) "U. S. military agencies may obtain copies of this report directly from DDC. Other qualified users shall request through \_\_\_\_\_."
- (5) "All distribution of this report is controlled. Qualified DDC users shall request through \_\_\_\_\_."

If the report has been furnished to the Office of Technical Services, Department of Commerce, for sale to the public, indicate this fact and enter the price, if known.

11. **SUPPLEMENTARY NOTES:** Use for additional explanatory notes.

12. **SPONSORING MILITARY ACTIVITY:** Enter the name of the departmental project office or laboratory sponsoring (*paying for*) the research and development. Include address.

13. **ABSTRACT:** Enter an abstract giving a brief and factual summary of the document indicative of the report, even though it may also appear elsewhere in the body of the technical report. If additional space is required, a continuation sheet shall be attached.

It is highly desirable that the abstract of classified reports be unclassified. Each paragraph of the abstract shall end with an indication of the military security classification of the information in the paragraph, represented as (TS), (S), (C), or (U).

There is no limitation on the length of the abstract. However, the suggested length is from 150 to 225 words.

14. **KEY WORDS:** Key words are technically meaningful terms or short phrases that characterize a report and may be used as index entries for cataloging the report. Key words must be selected so that no security classification is required. Identifiers, such as equipment model designation, trade name, military project code name, geographic location, may be used as key words but will be followed by an indication of technical content. The assignment of links, roles, and weights is optional.